Precision Medicine in Pancreatic Cancer

A dissertation submitted to the Faculty of

The School of Engineering and Applied Science

University of Virginia

In partial fulfillment of the requirements for the degree of Doctor of Philosophy in

Biomedical Engineering

By

Jaymes Ryan Beech

May

2015

APPROVAL SHEET

This dissertation is submitted in partial fulfillment of the requirements for the degree of Doctor of Philosophy in Biomedical Engineering

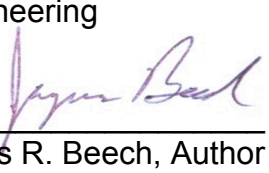

Jaymes R. Beech, Author

This dissertation has been read and approved by the Examining Committee:

Jason Papin, Ph.D., Chair of Committee

Kimberly Kelly, Ph.D., Thesis Advisor

Kevin Janes, Ph.D.

David Brautigan, Ph.D.

J. Thomas Parsons, Ph.D.

Accepted for the School of Engineering and Applied Science:

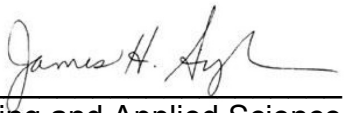

Dean, School of Engineering and Applied Science

May

2015

ACKNOWLEDGEMENTS

This dissertation is the culmination of six years of research, hard work, luck, and at times sheer will, but most of all it is a product of the advice, ideas, and support from those whom I have had the pleasure of working with throughout my time at UVA. So many people have contributed to this dissertation, some directly and many more indirectly; for everyone who has supported me during this process, I express my sincerest gratitude. There are several key individuals who have had the largest contribution to this work and my development that I would like to address specifically.

First, to my parents, Karla and Marty. Thank you for always believing in me and supporting me, no matter what the circumstances. Your constant faith in me, even in times when I doubted myself, has been so invaluable throughout my life. Nothing I have accomplished would have been possible without your love and support and for that I am eternally grateful. To my sister, Tiffany, and brother, Jason, seeing you on return trips home and during your visits to Charlottesville has always been some of the better memories of graduate school for me. Family is so important to me; thank you for always being someone whom I can rely on and who will be there for me no matter what.

To my girlfriend Brittany, your support and patience have been so helpful throughout this process. You are one of the kindest and most selfless people that I know. It's not just one or two things that you do, but a thousand small things that make me so grateful that you are in my life. Thank you for everything that you do for me.

To my friends and labmates, the last six years have brought so many fond memories that we have shared. Surviving clases and the extensive projects within, visiting wineries, negative data, discovering Foxfield, our ski trips to Snowshoe, regretting eating Fred's "manager's special" dish at the Kelly lab cook-off, dreading comps, and so much more. You have celebrated with me during the highs, and picked me up during the lows; I will cherish these memories and the many life-long friendships that we have formed here.

To my committee members and the biotechnology training program, you have helped me become a better researcher and broadened my understanding of the scientific world. Whenever my research took a turn for the worst (and it so often did), your expertise and insight would shed new light on the problems and helped me push forward with my work. Your ideas, opportunities, and support have been a large factor in the completion of this dissertation.

Finally, to Dr. Kimberly Kelly - my advisor, my mentor and my friend. Over the last six years, so much of my development, scientifically, professionally and personally can be attributed to you. In my research, you have always known just how much to push me and to let me develop my own ideas independently, but whenever I would begin to stumble you have always been there to guide me back to the right path. I know that in the years to come, you will always be there to support me, to offer advice and to help me however you can and for that I am grateful.

TABLE OF CONTENTS

ABSTRACT

Pancreatic ductal adenocarcinoma (PDAC) is one of the most deadly human cancers due to a lack of early detection and its resistance to conventional chemo- and radiotherapy. Precision medicine using small molecule inhibitors is an alternative therapeutic strategy. The *KRAS* oncogene is mutated in >90% of pancreatic cancer tumors and presents an exploitable therapeutic opportunity. KRAS mutations render it constitutively active, signaling through effector molecules to stimulate growth and survival in cancer cells. One of the most predominant pathways through which KRAS signals is the RAF-MEK-ERK pathway. Many inhibitors of this pathway have gone to clinical trials, but ultimately failed in treating pancreatic cancer due to a lack of overall efficacy and an acquired resistance in tumors. Often, the studies noted that a method of selecting for patients who are predicted to respond to the therapy could improve therapeutic efficacy. Therefore, we set out to find markers that could be used to predict when MEK inhibition will be effective or should conversely be avoided.

To discover such markers, we tested a panel of pancreatic cancer cell lines for sensitivity to the MEK inhibitor AZD6244. After grouping them as either sensitive or resistant, RTqPCR and cDNA microarray analyses identified genes that were differentially expressed between the two groups. Most notable were *MERTK* and *MAPK8*, which were both upregulated in resistant lines. Correlation studies with the protein products of these genes (MERTK and JNK1 respectively) showed both protein expression levels significantly correlated with resistance to the small molecule inhibitor. The MERTK protein in particular was

found to be upregulated in both innate and acquired resistant cell lines. Knockdown of either *MERTK* or *MAPK8* yielded a noticeable decrease in proliferation. Inhibitor targeting of JNK1 also resulted in combinatorial benefits with MEK inhibition, particularly in resistant cell lines. Our findings suggest that these two proteins can serve as markers of resistance and potential new therapeutic targets in pancreatic cancer.

In addition to predictive and therapeutic targets, precision medicine needs effective techniques to select for moieties that can target these key proteins. One powerful approach for identifying such moieties is the use of phage display. The technique uses combinatorial peptide libraries on the surface of bacteriophages to offer a rapid, economical way to screen billions of peptides for specific binding properties. As a modification to this approach, we have created a system that enables specific insertion of selenocysteine (Sec) residues into the peptides displayed for screening. These Sec residues allow for site-specific tethering of small molecules to create a hybrid screening technique capable of much higher chemical diversity than current phage screens. As a proof of concept, we tethered a small molecule agonist of the adenosine A_1 receptor to Sec phage and showed enhanced binding of this modified phage to the A_1 receptor compared to unmodified phage. Further, we showed that the modified phage are capable of activating the receptor and its downstream signaling pathways because of the small molecule agonist tethered to the phage. This technique will provide new screening capabilities for small molecule-peptide hybrids and provide a new tool for advancing precision medicine.

NOMENCLATURE

5-FU	5-Fluorouracil
ADM	Acinar-ductal metaplasias
AUC	Area Under the Curve
bid	Twice a day
Bt	Biotin
cDNA	Complementary DNA
COSMIC	Catalogue of Somatic Mutations in Cancer
Cys	Cysteine
DMEM	Dulbecco's modified eagle's medium
DPBS	Dulbecco's phosphate-buffered saline
DTT	Dithiothreitol
EC_{50}	Concentration to achieve 50% of maximal effect
E_{inf}	Effect at an infinite concentration
ELISA	Enzyme Linked Immunosorbent Assay
E_{max}	Effect at the maximum concentration tested
FBS	Fetal bovine serum
FOLFIRINOX	Chemotherapy regimen consisting of folinic acid, fluorouracil, irinotecan and oxaliplatin
GAP	GTPase-activating protein
GBS	Glycine buffered saline
GEF	Guanine nucleotide exchange factor
GI_{50}	Concentration to inhibit growth by 50%
GI_{80}	Concentration to inhibito growth by 80%
hA_1-CHO	CHO cells transformed to express the human adenosine A_1 receptor

HBSS	Hank's balanced salt solution
IC_{50}	Concentraiton to achieve 50% of max inhibition
IMDM	Iscove's modified dulbecco's medium
IPMN	Intraductal papillary mucinous neoplasms
JNKi	JNK inhibitor/inhibition
MAPK	Mitogen-activated protein kinase
MCN	Mucinous cystic neoplasm
MEKi	MEK inhibitor/inhibition
MEM	Minimum essential medium
MERTKi	MERTK inhibitor/inhibition
MeV	Multi-experiment Viewer
mRNA	Messanger RNA
NOAMI	N6-octylaminoadenosine modified with an iodoacetyl group
NSCLC	Non-small cell lung carcinoma
PanIN	Pancreatic intraepithelial neoplams
PBS+	Phosphate buffered saline plus calcium and magnesium
PDAC	Pancreatic ductal adenocarcinoma
PVDF	Polyvinylidene difluoride
qPCR	Quantitative polymerase chain reaction
qWestern	Quantitative western (blot)
RPMI	Roswell park memorial institute (medium)
RTqPCR	Real time quantitative polymerase chain reaction
SAM	Significance analysis of microarrays
Sec	Selenocysteine
shRNA	Short hairpin RNA

siRNA	Short interfering RNA

LIST OF FIGURES

LIST OF TABLES

Chapter 1

Introduction

1.1. The Clinical Problem of Pancreatic Cancer

1.1.1. An Overview Pancreatic Cancer

Pancreatic cancer is a devastating disease and one of the most lethal human cancers. In 2014, the estimated incidence of the disease in the United States was 46,420 and an estimated 39,590 people died from the disease (1). These statistics place it tenth in cancer incidence but fourth in cancer deaths (2). By 2030, it is projected to be ranked second in cancer deaths (3). Part of the problem is pancreatic cancer has few symptoms and by the time most patients present, they are already in the later stages of the disease (4). An estimated 9% of patients have localized, resectable tumors while the remaining 91% of individuals diagnosed have regional tumors or metastases. Only 10% of this group are candidates for surgery (1). Further, most forms of the disease are refractory to therapeutic strategies; this results in the poorest prognosis of any major cancer type having a 5-year survival rate of 6% (2). Sadly, while many cancers have seen significant improvement in patient outcome over the past three decades, progress in pancreatic cancer has been minimal. Recognizing the need for improvement, the *Recalcitrant Cancer Research Act* was signed into law in 2013 intending to focus the National Cancer Institute's (NCI) funding more on diagnostic and therapeutic research in difficult cancers such pancreatic. Hopefully, this additional support will result in better patient outcomes in the future.

1.1.2. Risk Factors for Pancreatic Cancer

Epidemiologically, smoking is the only conclusive cause of the disease. Smokers have ~2-fold higher risk than nonsmokers, but this varies by extent and of cigarette use; heavy smokers (>20 pack-years) are ~1.4-fold more at risk than light smokers (≤20 pack-years). Excessive alcohol consumption has also been linked to pancreatic cancer. Those who consume more than 60 mL of ethanol/day have a 60% higher risk than moderate or non-drinkers (5). Links between *Helicobacter pylori* infection and chronic pancreatitis to pancreatic cancer has also been reported (6, 7). Other reported, but less conclusive, risk factors for pancreatic cancer include a history of diabetes (8, 9), poor diet (10), and having type A, B or AB blood type (11).

Familial history can also be an important factor in pancreatic cancer. Those with four or more affected family members are a staggering 57 times more likely to contract pancreatic cancer (12) and approximately 5-10% of presenting patients have a family history with the disease (13). Genetic links to familial pancreatic cancer are largely unknown and is still an area of active research. Hereditary mutations are thought to be heterogeneous between families, but several subgroups in familial pancreatic cancer have emerged, centered around several key genes – *BRCA1*/*BRCA2*/*PALB2*, *PRSS1*/*SPINK1,* and *CKDN2A* (13, 14). Families with germline *BRCA1, BRCA2* (15), and *PALB2* (16) mutations fall into the *breast and ovarian cancer syndrome* category (17, 18) and have been shown to be 3.5- to 10-fold more susceptible to pancreatic cancer. Mutations in the *PRSS1* or *SPINK1* (19, 20) genes results in increased trypsin activity within

the pancreas and make up the second category of families with chronic pancreatitis. This group is the most susceptible to pancreatic cancer having a 53-fold higher chance of contracting the disease. A third subgroups of individuals, *familial atypical multiple mole melanoma*, harbor a *CKDN2A* germline mutation, and have a 13- to 22-fold higher chance of pancreatic cancer (21). Other subclasses have been formed including the *Peutz-Jeghers syndrome* associated with *STK11* and *LKB1* gene mutations (22), *hereditary nonpolyposis colorectal cancer syndrome* with mismatched repair genes (23) and *familial adenomatous polyposis* and the *APC* gene (24). Still, these subgroups and their associated mutations only account for 10% of the cases of familial pancreatic cancer (14) and the major gene defect has yet to be found (25).

1.1.3. Current Methods of Detecting and Diagnosing Pancreatic Cancer

One of the main reasons pancreatic cancer has such dismal survival statistics is because patients are rarely diagnosed in an early stage of the disease. Patients rarely have symptoms until after the tumor has metastasized and is no longer resectable. The location of a tumor in the pancreas also contributes to the presenting symptoms. The majority of tumors develop in the head of the pancreas and cause obstructive cholestasis or, less commonly, duodenal obstruction. Abdominal discomfort, nausea and gastrointestinal bleeding are the most common symptoms in these cases. Tumor obstruction of the pancreatic duct can also result in pancreatitis. Acute pancreatitis and newly diagnosed diabetes are two warning signs of pancreatic cancer. Other symptoms may include asthenia, anorexia, and weight loss (26).

Typically, contrast-enhanced, helical computed tomography (CT) is initially used to diagnose pancreatic cancer (27) and determine resectability with 80-90% accuracy (28). Endoscopic ultrasonography, endoscopic retrograde cholangiopancreatography (ERCP), and biopsies are possible follow-up procedures to help identify tumors not visible by CT. Although these procedures improve diagnostic accuracy, they are invasive and can cause adverse side affects such as injury to the pancreas (29). Recently, scientific research has focused on less invasive alternatives to diagnose the disease. Several serum biomarkers have been proposed as such an alternative (30) but only CA19-9 has shown any clinical success (31). For patients that have tumors secreting CA19-9, changes in the marker expression level can be indicative of therapeutic efficacy or recursion (32). However, the marker overall has poor sensitivity and specificity as a means of early tumor detection (33).

1.1.4. Treatment Strategies for Early Pancreatic Cancer

Therapeutic strategies for patients with pancreatic cancer are limited and will depend on the stage and grade of the tumor. Approximately 20% of recently diagnosed tumors are localized and candidate for surgery (34). Tumor resection is the treatment of choice in these cases because it offers the best patient survival rates and is the only potentially curative option (35). The most common type of surgery is known as a Whipple procedure, or pancreaticoduodenectomy, which removes the head of the pancreas, a portion of the bile duct, the gallbladder and the duodenum. Alternatively, depending on where the tumor is located, a distal pancreatectomy or total pancreatectomy might be performed.

Even with surgery, patient survival rates are poor with the average life expectancy still under two years, but this can be improved with adjuvant chemotherapy after surgery (36). Recently, studies have shown that using adjuvant chemotherapy before surgery can be just as effective as postoperative treatment due to improved positive margin rates. This is a particularly good strategy for patients who are borderline for surgery (37).

1.1.5. Treatment Strategies for Non-Resectable Pancreatic Cancer

For the majority of patients, diagnosis comes too late for resection; the tumor has already metastasized and alternative therapeutic strategies are needed. In these cases, the standard treatment is systemic chemotherapy, or a combination of chemoradiation therapy and chemotherapy. Historically, 5-fluorouracil (5-FU) was used to treat pancreatic cancer patients, but in 1997, a seminal report by Burris, et al. showed gemcitabine to be more effective in relieving patient symptoms and extending patient survival than 5-FU. Studies found 23.8% of patients treated with gemcitabine to experience clinical benefit compared to only 4.8% of those who received 5-FU. Further, the median survival rate was extended from 4.41 months to 5.65 when comparing 5-FU to gemcitabine (38). Still, these statistics leave much room for improvement.

Unfortunately, little progress has been made clinically since the gemcitabine discovery almost two decades ago. Numerous drug combinations utilizing a number of different mechanisms of action have been tried and until recently almost all have been unsuccessful. Combination therapy using

gemcitabine with docetaxel (39), cisplatin (40), oxaliplatin (41), 5-fluorouracil (42), and irinotecan (43) have gone to clinical trials, but none have shown benefit by phase III. Recently, the combination regime FOLFIRINOX, consisting of oxaliplatin, irinotecan, fluorouracil, and leucovorin, has been shown be more effective than gemcitabine in stage III clinical trials. A study by Singhal, et al. showed in patients with metastatic pancreatic cancer, FOLFIRINOX had a median survival of 10.8 months compared to gemcitabine's 7.4 months. This led the researchers to conclude that FOLFIRINOX is a good treatment option for patients, but warns that the survival benefits come with increased toxicity (44). For those in relatively good health and who can withstand the treatment, FOLFIRINOX has become the standard of care.

Alternatively, a combination of gemcitabine and Nab-paclitaxel has shown great promise clinically. Nab-paclitaxel is albumin-bound paclitaxel molecule designed to overcome anaphylactic reactions associated with the Cremophor EL formulation of paclitaxel (45). In a recent study published in the New England Journal of Medicine, rsearchers found adding nab-paclitaxel as an adjuvant therapy to gemcitabine increased median survival in patients from 6.7 months to 8.5 months. In addition to an improved overall survival, patients had prolonged progression-free survival and better response rate than with monotherapy, but again, additional toxicity and decreased quality of life were noticed (46). Nonetheless, the FDA approved the combinatorial therapy in 2013 for patients with metastatic pancreatic cancer as one of the few available treatment options.

The only other drug combination to show efficacy in phase III clinical trials was gemcitabine plus erlotinib. Different from the aforementioned drugs, erlotinib is a reversible tyrosine kinase inhibitor targeting the epidermal growth factor receptor (EGFR). EGFR inhibitors have been effective in several other cancers with high EGFR expression, including colorectal cancer and non-small-cell lung carcinomas (NSCLC) (47). In pancreatic cancer, gemcitabine–erlotinib therapies have resulted in increased instances of pneumonitis, sepsis, and other adverse effects (48) but comparative studies show modest, yet significant, patient survival compared to gemcitabine alone (6.2 vs. 5.9 months) (49). The mechanism attributed to this benefit is thought to be a limiting of the MAP kinase pathways, which promote growth and survival (50). The FDA approved the combinatorial therapy in 2005, but the use of this therapy is somewhat controversial and many do not feel the benefits outweigh the risks (45).

1.2. The Development and Molecular Biology of Pancreatic Cancer

1.2.1. Pancreatic Cancer Progression

There are several types of pancreatic cancer including acinar cell carcinoma, colloid carcinoma, and pancreatoblasoma, but the most common subtype of the disease, accounting for approximately 85% of pancreatic cancer cases, is pancreatic ductal adenocarcinoma (PDAC) (51). The conversion of normal pancreas to PDAC is a well-characterized progression with several progression pathways having been identified. The most common pathway is through pancreatic intraepithelial neoplasms (PanINs). Other pathways include

mucinous cystic neoplasms (MCNs), acinar-ductal metaplasias (ADMs) and intraductal papillary mucinous neoplasms (IPMNs), and are less commonly studied (52). PanINs can be further broken down into three grades with distinct histological characteristics: PanIN-1, PanIN-2 and PanIN-3. PanIN-1 lesions (sometimes broken down even further to PanIN-1a and PanIN-1b) are low-grade lesions and often considered benign. In fact, it has been estimated that 50% of individuals over 50 years of age have these precursor lesions without any adverse effects (53). However, high-grade lesions (PanIN-3) will ultimately transform into PDAC, and are of clinical concern.

1.2.2. The Molecular Genetics of PDAC

The major genetic mutations associated with PDAC and their relative onsets in cancer development are fairly well known. One of the most widespread of these mutations is *KRAS*. The mutation has been reported in over 90% of PDAC (54). In precursor lesions, *KRAS* mutations occur at the rate of 36%, 44% and 87% for PanIN-1a, PanIN-1b and PanIN-2/3 respectively (55). The most common mutation type is a point mutation at the 12th amino acid, replacing a glycine with an aspartic acid (*KRAS*^{G12D}) accounting for over a third of PDAC *KRAS* mutations (56). The RAS protein is a key regulator of growth and proliferation, and activating mutations cause increased downstream signaling in cells. However, evidence suggests that *KRAS* mutations alone are not sufficient to cause PDAC due to the low frequency of spontaneous progression of early stage PanINs to PDAC (57). The effects of this mutation and KRAS's downstream signaling will be discussed further in section 1.3.

Another key mutation that is common in PDAC is at the 9p21 locus (*CDKN2A* gene) causing the loss of two overlapping tumor suppressors, *INK4A* and *ARF*. The frequency of this occurrence is between 80%-95% (58, 59). These two genes code for $p16^{INK4A}$ and $p14^{ARF}$ respectively. $p16^{INK4A}$ inhibits entry into the S phase of the cell cycle by inhibiting cyclin dependent kinases 4 and 6 phosphorylation of retinoblastoma protein (Rb) (51). Without $p16^{INK4A}$, Rb phosphorylation levels become abnormally high, inactivating Rb's inhibitory effects on cell cycle progression. $p14^{ARF}$ ($p19^{ARF}$ in mice) is an alternate reading frame product of *CDKN2A* and promotes the stabilization of the tumor suppressor p53 via Mdm2 inactivation (60); MDM2 is a p53 E3 ubiquitin ligase (61). The loss of *INK4A* and *ARF* is typically associated with moderately advanced precursor lesions.

The loss of another tumor suppressor protein, p53, occurs in approximately 50-75% of pancreatic cancers (62). Mutations in the *TP53* gene, which encodes for p53, often happen in the later stage of PanIN progression when the tissue is already dysplastic (63). The loss of this third tumor suppressor almost ensures eventual PDAC and results in increased tumor resistance to therapeutics.

Other common mutations in PDAC include *SMAD4* (~50% of patients) (64) and *EGFR*. SMAD4 mutations cause aberrant signaling in the TGF-β pathway that regulates proliferation, differentiation, and apoptosis. The TGF-β pathway is complex, and reports have shown it to exhibit both growth promoting (65) and growth inhibiting (66) characteristics in tumors depending on context. Because of

this duality, it is still uncertain how significant *SMAD4* mutations are in PDAC. The EGFR, epidermal growth factor receptor and its ligands, EGF and TGF-α, are often found overexpressed in pancreatic cancers. Although the receptor is not typically mutated, targeting EGFR in tumors overexpressing the protein has shown to be an effective strategy in fighting the disease.

1.3. The KRAS Protein

1.3.1. An Overview of the RAS Superfamily Proteins

The RAS superfamily proteins (Rat sarcoma proteins) are a set of GTPases that have a central role in cellular signal transduction and affect virtually every aspect of cell function. Over 35 different proteins have been reported as member of this family with HRAS, NRAS, and KRAS being the most prominent three in cancer (67).

1.3.2. RAS's Mechanism of Action

All RAS members cycle between an inactive, guanosine diphosphate-bound (GDP-bound) state and an active guanosine triphosphate-bound (GTP-bound) state. In the GTP-bound form (RAS-GTP), the protein can bind and activate a number of effector proteins. Two proteins facilitate the transition of RAS between the GDP-bound and GTP-bound states; guanine nucleotide exchange factors (GEFs) activate RAS and GTPase-activating proteins (GAPs) deactivate RAS. GEFs work by promoting the dissociation of GDP from RAS and once separated, RAS is free to bind GTP, which is 10-fold more abundant than

GDP in cells (68). Well known examples of GEFs include son of sevenless (SOS) and CDC 25. GAPs function by stabilizing and augmenting the catalytic region of RAS, facilitating RAS's hydrolysis of GTP to GDP, and ultimately inactivating RAS. This process and how genetic mutations alter its signaling are depicted in Figure 1.1A RAS protein can switch states without the help of one of these two proteins but much more slowly, taking approximately 100,000 times longer (69). The balance between the active and inactive states is critical for proper cellular signaling and function.

1.3.3. RAS Mutations in Cancer

The oncogenic branch of the RAS family consists of three members, HRAS, NRAS and KRAS. Of all the activating mutations seen in cancer, none is more prevalent than KRAS. KRAS is estimated to be mutated in 40% of colon cancer (70), 15%-20% of lung cancer (71) and 90%-95% of pancreatic cancer (72). Most alterations are point mutations in the 12^{th}, 13^{th}, or 61^{st} codon that prevent the binding of GAPs (Fig. 1.2) (73). This prevents the enzymatic catalysis of GTP to GDP, essentially locking RAS in the GTP bound state. With only RAS's intrinsic GTPase activity to deactivate the protein it is considered constitutively active (74), signaling to downstream pathways. Other reported genetic alterations in cancer that act through RAS include a GEF enhancing mutation (75), increased basal activity of RAS (76), and indirect hyperactivity from overexpressed surface receptors upstream of RAS such as ERBB2 in breast cancer (77).

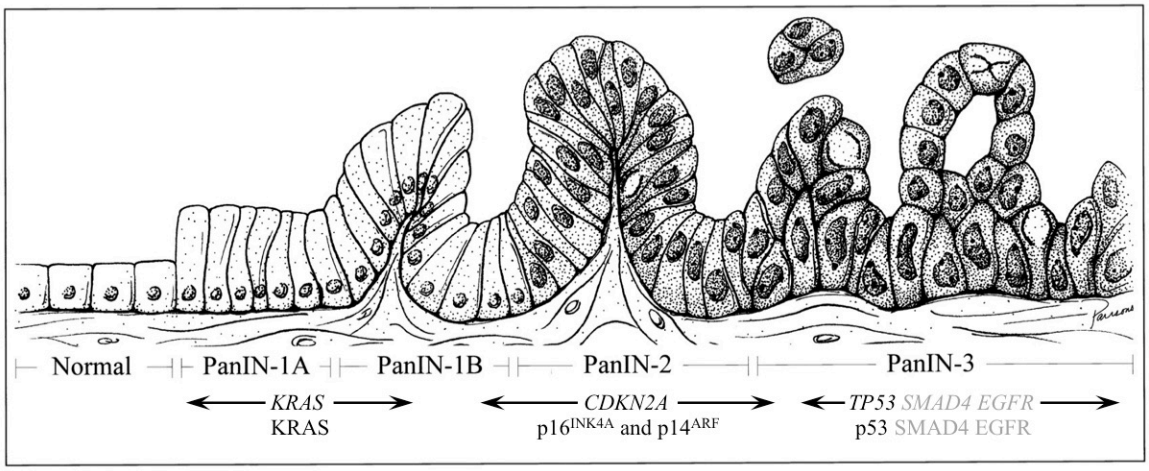

Figure 1.1 Model of pancreatic cancer progression from normal pancreas through PanINs to PDAC. Below the depiction of the progression are the PanIN lesion stages and associated genetic mutations. Figure adapted from Wilentz, R. E. et al. Loss of expression of Dpc4 in pancreatic intraepithelial neoplasia: evidence that DPC4 inactivation occurs late in neoplastic progression. *Cancer Res* **60**, 2002-2006 (78)

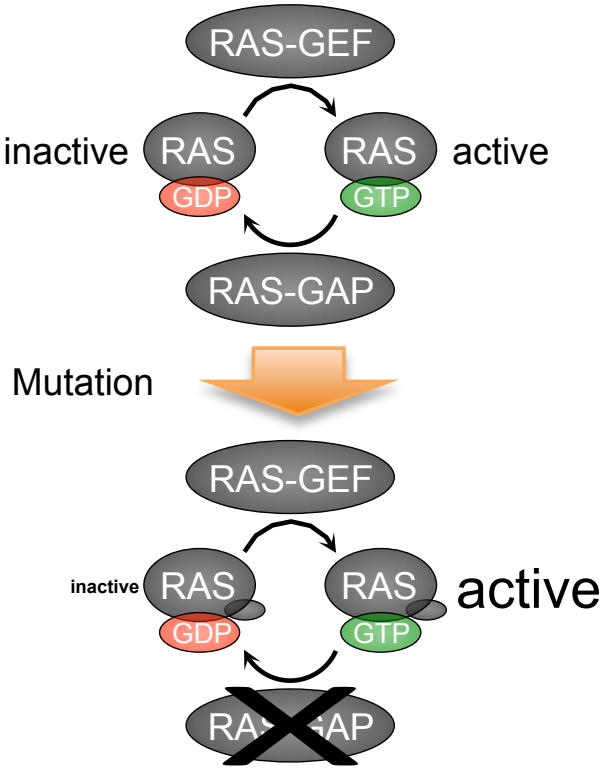

Figure 1.2 Ras activation and deactivation in normal and mutant form. Wild type RAS cycles between a GDP- and GTP-bound states with the help of RAS-GEFs and RAS-GAPs, keeping a necessary balance between the two states. In cancer, a mutation prevents the GAPs from binding and deactivating RAS, locking it in the active, GTP-bound state.

1.3.3.1. Downstream Pathways of Oncogenic RAS

Overactive RAS signals through a large number of downstream effectors to trigger growth, proliferation, and survival in cancer. Several notable pathways are summarized in Figure 1.3, of these three play the largest role in cancer: the Raf-mitogen-activated kinase (MAP kinase or MAPK), phosphoinositide-3-kinase (PI3K), and the Ral guanine nucleotide exchange factor (RalGEF) pathway (52). RalGEFs are thought to be activated by RAS and are exchange factors for RAL GTPases, specifically RalA and RalB in pancreatic cancers. These two proteins have been found to mediate tumor growth and metastasis in PDAC, respectively (79). Further, limiting RAS-Ral signaling by inhibiting cyclin-dependent kinase 5 (CDK 5) was shown to block pancreatic cancer formation and progression (80).

1.3.3.1.1. The PI3K-AKT Pathway in Cancer

The PI3K-AKT pathway is important in cell cycle regulation, proliferation, cell size, and survival. In an over-simplified procession, RAS activates PI3K, which is a lipid kinase that produces PIP3. PIP3 is a docking site for PDK1, it facilitates PDK1's phosphorylation of AKT. AKT can activate a number of effector molecules to control cellular actions including mTORC1 to promote growth. Mutations in this pathway are seen throughout cancer. For example, PI3K is a heterodimer that is comprised of 2 subunits: a p110 catalytic subunit and a p85 regulatory subunit (81). Mutations in the p110 protein, specifically p110α coded for by the PIK3CA gene, cause the kinase to become more active, increasing pro-tumor signaling. These mutations are seen in more active, increasing pro-

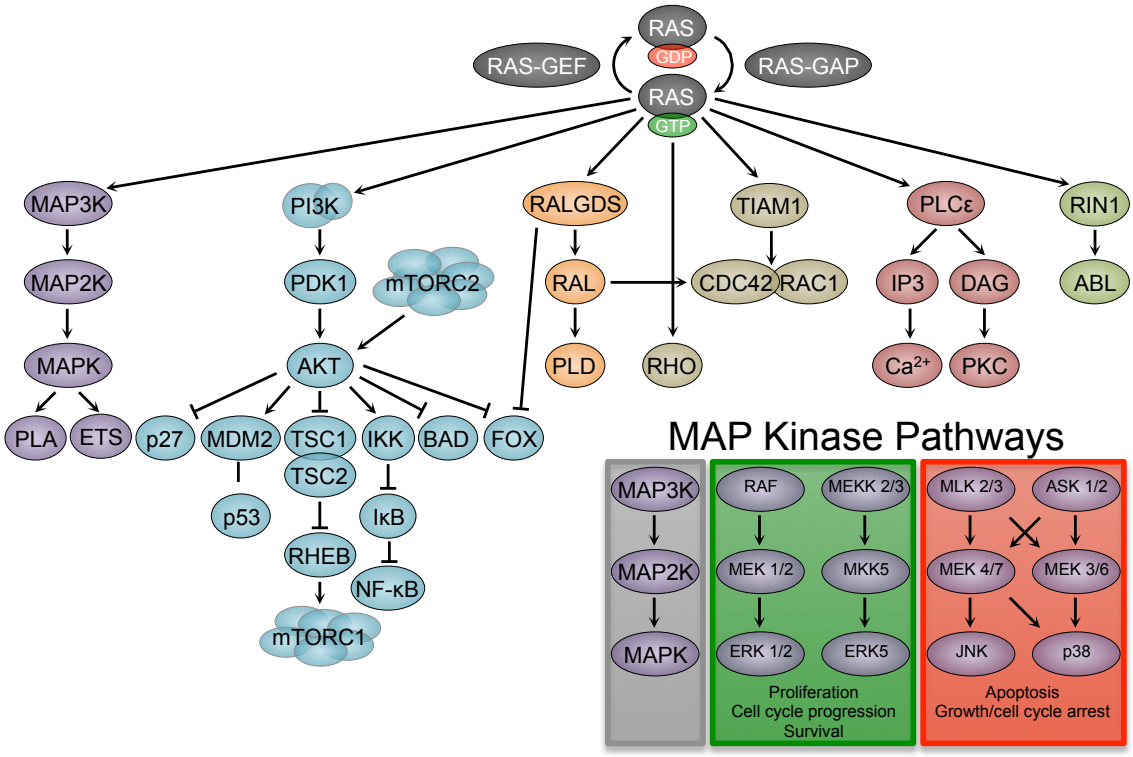

Figure 1.3 Ras signaling. Ras signals through a number of effector molecules to activate pathways that lead to growth, proliferation, cell cycle progression, and apoptosis. The major pathways depicted include the MAP kinase pathways, the PI3K/AKT pathway, and Ral-GEF. Figure was adapted from Berndt et al. (82).

tumor signaling. These mutations are seen in many cancers including colon, breast, liver and lung (83). Other activating mutations in this pathway, although less common, include the PI3K regulatory subunit 1 and AKT family members (84).

Hyperactivity of the PI3K-AKT pathway can also be achieved by the loss of certain tumor suppressors. This is the case when phosphatase and tensin homolog (PTEN) becomes mutated. PTEN is a PIP3 phosphatase that ultimately reduces AKT phosphorylation levels. PTEN mutations (or reduced expression) are seen in lung, breast and prostate cancers; up to 70% of prostate tumors have lost at least one PTEN allele (85). Interestingly, PI3K pathway mutations are largely absent in PDAC (86), but the pathway still plays an important role in pancreatic cancers. Low expression levels of PTEN have been reported in PDAC and the activation of the AKT pathway is sometimes necessary for tumor maintenance after the quiescence of oncogenic RAS (87, 88).

1.3.3.1.2 Mitogen-Activated Protein Kinase Cascades in Cancer

The MAPK cascades are some of the most canonical pathways in cell signaling. They are responsible for a number of cellular functions including proliferation, mitosis, cell survival and apoptosis (89). A typical signal transduction pathway starts with RAS, which can activate a MAP3K. In turn, the MAP3K activates a MAP2K, and the MAP2K activates a MAPK. Several different cascades are known and a simplified summary of these pathways with their general effects is shown in Figure 1.2. The RAS > RAF > MEK 1/2 > ERK 1/2

pathway specifically is well associated with many forms of cancer and is a popular area of research. In many cancers where RAS is not mutated, mutations in BRAF can be found to hyperactivate this pathway; such is the case in skin cancer where two thirds of malignant melanomas have BRAF mutations (90). Inhibition of this pathway in PDAC cells results in decreased proliferation and cell cycle arrest, highlighting the pathway's important role in pancreatic cancer (91, 92). Less studied, the MEKK 2/3 > MEK 5 > ERK 5 cascade has been shown to promote cell cycle progression as well (93, 94). MEK 5 overexpression has been seen in a number of different cancers including colon, breast, and mesothelioma (95-97).

In contrast to the previous two pathways, some MAPK cascades can have the opposite effects in cells. The MLK 2/3 > MEK 3/6 > p38 and the MLK 2/3 > MEK 4/7 > JNK pathways are more associated with growth arrest and apoptosis (98, 99). Because either pathway can result in tumor suppression, decreased activity of these pathways is often seen in cancer (100, 101). It is interesting that RAS has the ability to stimulate all four of these pathways and yet the pathways have inverse effects.

Several feedback loops, both positive and negative, also contribute to the dynamic behavior of MAP kinase signaling. Studies have shown ERK-SOS signaling to be one example of pathway activity regulation. ERK can inhibit the RAS-GEF protein SOS to decrease RAS signaling in a negative feedback loop (102). Conversely, ERK can also signal through a positive feedback loop by inhibiting the RAF kinase inhibitor protein (RKIP) and increasing RAF signaling

(103). These contradictory signals can result in an oscillatory activation ERK and spatiotemporal factors become important for ultimate cellular response (104). Other regulatory signals can occur through crosstalk with other pathways. MEK-ERK signaling and PI3K-AKT signaling are known to inhibit one another. MEK can stimulate PTEN's inhibition of PI3K and AKT has been shown to inhibit RAF (105, 106). Crosstalk also occurs between different MAP kinase pathways. For example, the JNK pathway has been reported to inhibit MEK-ERK signaling by blocking ERK's phosphorylation by MEK (107). The reality of cellular signaling is immensely more complex than the simplified representations that the pathways are usually depicted as. Additional affecting proteins, cross talk, spatiotemporal factors and other aspects not considered all contribute to the end cellular response. How cells ultimately integrate these factors can be very context dependent and difficult to predict.

1.3.3.2. Limiting Aberrant RAS Signaling

For over three decades, researchers and pharmaceutical companies have tried to devise a method to inhibit RAS signaling because of its pivotal role in cancer. Unfortunately, with billions of dollars spent and no clinically approved inhibitor, these attempts have largely been unsuccessful, earning RAS the title of "undruggable". Unlike with aberrant kinases, where inhibitors will often bind and/or block the ATP binding pocket (108), RAS mutations decrease the rate of GTP hydrolysis and prevent GAPs from binding. So far, no small molecule has been successful at restoring either of these functions. Attempts to use a competitive inhibitor for the enzymatic site in RAS have only served to block

GAPs from binding completely (109). Because RAS's localization to the plasma membrane is crucial for signaling (110), methods of inhibiting the farnesylation of RAS, a post-translational modification needed for RAS's trafficking, have been attempted. Unfortunately, inhibitors blocking this modification failed in clinical trials because a compensatory geranylgeranyl group modification still allowed KRAS to associate with the plasma membrane (111). Recently, inhibitors that prevent RAS's localizing chaperone PDEδ have shown some promise pre-clinically by disrupting PDEδ-RAS bonding and displacing RAS to endomembranes (112). It is still uncertain how these inhibitors will do clinically and the adverse side effects of disrupting all PDEδ-protein binding could be significant. Other current attempts to modulate RAS signaling include preventing RAS-GEF interactions (113), locking RAS in the GDP-bound state (114), and blocking RAS-effector interactions (115) – each strategy with its own challenges. While one of these attempts may ultimately prove successful, no direct method of inhibiting RAS has yet to pass clinical trials (82).

Even if RAS can be inhibited, questions remain concerning how effective an inhibitor would be. Studies by Ying et al. used mouse models with an oncogenic KRAS that can be switched on and off and found RAS necessary for PDAC progression and maintenance (116). Similar results were found by Collins et al. (117). However, other studies in human PDAC and NSCLC cell lines with mutant KRAS found the diseases to be very heterogeneous in response to KRAS knockdown; some cell lines were KRAS dependent whereas others were KRAS independent. The researchers suggested that for some tumors, KRAS might be

important in disease initiation, but once established, the tumors may no longer need KRAS signaling to maintain tumorigenicity (118). Most likely, a RAS inhibitor would be a very potent tool in fighting cancer, but may not be sufficient to control PDAC alone. Ultimately, mutant RAS does not causes cancer, rather its downstream signals for growth, survival and proliferation do. Therefore, as an alternative to developing a RAS inhibitor, efforts have focused on targeting the downstream pathways, specifically the PI3K/AKT and MAPK pathways, with some, albeit limited clinical success.

1.3.3.2.1. PI3K/AKT Inhibitors

As one of the major downstream effectors of RAS, the PI3K/AKT pathway has been of interest as a therapeutic target for over 25 years. In 1993, the first PI3K inhibitor (wortmannin) was discovered (119). Unfortunately, wortmannin had too poor specificity for clinical use. As an alternative, mTOR inhibitors began growing in popularity with rapamycin being the first mTOR inhibitor to have clinical success. Although originally approved in 1999 for transplant rejection, a translation into cancer seemed apparent and derivatives of the molecule, such as temsirolimus, had initial success treating renal cell carcinomas. Temsirolimus gained FDA approval in 2007, becoming the first inhibitor to do so of its type (120). Unfortunately, the rapamycin-derived inhibitors were easy to circumvent, and cancers quickly developed a resistance to them (121). Despite numerous PI3K and AKT inhibitors moving to clinical trials since [a nice summary was compiled by Dienstmann et al. (122)], none have yet to gain FDA approval for any cancer type. Much hope was riding on perifosine, an AKT inhibitor that

progressed to Phase III trials (84), but AstraZeneca ultimately ceased clinical trials due to safety concerns (AstraZeneca news release, March 11, 2013). Recently, Novartis's BKM120 (buparlisib), a pan PI3K inhibitor, has begun phase III testing in breast cancer and the trial is expected to complete in 2017 (*ClinicalTrials.gov*).

Much research is still being conducted in this field with the hope of finding a safe and effective inhibitor of the PI3K/AKT pathway. A major focus has been on further understanding the pathway's role in cancer and the activating mutations that cause aberrant signaling. Development of better therapeutics could follow, particularly if drugs can be developed to selectively target mutated proteins over wild type. More likely, a deeper understanding of this pathway will at least expand our knowledge of how tumor heterogeneity affects inhibitor effectiveness.

1.3.3.2.2. RAF/MEK Inhibitors

The MAP kinase family is the other major signaling target downstream of RAS, particularly the RAF > MEK > ERK pathway. RAF inhibitors are one possible avenue for limiting MAPK pathway signaling. Clinical trials of early RAF inhibitors such as sorafenib were disappointing and showed little to no benefit (123). However, a breakthrough occurred with the development of vemurafenib and dabrafenib, two BRAF inhibitors that only target the mutant form of the enzyme. These inhibitors have shown great promise in cancers such as melanoma, where BRAF mutations occur in two thirds of patient tumors (124).

However acquired resistance to RAF mutations is common (125). Further, tumors that initially have mutant RAS show no silencing of ERK by RAF inhibitors (126). In pancreatic cancer, where RAS is mutated >90%, RAF monotherapies do not appear to be a good therapeutic strategy.

Targeting MEK has been another well-explored avenue of therapeutics. Unlike most small molecule kinase inhibitors, many MEK inhibitors are ATP non-competitive. Instead of competing for the ATP-binding pocket of MEK, they bind to a unique allosteric pocket adjacent to the ATP-binding site. This feature results in MEK inhibitors' high selectivity and specificity (127). Co-crystallization of MEK with an inhibitor and MgATP first identified this allosteric pocket, separated from the MgATP binding pocket by the conserved side chains of Lys97 and Met143 (128). Subsequent studies showed that the diaryl amine structure of the inhibitors (A and B rings) stabilized the small molecules in the allosteric site, forming a hydrogen bond and non-covalent interactions to cause a conformational change in MEK that interferes with the catalytic site. This mechanism of action is believed to be the same for all of the MEK 1/2, ATP non-competitive inhibitors (128, 129).

The first MEK inhibitor was PD098059, originally disclosed in 1995 (130). It is ATP non-competitive with a reported IC_{50} ~10 μM (131) and the nearest off target effects are on MEK 5 at ~100 μM (132). Unfortunately, this inhibitor did not have sufficient solubility to go to clinical trials, but laboratory use of the inhibitor shed enormous light on the MEK-ERK signaling pathway and it effects in cancer (133). Subsequently, PD184352 (CI-1040; MEK 1: IC_{50}=300 nM) was screened to have better bioavailability and has been used *in vitro* (134) and in clinical trials

(135). However after phase II studies, testing was terminated due to lack of efficacy in favor of more potent inhibitors (133).

As of 2013, there has been a total of 13 MEK inhibitors to enter clinical trials; all inhibit MEK 1, MEK 2 or both. Many of these are in phase I or phase II clinical trials, but two show great promise as therapeutics: AZD6244 and GSK1120212. AZD6244 (Arry-142886 or selumetinib) is a second-generation inhibitor based on the PD184352 structure and, therefore, also a non-competitive inhibitor with high potency (MEK 1: IC_{50}=14.1 nM) and no off target effects (136). It is currently in phase III trials for thyroid cancer, NSCLC, and melanoma. It was tested in phase II pancreatic cancer and although a few patients responded well, no significant difference was seen over a secondary chemotherapeutic (137). GSK1120212 (trametinib) has progressed even further, being the first (and only) MEK inhibitor approved by the FDA (used in advanced melanomas). It too is ATP non-competitive and bind to the same allosteric domain as the other small molecules detailed above (MEK 1: IC_{50}=0.92 nM; MEK 2: IC_{50}=1.8 nM; no off target effects) (138). Clinical trails for using GSK1120212 in pancreatic cancer also have made it to phase II but no therapeutic benefit was seen vs. chemotherapy alone (139). It is of note that in all trials, no discrimination towards mutational status was performed, and researchers often note that some form of screening, such as for RAS and BRAF mutations, could benefit the outcome of the studies (140-143).

1.3.3.2.3. Acquired Resistance to Small Molecule Inhibitors

A common problem with small molecule monotherapies is the development of acquired resistance. This can happen through several different mechanisms, one of which is alterations in the drug target, typically through the development of a mutation. The best example of this is with EGRF inhibitor therapies, such as gefitinib and erlotinib, where secondary mutations to the receptor account for over half of the reports of acquired resistance (144). The development of parallel signaling pathways, or “bypass track signaling” is another form of resistance seen with small molecule inhibitors. This is one of the main known mechanisms of MEK inhibitor resistance where increased signaling in the PI3K-AKT pathway, possibly by a mutation, can confer resistance to the MEK therapy (145). Another example is RAF inhibitor resistance by COT activating MEK-ERK independent of RAF signaling. Bypass tracks can occur in the same cells as a second driver or result in the emergence of distinct clones resistant to the therapy (146). Downstream pathway alterations are yet another form of acquired resistance. EGFR therapies have limited effect in cells that also harbor or gain KRAS or BRAF mutations because any upstream signaling inhibition becomes reactivated by these protein mutations. Other reported mechanisms of acquired resistance include increased gene copy number for the drug target (147), phenotypic changes in the tumor cells (148), and pharmacological mechanisms of resistance. Examples of the latter include increased metabolism of the drug, and decreased absorption of the drug in the target tissue (149, 150).

1.3.3.2.4. Combination Therapies

Often, small molecule inhibitors alone are not sufficient to cause a positive change in patient outcome even before an acquired resistance forms. Because monotherapies pinpoint one pathway, when usually several are aberrant in cancer, combination therapies tend to be much more successful. For example, when AZD6244 was used as a monotherapy in NSCLC, phase II trials found no benefit to patients (141), but it was efficacious when used in conjunction with docetaxel. Currently, this drug combination is recruiting for phase III trials in NSCLC (151). In pancreatic cancer, current phase II trials are being conducted to evaluate the effects of AZD6244 plus the AKT inhibitor MK2206 and AZD6244 plus the EGFR inhibitor erlotinib. The studies have noted that higher toxicity was seen with the drug combination than with either drug alone. This is a common observance in combinatorial therapies and one of the largest barriers to clinical success. Shimizu et al. performed an in depth analysis of RAF/MEK and PI3K/AKT monotherapies vs. combination therapies in clinical trials and found that dual inhibition has the ability to exhibit favorable efficacy but almost always at the expense of higher toxicity. They go on to recommend that proper patient profiling and patient pairing with the correct therapy is needed (142). It is clear that combinatorial therapy has great promise, but only when used properly.

1.4. Precision Medicine in PDAC

The concept of precision medicine, or what many have previously refereed to as personalized medicine, has been around for well over a hundred years. The

well-known physician, and one of the four founding professors of Johns Hopkins Hospital, Sir William Osler once stated, “as no two faces are the same, so no two bodies are alike, and no two individuals react alike and behave alike under the abnormal conditions we know as disease” (152). Indeed inter-tumor heterogeneity is one of the biggest challenges in oncology. Two patients can have tumors in the same tissue, with the same morphology, but respond completely different to a particular therapy. It takes a deeper understanding of each patient’s tumor to determine why the individuals responded differently and more importantly what therapeutic strategies can be used to address the differences. The need to do just that is why there is such interest in precision medicine.

Precision medicine is the use of genomic, transcriptomic, proteomic, and metabolomics data, combined with environmental factors and family history to understand the biology of a patient’s disease and to chose the best therapeutic strategy for that individual. Often the use of clinical decision support systems is needed to integrate this wealth of information (152). Over the past few decades advances in DNA sequencing techniques and microarrays have resulted in the bulk of information being genomic data and mRNA transcript expression levels. This has resulted in a number of “gene signatures” that can be used for prognoses and determining therapeutic efficacy with some success (153-157). However, Dietel and Sers note that many of these signatures have been found to be platform dependent and unstable due to tumor heterogeneity. They go on to recommend that a strategy using multiple, parallel analyses including gene

expression, methylation, and protein based analyses (overexpression and phosphorylation) is the method of choice moving forward (158).

Building upon these recommendations, we set out to find markers in PDAC that could predict sensitivity or resistance to MEK 1/2 inhibition. We took a multi-level approach beginning with transcriptome datasets and analyzing differentially expressed genes between sensitive and resistant groups of pancreatic cancer cell lines. From this, we identified *MERTK* and *MAPK8* to be overexpressed in resistant cell lines. First focusing on *MERTK*, a tyrosine kinase receptor, we explored its protein expression level and found it to be elevated in cell lines that had either innate or acquired resistance to MEK 1/2 inhibition. Protein knockdown studies revealed MERTK was important for tumor growth. Inhibition of MERTK however, did not sensitize resistant cell lines to MEK inhibitors.

Studies on JNK1, the protein coded for by *MAPK8*, show the protein levels to be elevated in cell lines with innate resistance to MEK 1/2 inhibition. However JNK1 levels did not correlate with acquired resistance. Knockdown of JNK1 significantly slowed cancer cell growth, and inhibiting the kinase sensitized resistant cell line to MEK 1/2 inhibition. These findings support the exploration of combination therapies in pancreatic cancers that are resistant to MEK inhibitor monotherapies.

To fully exploit predictive markers and new therapeutic targets in PDAC, techniques that can be used to identify targeting mechanisms are needed. Many

powerful screening techniques, such as small molecule screens and phage display, have been instrumental in the development of imaging and therapeutic agents. For medicine to continue to become more precise, improvement on the technical front must continue to evolve as well. Therefore, we set out to develop a new phage display library that would have a significantly larger diversity than the existing ones today. By incorporating a selenocysteine (Sec) in the middle of the screened peptide, we were able to tether small molecules to the phage to create a small molecule-peptide hybrid. By tethering an agonist of the adenosine A_1 receptor to Sec-phage, we were able to demonstrate that the modified phage bound the A_1 receptor with high affinity due to the tethered small molecule. Further, we showed that when bound to the receptor, the modified phage could activate signaling pathways downstream of the A_1 receptor. This showed that the small molecule still maintains its functionality when tethered to phage. The work on this new phage display system provides a proof-of-concept for a powerful new screening technique that can be used to help design future imaging agents and therapeutics with precise targeting abilities.

Chapter 2

Potential Markers of Sensitivity or Resistance to MEK Inhibition in PDAC

2.1 Introduction

Due to the prevailing resistance of pancreatic cancer to current therapeutics, it is clear that alternative strategies are needed. Several mutations are common among patients, the most prominent of these being KRAS, mutated in >90% of patients (159), which signals through a number of effector proteins including the MAPK pathways. Of the four cascades in mammalian cells, the RAF-MEK-ERK pathway is the most characterized and studied due to its prevalent role in human cancer (160). In addition to increased proliferation (161, 162), and apoptosis evasion (163-165), overactivity of this pathway contributes to chemotherapy resistance (166, 167) and growth factor-independence (168, 169), making it difficult to treat patients effectively. Small molecule inhibitors present an attractive therapeutic option in these cases because they can govern the oncogenic signaling of this pathway by pinpointing key proteins, such as MEK, within the cascade and limit its overall activity. Several such inhibitors include trametinib and selumetinib, which target the MAP kinase pathway via MEK 1/2 inhibition. These molecules are showing great clinical success in other cancers such as in NSCLC, where selumetinib (AZD6244) is in phase III clinical trials (151), and melanoma, where trametinib has been FDA approved for advanced cancers (170). As a result, thirteen different small molecule MEK inhibitors have entered clinical trials for various forms of cancer (143). A transition to pancreatic cancer is logical, but unfortunately clinical inhibition of MEK in this disease has found limited success. Studies of AZD6244 as a second-line therapeutic have shown only a slight improvement over chemotherapy, leading to a statistically

insignificant increase in median survival from 5.0 to 5.4 months (171). However, 5% of patients did have a partial response to the inhibitor and 32% showed disease stability, suggesting MEK inhibition might be effective on a subset of pancreatic tumors. Despite the disconnect between genetic mutations and therapeutic effectiveness, other means might be used to distinguish those who are likely to be responsive from those likely to be resistant, prior to administration of the inhibitor. Further, understanding why resistant patients are minimally responsive to the small molecule inhibitors could help guide a better therapeutic strategy for these individuals, including rational design of combination therapies.

Therefore, we sought to find markers capable of predicting patient sensitivity to MEK inhibition that could be used clinically to help doctors pair their patients with the proper therapeutic strategy. To do this, we began with a panel of pancreatic cancer cell lines and evaluated their response to the MEK 1/2 inhibitor AZD6244 *in vitro.* We validate these results with *in vivo* tumor models. We separated 19 cell lines into two groups, 13 sensitive and 6 resistant. We then used an RTqPCR surface transcriptome array to compare 196 surface receptor transcript expression values between the two groups identifying potential markers of both sensitivity and resistance. We further compared the two cell line groups using cDNA microarray data to identify additional transcripts of importance. Of the top hits from this study, only one surface receptor was also found in the RTqPCR analysis, *MERTK*. Deeper analysis of the microarray data found the JNK1 pathway was overexpressed, with *MAPK8*, the gene that codes for JNK1, to be most differentially expressed gene in the analysis. For these

reasons, *MERTK* and *MAPK8* were selected for further analysis as distinguishing markers.

2.2. Results

2.2.1. Establishing Sensitive and Resistant PDAC Cell Lines by GI_{50} Value

To find markers of sensitivity or resistance to AZD6244, we sought to compare a panel of 19 pancreatic cell lines for differentially expressed genes between sensitive and resistant groups. Eighteen pancreatic cancer lines plus one non-cancerous, transformed line (HPDE) were chosen for the panel. Figure 1 summarizes the key characteristics of these cell lines, including their mutational statuses for the four key genes in PDAC (172-176). When compared to clinical statistics, the *CDKN2A* gene is slightly less mutated in the panel, but otherwise the chosen cell lines effectively recapitulate the key genetic alterations seen in patients' tumors. We determined the cell line responses to AZD6244 inhibition by treating each line with 12 different concentrations of AZD6244, ranging from 20 μM down to 63.2 pM by half-log units. After 3 days of inhibition, growth curves could be constructed as shown in Figure 2.2. Plotting the curves together showed a range of different response rates (Fig. 2.3). Using the concentration of AZD6244 required to decrease cellular growth by 50% (GI_{50}), we were then able to compare the growth response of each cell line to the MEK inhibitor. Two cell lines, Yap-C and Panc-1, did not have a 50% decrease in growth at any tested concentration of AZD6244, and therefore their GI_{50} values are unknown but greater than 20 μM. For comparative purposes, we consider this concentration to

Cell Line	Cancer Type	Derivation	Mutations / Deletions and Suppressions				Notes
			KRAS	*TP53*	*CDKN2A*	*SMAD4*	
AsPC-1	PDAC Grade II	Ascites	G12D	Frameshift	Frameshift	Heterozygous	
BxPC-3	PDAC Grade II	Primary Tumor	Wildtype	Y220C	Mutation	Mutation	Do Not Express CFTR
Capan-1	PDAC Grade I	Liver Metastasis	G12V	A159V	Mutation	Mutation	Do Express CFTR
Capan-2	PDAC Grade I	Primary tumor	G12V	Wildtype	Insertion	Low Expression	
CFPAC-1	PDAC	Liver Metastasis	G12V	C242R	Methylation	Deletion	Patient Had Cystic Fibrosis
HPAF-II	PDAC Grade II	Ascites	G12D	P151S	Deletion	Wildtype	Derived from Static HPAF-I Cells
HPDE	Normal	Immortalized Ductal Epithelial	Wildtype	Wildtype but low	Wildtype	Wildtype	
Hs 766t	PDAC	Lymph Node Metastesis	Q61H	Wildtype	Wildtype	Deletion	
L3.6 pl	PDAC	Liver Metastasis from Nude Mice Implanted with COLO 357 Tumors	G12D	Wildtype	Methylation	Deletion	Highly Metastatic
MIA PaCa-2	PDAC Grade III	Primary Tumor	G12C	R248W	Mutation	Wildtype	
Panc 02.03	PDAC	Primary Tumor	G12D	Mutation	Frameshift	Mutation	
Panc 03.27	PDAC	Primary Tumor	G12V	Mutation	Wildtype	Wildtype	
Panc 08.13	PDAC	Primary Tumor	G12D	Wildtype	Wildtype	Frameshift	
Panc-1	PDAC Grade III	Primary Tumor	G12D	R273H	Methylation	Wildtype	
PaTu 8902	PDAC Grade II	Primary Tumor	G12V	C176S	Wildtype	Wildtype	
PL45	PDAC	Primary Tumor	G12D	Wildtype	Unknown	Unknown	Derived from Same Tumor as Panc 10.05
SU.86.86	PDAC	Liver Metastasis	G12D	G245S	Deletion	Wildtype	Produce CEA
SW1990	PDAC	Spleen Metastasis	G12D	Deletion	Wildtype	Wildtype	
Yap-C	PDAC	Ascites	G12V	H179R	Wildtype	Deletion	Dependent on Autocrine IL-1α

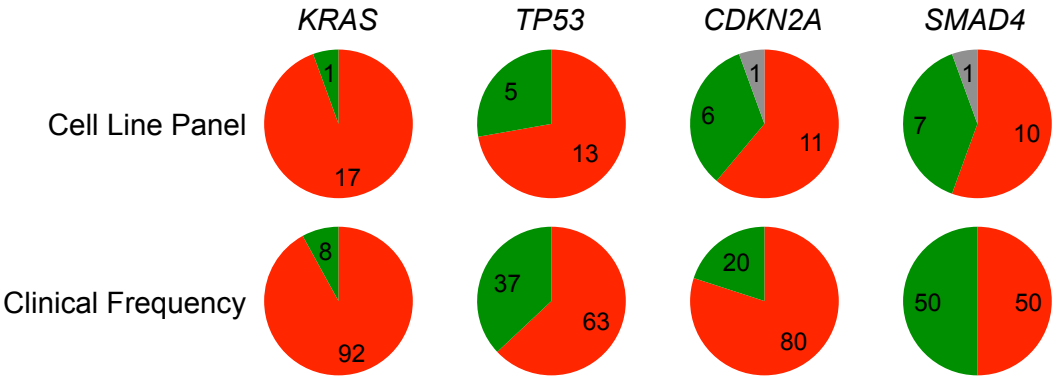

Figure 2.1 Cell Line Characterization. *Top)* Table of the 19 pancreatic cell lines used characterizing their tumors of origin, key genetic mutations, and other notable qualities. *Bottom)* Comparison the 4 key PDAC mutations in the cell line panel to clinical occurrence (172-176).

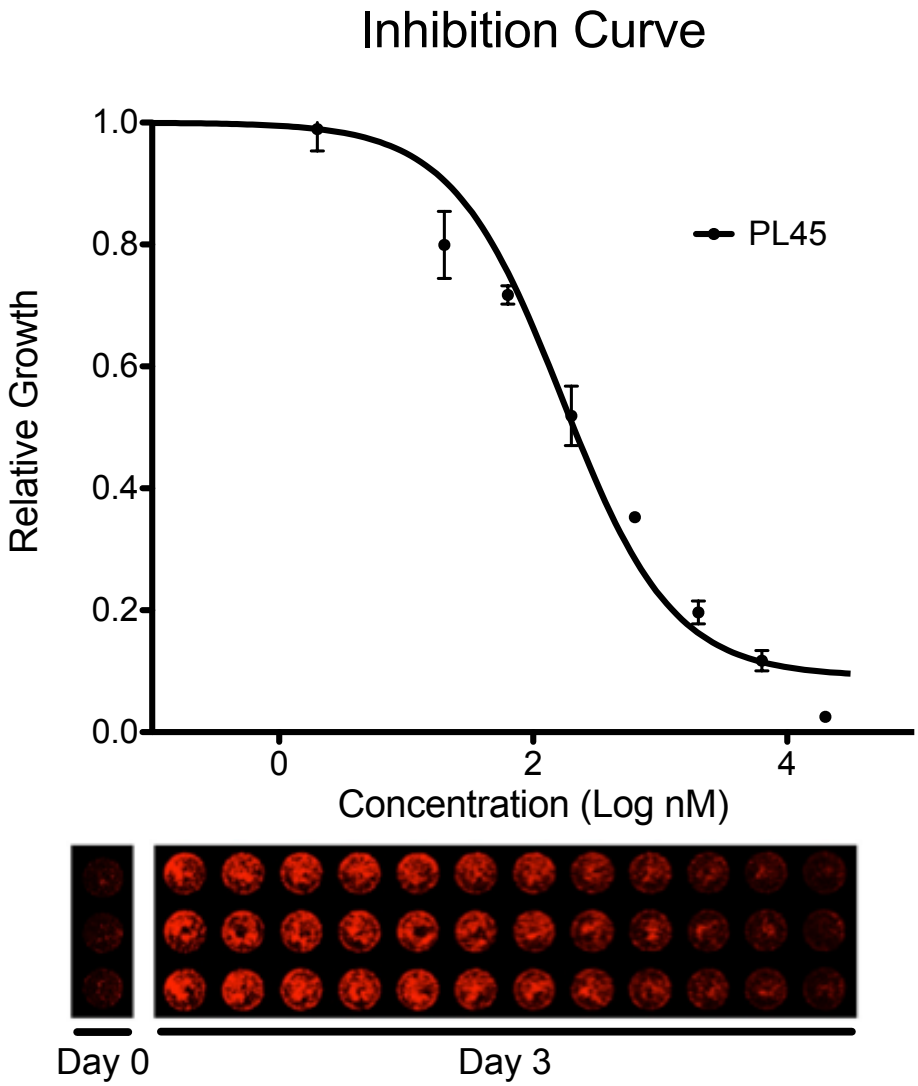

Figure 2.2 Establishing Cell Line Sensitivity to AZD6244. *Bottom* Cells were treated with varying concentrations of the inhibitor AZD6244 ranging from 63 nM to 20 μM. After 72 hrs they were stained with Syto® 60 and imaged. *Top* Fluorescent activity at each concentration was measured and used to construct an inhibition curve to determine the cell lines sensitivity.

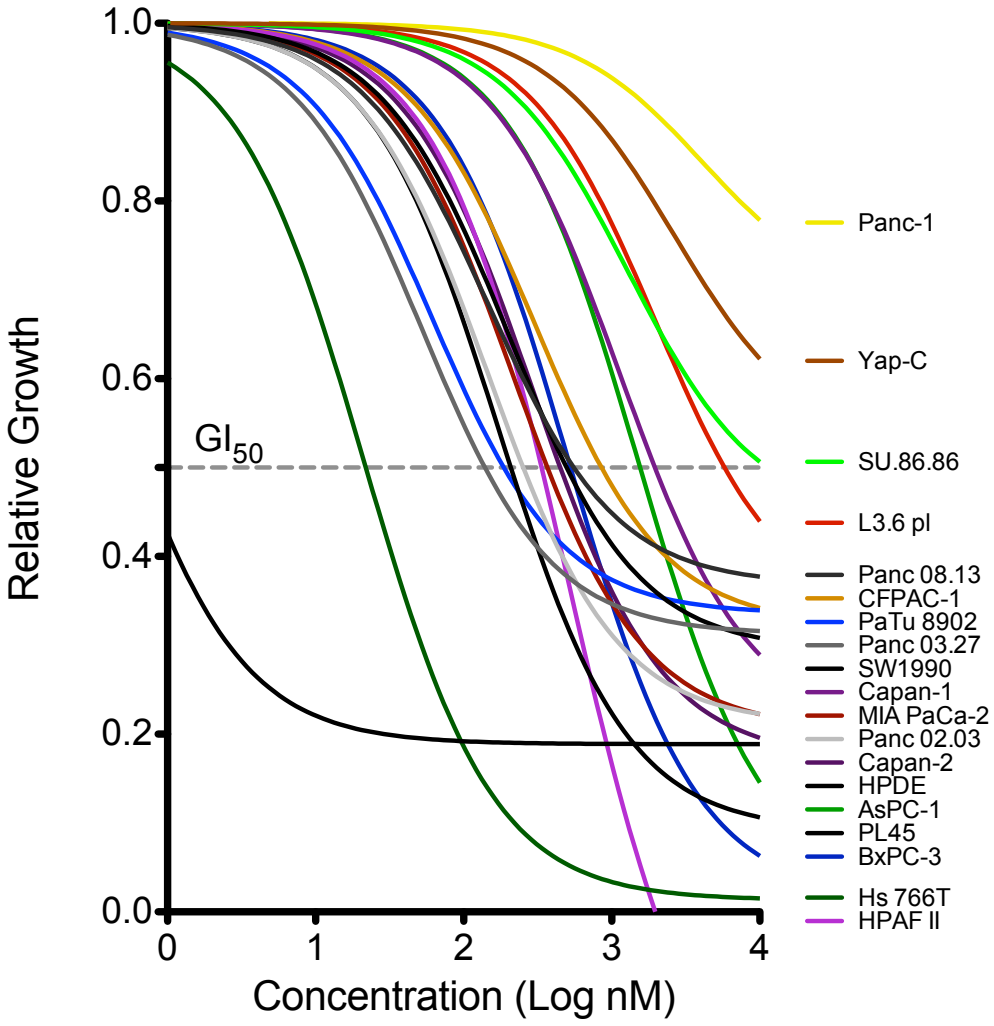

Figure 2.3 AZD6244 cell line inhibition curves. *A)* A complete set of inhibition curves for 19 PDAC cell lines in response to the MEK inhibitor AZD6244.

be their GI_{50} value. We used two methods to establish sensitive and resistant groups. First, a K-means analysis using the GI_{50} values was performed to cluster the cell lines into two groups (Fig. 2.4A). By using GI_{50}, and not IC_{50}, we framed "sensitivity" by the overall effect on cell growth, and not necessarily the inhibitors ability to limit MEK-ERK signaling. Therefore, a cell line's ERK signaling could be silence with a very low dose of AZD6244, but if no changes to the rate of ceullular growth occur, then it is considered a resistant line. From the K-means analysis, a separation forms between CFPAC-1 and AsPC-1; this occurs both with and without HPDE being included in the analysis. Secondly, we performed hierarchical clustering on the cell lines using their entire set of dose responses and again a break can be seen after CFPAC-1 (Fig. 2.4B). From the K-means analysis, the threshold was 1.35 μM; therefore, cell lines with a GI_{50} value below 1.35 μM were considered sensitive, and above, resistant. This resulted in 12 pancreatic cancer cell lines being considered sensitive, as well as the non-cancerous pancreatic line HPDE. The remaining 6 cell lines were considered resistant (Fig. 2.5).

2.2.2. Validating Cell Line Sensitivity by In Vivo *Tumor Models*

The cell line sensitivity classifications are based on *in vitro* assays, which may not be representative how tumors would respond to the inhibitor. Because of this, we selected four cell lines, two from each group, for *in vivo* tumor models to determine if the sensitivity classifications are accurate. Hs 766T and HPAF-II lines were selected from the sensitive group because of their low GI_{50} value and maximum predicted therapeutic response [effect at infinite concentration (E_{inf})]

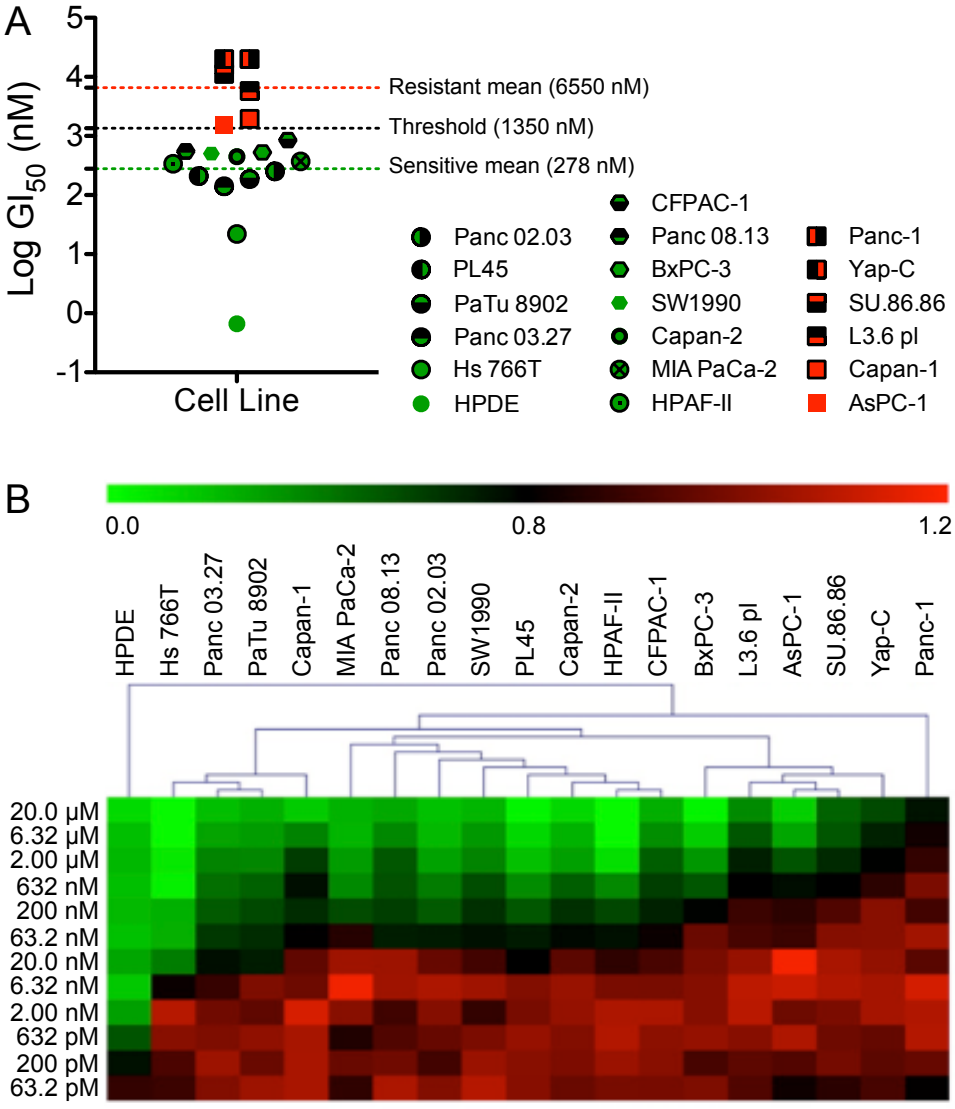

Figure 2.4 Cell line clustering. *A)* A K-means 2 group clustering was performed using the log GI_{50} values for the 18 cancer cell lines. A separation occurs between CFPAC-1 and AsPC-1 with a threshold of 1350 nM. Cell lines below this value are considered sensitive, and above resistant. *B)* Additionally, cell line growth response data for the different concentration of AZD6244 was uploaded into MeV for analysis. After hierarchical clustering, a break can again be seen after CFPAC-1.

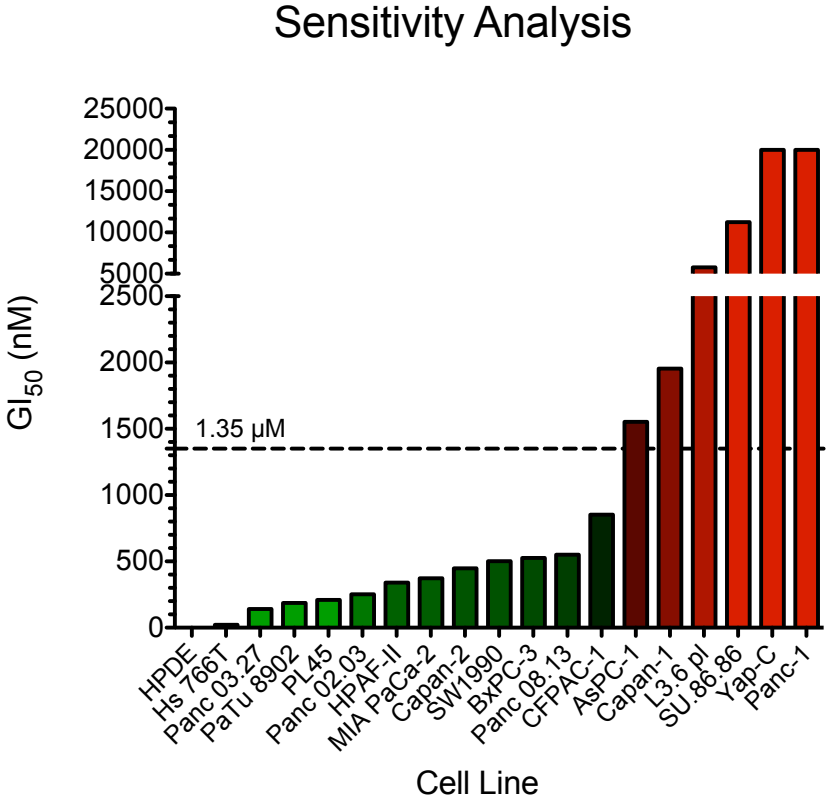

Pancreatic Cell Line	GI_{50} (nM)
HPDE	0.662
Hs 766T	21.9
Panc 03.27	141
PaTu 8902	187
PL45	209
Panc 02.03	252
HPAF-II	340
MIA PaCa-2	372
Capan-2	448
SW1990	502
BxPC-3	526
Panc 08.13	551
CFPAC-1	853
AsPC-1	1552
Capan-1	1954
L3.6 pl	5768
SU.86.86	11247
Yap-C	20000
Panc-1	20000

Figure 2.5 Cell line GI_{50} values. The concentration of AZD6244 needed to inhibit growth by 50% for each cell line is plotted (*left*) and arranged with increasing resistance. From the clustering analysis, CFPAC-1 was the cutoff for sensitive cell lines so a value of 1.0 µM was chosen for the sensitivity threshold. *Right)* Individual GI_{50} values for each cell line.

respectively. Yap-C and Panc-1 cell lines were chosen to represent the resistant group because they showed the least response to MEK inhibition. Subcutaneous tumors were created by implanting cancer cells mixed in Matrigel (BD Biosciences) into the backs of mice (two tumors per mouse). Once palpable (approximately 200 mm^3), the mice were broken into two groups, and treated with 2.5 mg/kg AZD6244 or vehicle control *bid*. Tumor measurements were taken twice a week for up to four weeks or until tumor burden required a termination of the study. In confirmation of the *in vitro* results, there was a significant reduction in tumor growth in animals with tumors derived from sensitive cell lines, whereas the tumors from the two resistant cell lines had no significant response to the inhibitor (Fig. 2.6). These findings confirmed the classification of the cell lines as sensitive or resistant.

2.2.3. Finding Potential Markers of Sensitivity and Resistance in Surface Receptor Transcriptome Data

Ideally, any marker that would translate to clinical use would be accessible to non-invasive imaging agents, so that diagnoses could be made without the need for a biopsy. Unfortunately, many agents such as antibodies and peptides cannot pass freely through the plasma membrane of a cell. Further, as a targeting mechanism for therapy, delivering a large payload such as nanoparticle would require targeting to be achieved extracellularly (177). It follows that a protein expressed on the cell surface, such as a receptor, would make the ideal candidate for a marker. Because receptors are the initiating protein in many

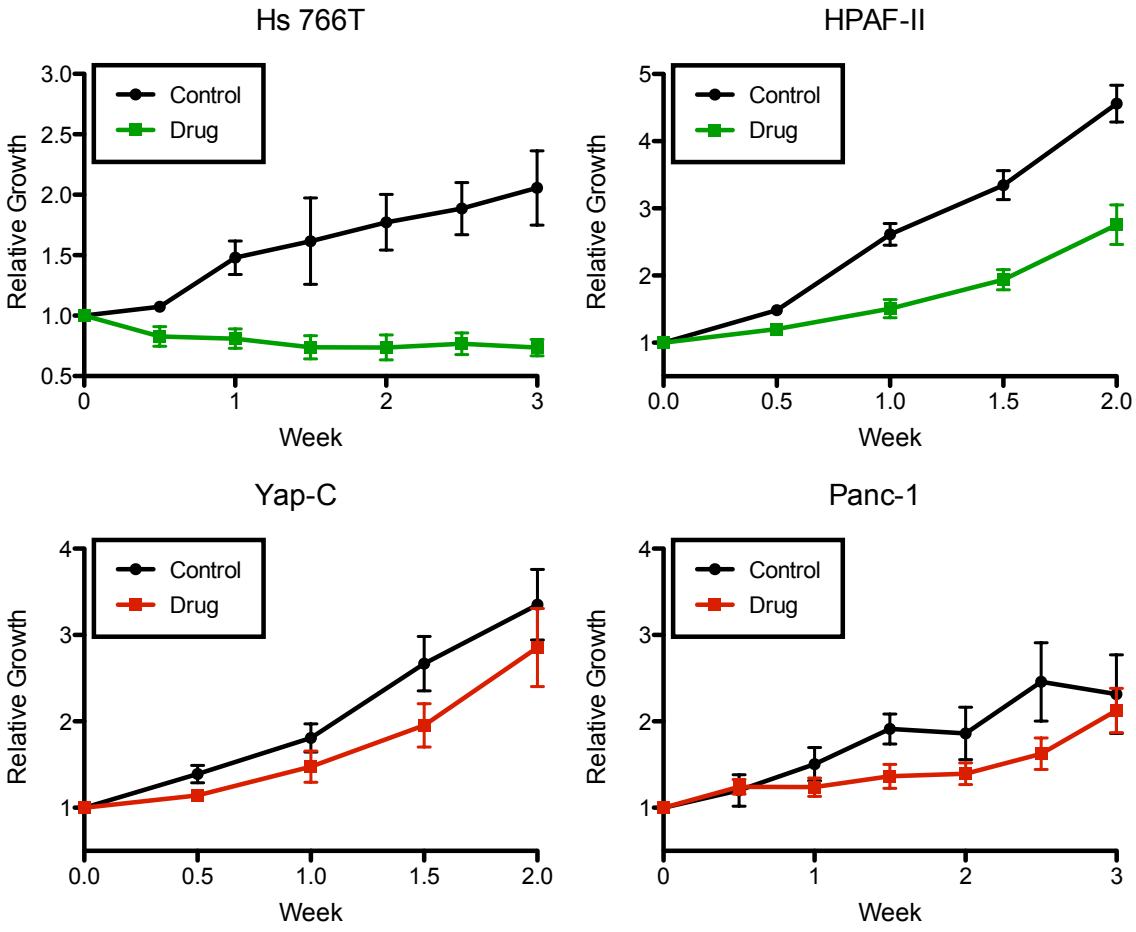

Figure 2.6 *In vivo* validation of sensitive and resistant cell line classifications. Subcutaneous tumor models of the indicated cell lines were used to confirm the *in vitro* sensitivity findings for the inhibitor AZD6244. Both sensitive lines had a significant decrease in tumor volume from the inhibitor (2.5 mg/kg *bid*) whereas the resistant lines were not responsive.

cellular signals, if a surface receptor is a marker of resistance, it may also serve as a therapeutic target itself.

For these reasons, a surface receptor transcriptome dataset constructed using RTqPCR mRNA expression levels was used in our initial search. The dataset included 194 major signaling receptors in the array (178). 5 sensitive (HPDE, PaTu 8902, HPAF-II, MIA PaCa-2 and Capan-2) and 5 resistant (AsPc-1, Capan-1, SU.86.86, Yap-C and Panc-1) cell lines were used for comparison. Multi-experiment Viewer (MeV) was used for the comparison. A rank test was performed (179), resulting in 27 genes of interest ($p \leq 0.05$; Fig. 2.7). The top result was *IL13RA2* ($p=3.35E-3$) being overexpressed in sensitive lines; the most overexpressed transcript in resistant lines was *TNFRSF10B* ($p=8.09E-3$). A full list of the significant transcripts can be found in Table 2.1.

2.2.4. Finding Potential Markers of Sensitivity and Resistance in Microarray Data

As a second means of comparison, we mined the extensive previously published microarray data available from gene expression omnibus (GEO) for a number of pancreatic cell lines (180). This additional comparison expanded the genes studied from 194 to over 38,000 genes and UniGenes (181), allowed us to examine the genes of intracellular proteins, and provided a potential means of cross-evaluation between datasets. Of the lines in the sensitive and resistant groups, 7 overlapped with GEO data and were used for microarray analysis. A t-test comparing the 4 sensitive lines (Hs 766T, PL45, HPAF-II and MIA PaCa-2) to 3 resistant lines (AsPC-1, SU8686 and Panc-1) was performed in MeV after

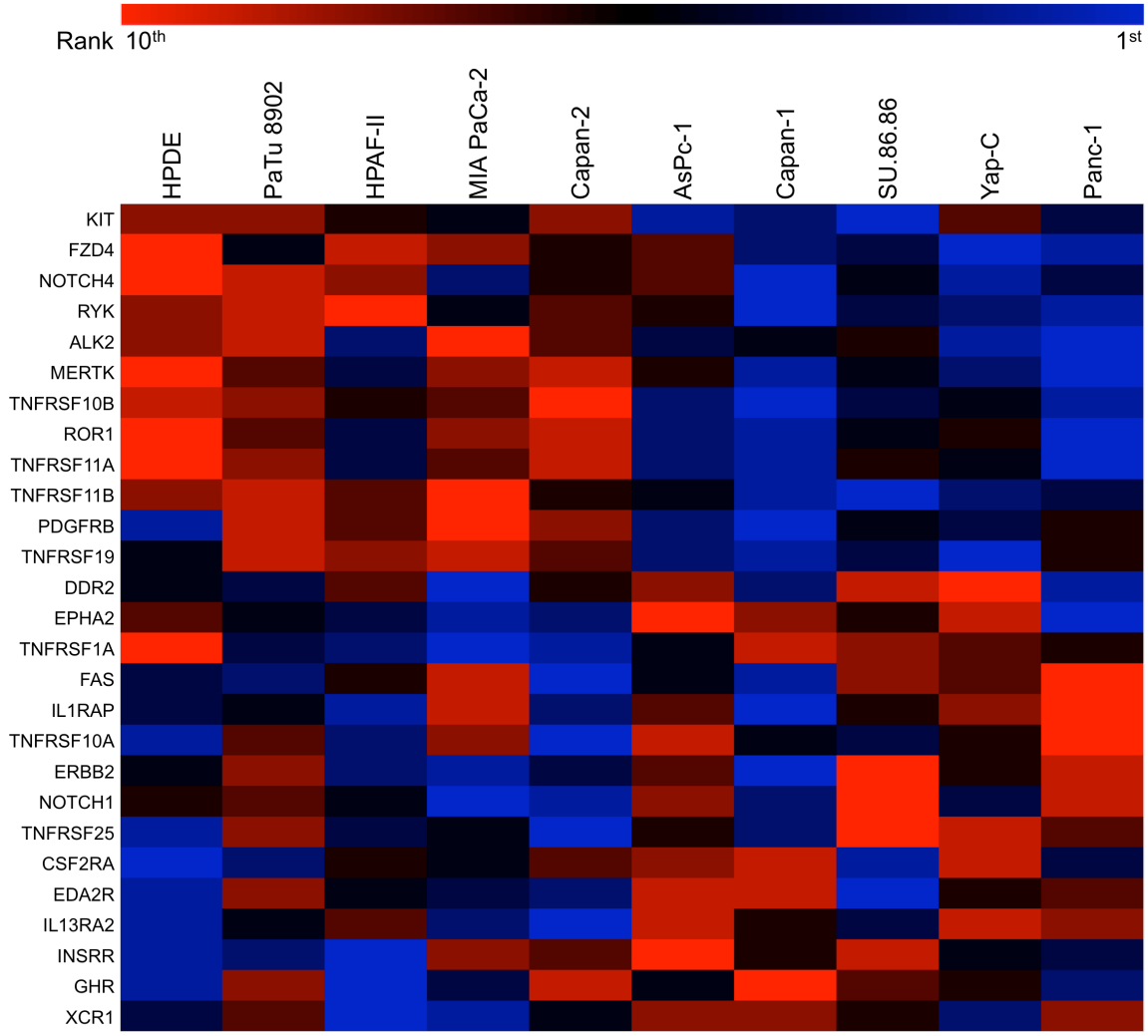

Figure 2.7 Surface receptor transcriptome analysis results. Surface receptor transcriptome data from RTqPCR was compared for 5 sensitive and 5 resistant cell lines by a ranked product test. 27 surface receptors were found to have transcripts differentially expressed between sensitive and resistant groups (p=0.05).

Hit	Gene Symbol	P Value	Microarray Location
1	*IL13RA2*	3.351E-03	19265
2	*INSRR*	6.649E-03	3002
3	*TNFRSF1A*	7.784E-03	23157
4	*EPHA2*	8.041E-03	46147
5	*TNFRSF10B*	8.093E-03	26429
6	*TNFRSF25*	8.608E-03	5938
7	*TNFRSF11B*	1.160E-02	33013
8	*TNFRSF10A*	1.330E-02	33469
9	*Notch1*	1.356E-02	8462
10	*RYK*	1.541E-02	13901
11	*CSF2RA*	1.773E-02	20152
12	*TNFRSF19*	1.907E-02	23803
13	*FZD4*	2.077E-02	8954
14	*DDR2*	2.129E-02	22137
15	*XCR1*	2.201E-02	12612
16	*FAS*	2.284E-02	451
17	*TNFRSF11A*	2.289E-02	10275
18	*IL1RAP*	2.325E-02	43864
19	*ERBB2*	2.418E-02	2801
20	*ROR1*	2.593E-02	5691
21	*MERTK*	3.510E-02	10
22	*KIT*	3.619E-02	31141
23	*EDA2R*	4.098E-02	5034
24	*GHR*	4.299E-02	13132
25	*PDGFRB*	4.644E-02	11658
26	*ALK2*	4.660E-02	7757
27	*Notch4*	4.701E-02	7870

Table 2.1 Significant genes from the RTqPCR surface receptor transcript studies. The microarray location column is taken from the cDNA analysis (see below).

the data was normalized across genes. Of the 47,400 transcripts tested, 411 were found to have a significance of $p<0.02$. These were then ranked by p value with the top 43 shown in Fig. 2.8, all with a $p<0.002$. The top gene was found to be *MAPK8* (p=8.42E-6), which codes for the protein c-Jun N-terminal kinase 1 (JNK1) and was upregulated in resistant cells. A more complete list of the top differentially expressed genes can be found in Table 2.2.

2.2.5. Extracting Potential Sensitivity Markers from Datasets

When working with the surface proteome or microarray data alone, it is difficult to find conclusive results due to a high false discovery rate. We performed a significance analysis of microarray (SAM) test with the surface transcriptome data (2 classed unpaired SAM, delta=0.15) and found the false discovery rate (FDR) =23.7% with only 4 genes to have a $q \leq 0.05$: *TNFRSF11B, TNFRSF10B, TNFRSF19,* and *RYK* (Fig. 2.9). After performing a SAM test on the microarray data (2 classed unpaired, delta =0.5) the FDR was 42.8%, and only 7 genes had a q-value ≤ 0.05: *CTCF, GHG1, TGM5, PRKRIP1, RPL23AP7, TMEM72,* and *MERTK* (Fig. 2.9). Therefore, the genes were ranked and the top results taken knowing they had a high chance of being false positives. As a means of improving robustness in the results, a comparison between the two arrays was performed. Only *MERTK* was found significant in both the surface transcriptome and the cDNA microarray datasets (RTqPCR: p=0.0351; microarray: p=3.66E-4). For this reason, we chose to pursue *MERTK* as a potential marker of MEK inhibition (in)sensitivity. Further, because we found

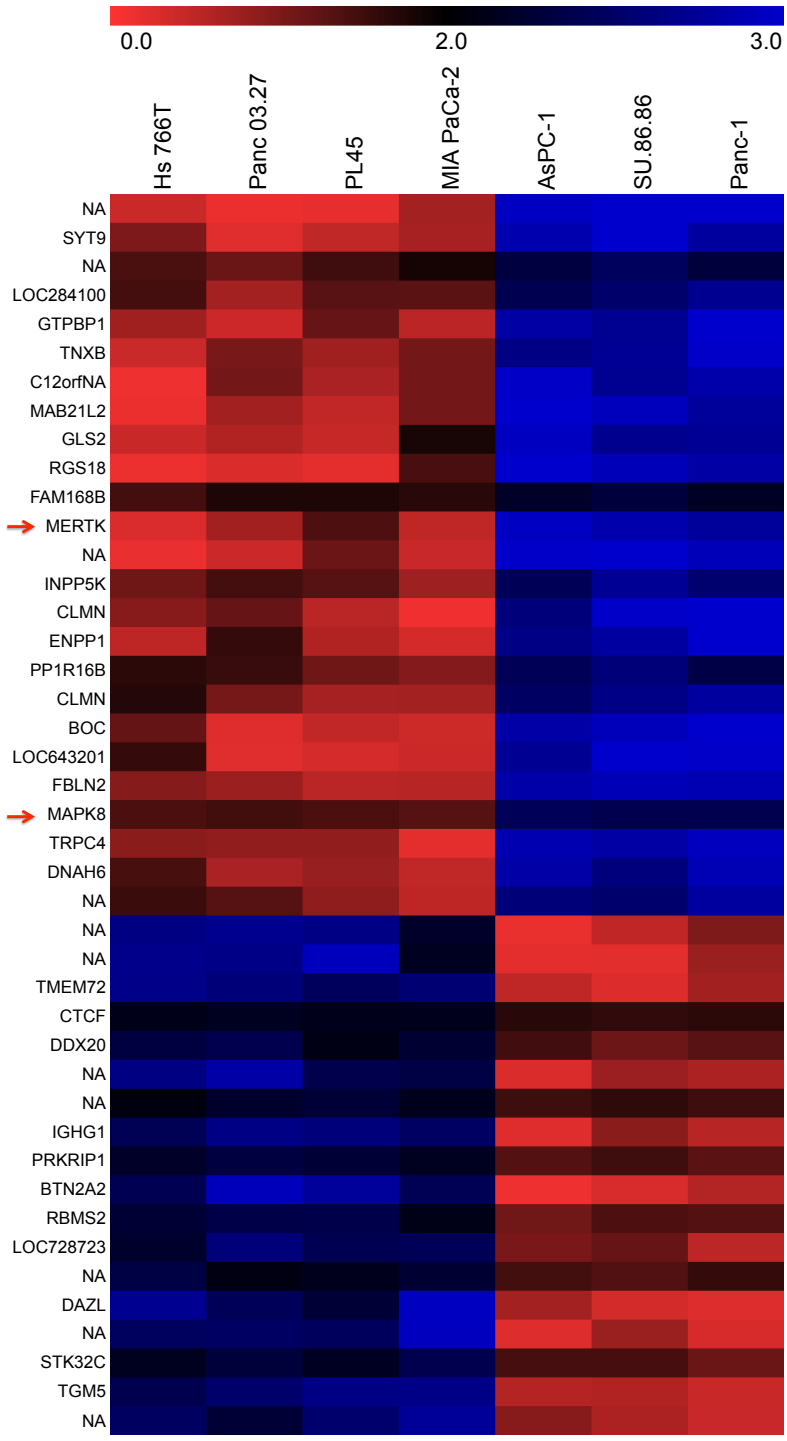

Figure 2.8 cDNA microarray analysis results. cDNA microarray data was used to compare sensitive and resistant cell line groups. 4 sensitive and 3 resistant cell lines were evaluated using a t-test. The 43 top differentially expressed genes ($p<0.002$) are shown. MERTK and MAPK8 were two target of interest from the microarray and transcriptome analyses.

Hit	Gene Symbol	Gene Name	P Value	Probe I.D.
1	*MAPK8*	mitogen-activated protein kinase 8	8.424E-06	210671_x_at
2	*CTCF*	CCCTC-binding factor (zinc finger protein)	1.213E-05	202521_at
3	NA	NA	4.471E-05	1560973_a_at
4	*TGM5*	transglutaminase 5	5.474E-05	207911_s_at
5	*TRPC4*	transient receptor potential cation channel, subfamily C, member 4	7.742E-05	224219_s_at
6	*FBLN2*	fibulin 2	8.461E-05	203886_s_at
7	*BOC*	Boc homolog (mouse)	2.886E-04	225990_at
8	*MAB21L2*	mab-21-like 2 (C. elegans)	3.457E-04	210303_at
9	*PRKRIP1*	PRKR interacting protein 1 (IL11 inducible)	3.648E-04	218378_s_at
10	*MERTK*	c-mer proto-oncogene tyrosine kinase	3.660E-04	211912_at
11	*GTPBP1*	GTP binding protein 1	4.061E-04	226359_at
12	*C12orf33*	chromosome 12 open reading frame 33	4.316E-04	1555040_at
13	*TNXB*	tenascin XB	4.587E-04	216654_at
14	*TMEM72*	transmembrane protein 72	5.057E-04	1558324_a_at
15	*DNAH6*	dynein, axonemal, heavy chain 6	5.071E-04	1561616_a_at
16	*BTN2A2*	butyrophilin, subfamily 2, member A2	5.584E-04	1564684_at
17	NA	NA	6.376E-04	228692_at
18	NA	NA	7.035E-04	242152_at
19	NA	NA	7.164E-04	1561128_at
20	NA	NA	7.450E-04	239737_at
21	*RBMS2*	RNA binding motif, single stranded interacting protein 2	9.856E-04	235558_at
22	*LOC643201*	hypothetical protein LOC643201	1.022E-03	235416_at
23	*INPP5K*	inositol polyphosphate-5-phosphatase K	1.042E-03	202782_s_at
24	NA	NA	1.144E-03	203579_s_at
25	*RGS18*	regulator of G-protein signaling 18	1.157E-03	223809_at

Table 2.2 Top differentially expressed genes from the microarray data analysis.

Hit	Gene Symbol	Gene Name	P Value	Probe I.D.
26	*CLMN*	calmin (calponin-like, transmembrane)	1.170E-03	225757_s_at
27	*DAZL*	deleted in azoospermia-like	1.224E-03	206588_at
28	NA	NA	1.289E-03	238276_at
29	*SYT9*	synaptotagmin IX	1.437E-03	1563658_a_at
30	*IGHG1*	immunoglobulin heavy constant gamma 1 (G1m marker)	1.460E-03	217039_x_at
31	*LOC284100*	hypothetical protein LOC284100	1.484E-03	1563945_at
32	*STK32C*	serine/threonine kinase 32C	1.492E-03	230934_at
33	*FAM168B*	family with sequence similarity 168, member B	1.505E-03	212017_at
34	*ENPP1*	ectonucleotide pyrophosphatase/ phosphodiesterase 1	1.539E-03	229088_at
35	*DDX20*	DEAD (Asp-Glu-Ala-Asp) box polypeptide 20	1.609E-03	223331_s_at
36	NA	NA	1.644E-03	1566868_at
37	*CLMN*	calmin (calponin-like, transmembrane)	1.697E-03	221042_s_at
38	*GLS2*	glutaminase 2 (liver, mitochondrial)	1.714E-03	1564707_x_at
39	*LOC728723*	hypothetical LOC728723	1.716E-03	241423_at
40	NA	NA	1.724E-03	238552_at
41	NA	NA	1.724E-03	1569644_at
42	NA	NA	1.803E-03	220932_at
43	*PPP1R16B*	protein phosphatase 1, regulatory (inhibitor) subunit 16B	1.880E-03	212750_at

Table 2.2 Cont. Top differentially expressed genes from the microarray data analysis.

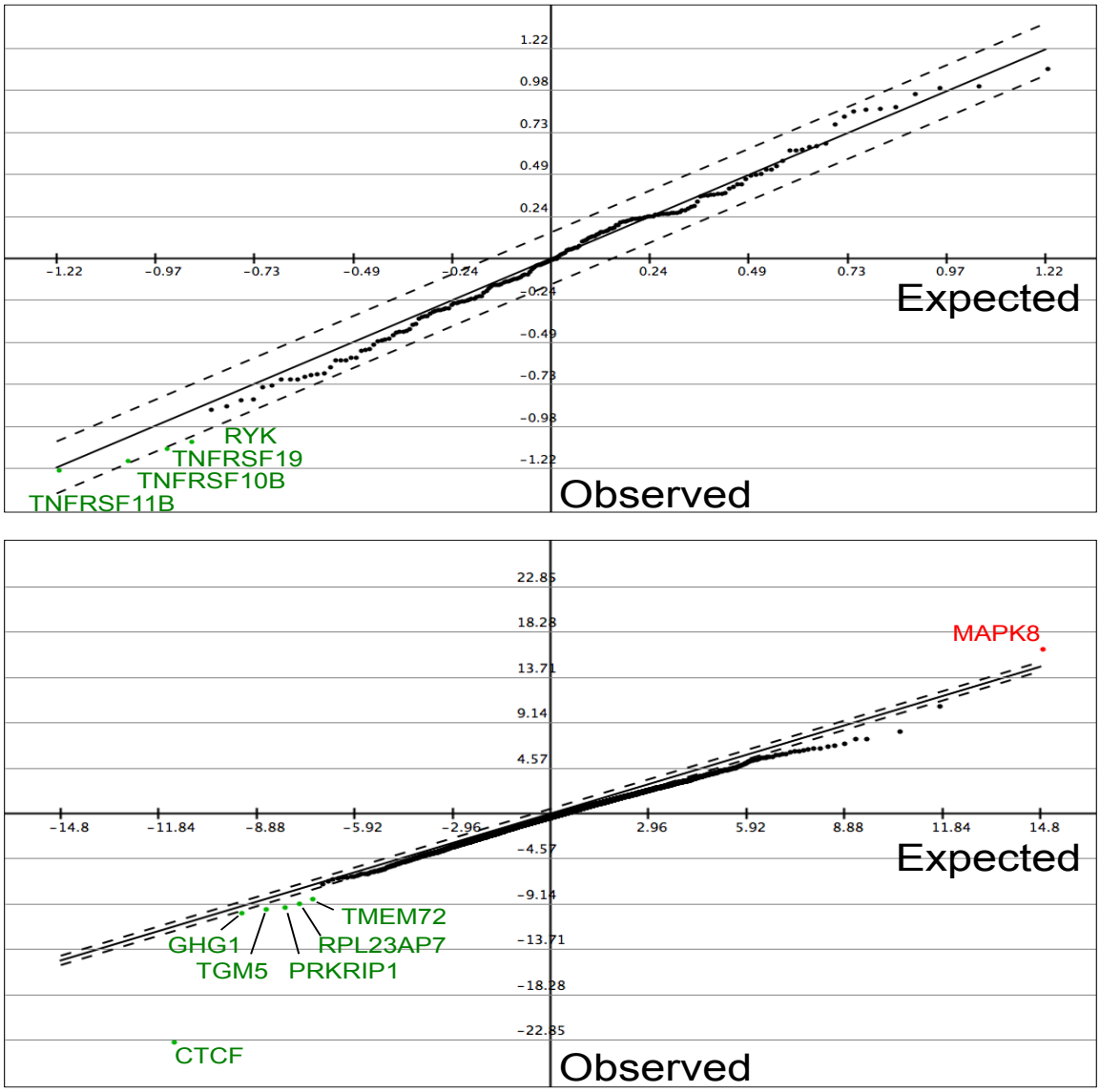

Figure 2.9 Significance Analysis of Microarrays. Analyzing the gene expression data for false positives. *Top)* A significance analysis of microarray (SAM) was performed on the surface proteome data using 2 classed unpaired test, delta=0.15. The False discovery rate was 23.7% with 4 genes having a q≤0.05 – *TNFRSF11B, TNFRSF10B, TNFRSF19,* and *RYK*. *Bottom)* Microarray SAM (2 classed unpaired, delta=0.5). False discovery rate=42.8%, and 7 genes, *CTCF, GHG1, TGM5, PRKRIP1, RPL23AP7, TMEM72,* and *MERTK* had q≤0.05. *C)* Quantification of *AXL* and *TYRO3* from the surface transcriptome analysis.

MERTK to be overexpressed in resistant lines, it could potentially serve as a new therapeutic target for tumors insensitive to AZD6244 inhibition.

Alternatively, we took a closer examination of the results from the cDNA microarray for potential targets of interest by importing the dataset into Ingenuity Pathway Analysis (IPA) to examine resistance from a higher order of complexity. Looking at the pathways that were differentially expressed, not just individual gene transcripts, we found several members of the JNK1 signaling pathway to be upregulated (Fig. 2.10A). The transcripts for JNK1 (*MAPK8*, p=8.42E-6 - our top hit from the microarray data), MEK 7 (*MAP2K7*, p=0.0149), and MEKK2 (*MAP3K2*, p=0.0358) were all upregulated in resistant lines (Fig. 2.10B). These three constitute a JNK pathway; MEKK2 phosphorylates MEK 7, MEK 7 then phosphorylates JNK1 (MEKK2 > MEK 7 > JNK1). Because *MAPK8* was our top hit from the microarray data, and two other pathway members are upregulated, we wanted to examine JNK1's importance in MEK 1/2 inhibition resistance as well.

2.3. Discussion

2.3.1. Fitting Dose Response Curves to the Inhibitor Data

12 different concentrations of AZD6244 were used to measure cell line growth response so that dose response curves, either 3-parameter (fixed hill slope) or 4-parameter (variable hill slope) could be fitted. Increasing the number of variables will always yield a closer fit, however doing so is not always necessary and can even sometimes result in overfitting. To evaluate the benefits

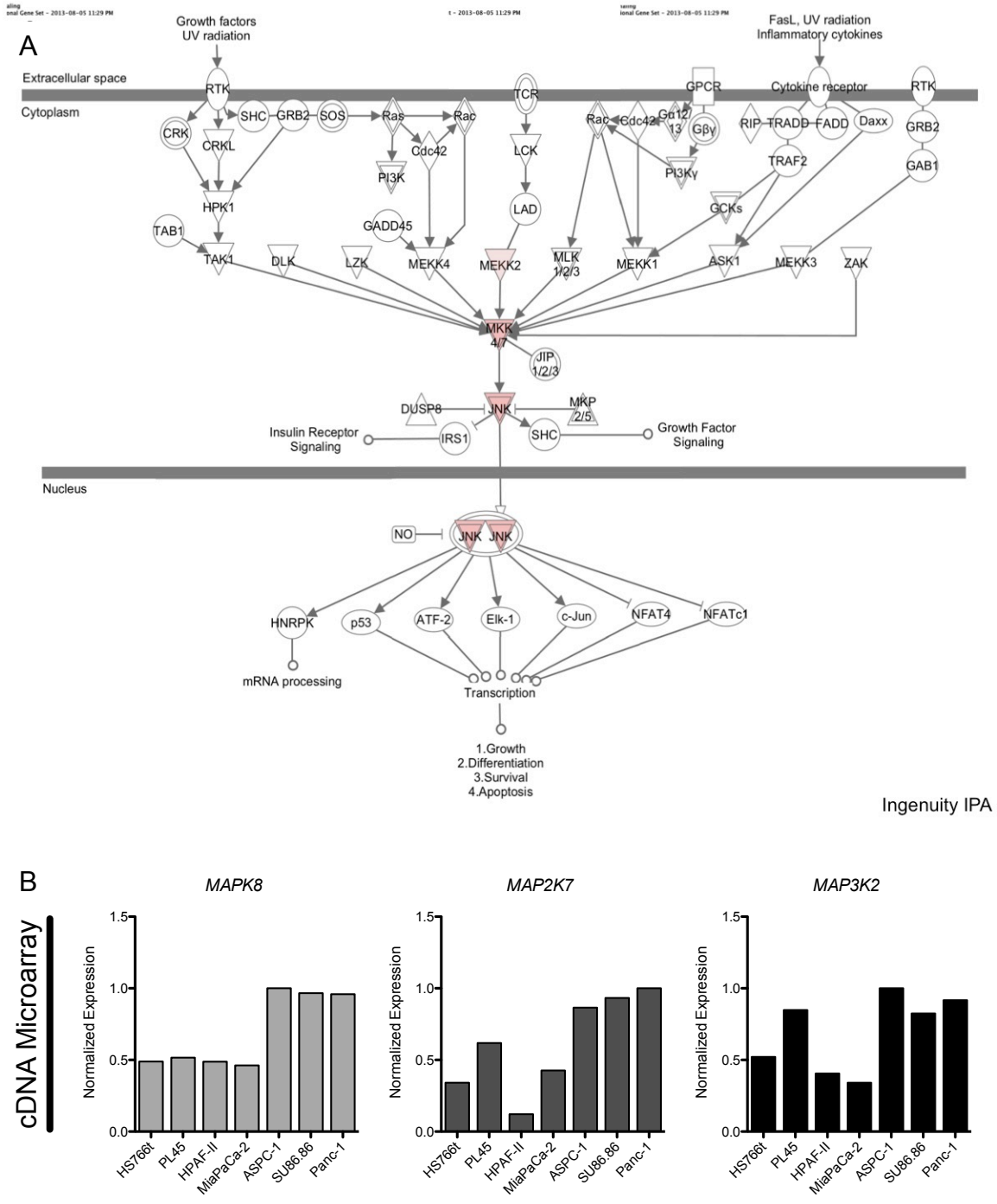

Figure 2.10 Ingenuity Pathway Analysis. *A)* Processing the microarray data through Ingenuity for differential pathway expression found the MEK7-JNK1 pathway to be overexpressed in resistant lines. *B)* Individual gene expression values for the MEK7-JNK1 pathway members JNK1 (*MAPK8)*, MEK 7 (*MAP2K7)* and MEKK2 (*MAP3K2).*

of the two, we performed both 3- and 4-parameter fittings to the cell line data and found that the 4-parameter curve did indeed fit better (Fig. 2.11A), but ultimately no meaningful difference was seen between the two fits (Fig. 2.11B). Calculating the GI_{50} values for both curve sets revealed slight differences in the cell line sensitivity order (Fig. 2.11C), but no line changed sensitivity groups. Further, when compared with the hierarchical clustering data, the 3-parameter fit aligned slightly better than the 4-parameter. Therefore, we chose to use the 3-parameter fit in our analyses.

2.3.2. Defining MEK Inhibition Sensitivity in PDAC Cell Lines

After establishing the inhibition curves for each cell line, difficulties arose when choosing a metric by which to compare the cell lines' sensitivities. A number of different variables exist for measuring sensitivity. Concentration based metrics include IC_{50}, EC_{50}, GI_{50} and any variation of these at a different response threshold (ex. GI_{80}). Alternatively, one could determine sensitivity based on cell line response at specific inhibitor concentration. These metrics include the maximum effect seen (typically at the highest dose; E_{max}), the highest response possible, or the bottom of growth curve (E_{inf}) or the effect at any another specific concentration. Further, parameters that incorporate multiple factors (ex. area under the curve or AUC) could also be used (182). Which parameter we chose would change the relative order of cell sensitivity. For example, Figure 2.12A compares two response curves for HPAF-II and Panc 03.27, depending on which criterion one chooses, either line could be considered more sensitive. Picking a specific concentration to measure growth response neglects the value of

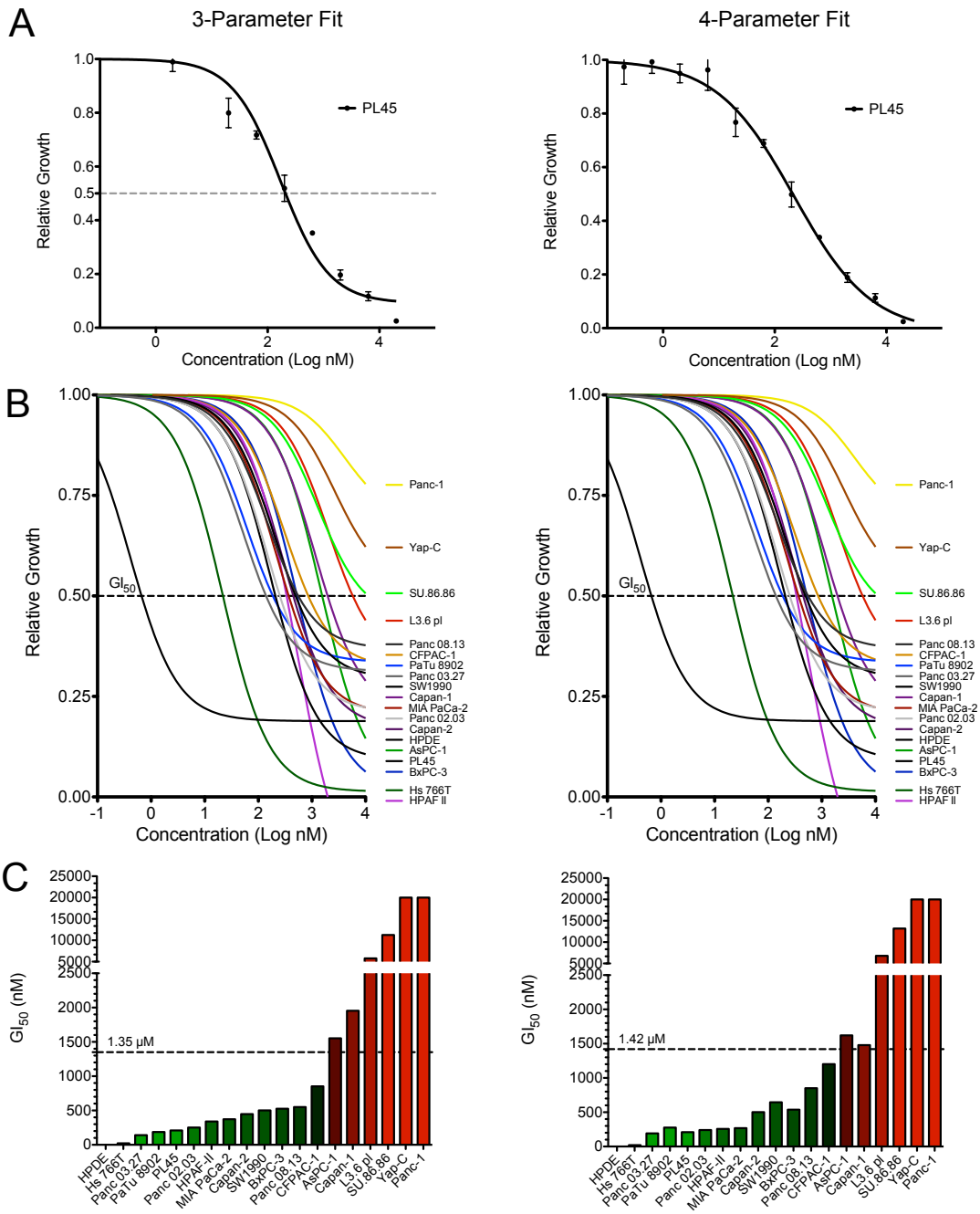

Figure 2.11 Comparing 3-parameter to 4-parameter curve fits. *A)* 3-parameter (*left*) and 4-parameter (*right*) curve fits for the PL45 cell line. *B)* Curve fits for all 19 pancreatic cell lines using the 3- (*left*) and 4-parameter (*right*) fits. *C)* Calculated GI_{50} values using the two fits.

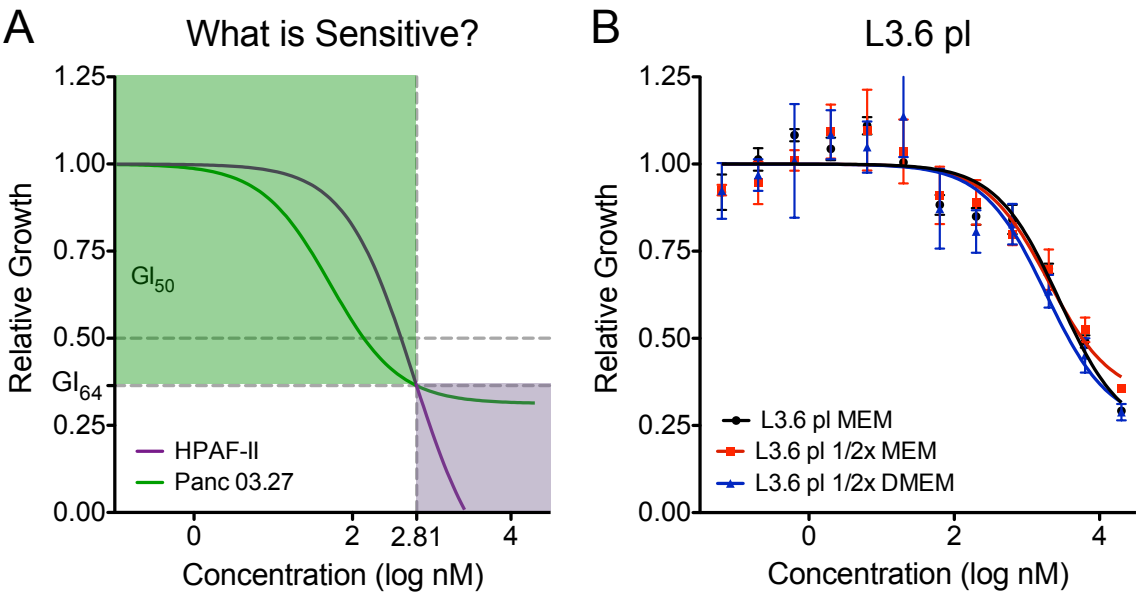

Figure 2.12 Evaluating the AZD6244 dose response curves of PDAC cell lines. *A)* Two sample curves for HPAF-II and Panc 03.27 illustrate how the use of different metrics for defining sensitivity can alter their relative sensitivity ordering. *B)* Evaluation of the robustness of cell lines in different media and seeding concentrations reveal limited differences in their response to MEK inhibition.

constructing a response curve. Using the EC_{50} devalues the overall effectiveness of the inhibitor at higher concentrations. For these reasons, we chose to use the GI_{50} metric because it incorporates both a specific response target (50% growth inhibition) and the concentration needed to achieve the target response.

2.3.3. The Robustness of Cell Line Inhibition Response

Several cell lines, including L3.6 pl, have been reported in literature to have different culture conditions (183-185). Whenever possible, we followed ATCC's recommended culturing protocol, but it raised the question how much variation in culturing technique could affect the inhibitor response. For example, plating too confluently could mask the decreased growth effects of an inhibitor or using a more robust medium with high glucose and amino acids could potential make cells more resistant to inhibition. We tested these variations, but found no meaningful difference in overall response (Fig. 2.12B). This, combined with the *in vivo* tumor models, gave confidence to our cell line sensitivity assessments.

2.3.4. Screening for Markers of Resistance

The HPDE line was the only non-cancerous cell line used in our studies. It is a transformed human pancreatic ductal epithelial line and was used for a few reasons. First, without the RAS mutation and other pro-growth changes that cancer cells acquire, we expected it to have a strong response to the inhibitor at low concentrations. This served as a positive control for our assays. Second, when performing the gene comparisons, designing it to find markers of resistance allowed us to find a potential therapeutic targets as well. As

mentioned previously, several qualities make a good marker including surface expression and differential expression between sensitive and resistant lines, but also having elevated expression over normal pancreatic tissue. By including HPDE in the sensitive group, markers of resistance would be low in both the sensitive cell lines and the HPDE line, hopefully translating to low expression in normal tissue as well.

2.3.5. Evaluating the Potential Markers Found from the Datasets

It is interesting that the JNK pathway was found to be overexpressed in resistant lines. The expressions of MAPK proteins are typically consistent across different cell types because of their importance in many cellular functions. Despite being the top hit from the array data, looking at the expression levels one can see that there isn't as large of a difference between groups as other genes, but the deviations within groups is small. The ingenuity analysis finding the rest of the pathway to have elevated expression does lend credibility to JNK's significance. It is important to note that the microarray analysis found gene expression differences, which may be completely unrelated to phospho-protein levels and pathway activity.

Lastly, *MERTK* was the only gene found in both the surface receptor transcriptome and the cDNA datasets, but other potential targets could still be explored. For example, *FAS* was the next best gene found in the surface receptor data (RTqPCR: p=0.023; microarray: p=0.022). The FAS receptor is a death receptor that signals for apoptosis in cells. It was found to be

underexpressed in resistant lines in both analyses and has been reported in literature to be disabled in many pancreatic tumors (186). It could be pursued as a marker of sensitivity. The gene arrays served as a starting point to identify potentially important proteins and further analyses are needed to establish their utility as markers.

2.4. Material and Methods

2.4.1. MEK 1/2 Inhibitor

The small molecule inhibitor AZD6244 was purchased from Selleck Chemical and prepared in dimethyl sulfoxide (DMSO) with a stock concentration of 10 mM.

2.4.2. Cell Culture

18 different PDAC cell lines and one transformed normal pancreatic cell line were chosen for this study. All cell lines except PaTu 8902, L3.6 pl and HPDE were acquired from American Type Culture Collection (ATCC). PaTu 8902 was purchased from the german culture core Deutsche Sammlung von Mikroorganismen und Zellkulturen (DSMZ). L3.6 and HPDE were both obtained from Dr. Craig Logsdon (University of Texas, MD Anderson Cancer Center). AsPC-1, BxPC-3, MIA PaCa-2, PaTu 8902, SU.86.86 and Yap-C were all growth in Roswell Park Memorial Institute (RPMI) medium supplemented with 10% (vol/vol) fetal bovine serum (FBS), 1% penicillin-streptomycin (pen-strep; ATCC 30-2300), and 2mM L-glutamine (L-glut). Panc 02.03, Panc 03.27, and Panc

08.13 were grown in RPMI supplemented with 15% (vol/vol) FBS, 1% pen-strep, 2 mM L-glut, 1.5% (vol/vol) NaHCO, 10 mM HEPES, 4.5 g/L glucose (final concentration), 1 mM Na Pyruvate, and 10 units/mL of human insulin. Hs 766T, L3.6 pl, Panc-1, PL45, and SW1990 were grown in Dulbecco's Modified Eagle's Medium (DMEM) supplemented with 10% (vol/vol) FBS, 1% pen-strep, and 2mM L-glut. CFPAC-1 cells were grown in IMDM supplemented with 10% (vol/vol) FBS, 1% pen-strep, and 2 mM L-glut. Capan-1 cells were grown in Iscove's Modified Dulbecco's Medium (IMDM) supplemented with 20% (vol/vol) FBS, 1% pen-strep, and 2 mM L-glut. Capan-2 cells were cultured in McCoy's 5A Medium supplemented with 10% (vol/vol) FBS, 1% pen-strep, and 2 mM L-glut. HPAF-II cells were grown in Eagle's Minimum Essential Medium (EMEM or MEM) supplemented with 10% FBS, 1% pen-strep, and 2 mM L-glut. Lastly, HPDE cells were cultured in Keratinocyte Growth Kit (ATCC PCS-200-040). All cells were incubated at 37°C, 5% CO_2.

2.4.3. Dose Response Curves

Cell lines were plated in two 96 well plates at a concentration of 2,500 cell/well. After 24 hrs, fresh media containing concentrations of AZD6244 ranging from 20 μM down to 63.2 pM by half-log units were added to each well in triplicate, after which the cells were incubated for three additional days. The second plate was used for an initial, "Day 0" reading. These cells were washed 3 times with phosphate buffered saline plus calcium and magnesium (PBS+) then fixed with 4% paraformaldehyde (PFA). The cells were again washed then incubated in Syto® 60 dye (Life Technologies) diluted 1:3,000 in PBS+ for 1 hr.

Cells were subsequently washed 6 times and imaged using a Li-Cor Odyssey at the 680 wavelength. Quantification was performed using the Li-Cor software. After the three-day incubation the inhibited cells in the first plate were processed the same way and quantified with the imager. Inhibition curves were reconstructed in Prism software using a 3-parameter (Bottom, Top, and IC_{50} with the hill slope constrained to -1) or 4-parameter (Bottom, Top, and IC_{50}, HillSlope) dose response curve. The equations used were Y=Bottom + (Top-Bottom)/(1+10^((X-LogIC_{50}))) and Y=Bottom + (Top-Bottom)/(1+10^((LogIC50-X)*HillSlope)) respectively. The curves were adjusted by subtracting the Day 0 intensity (therefore y=0 indicates no growth) and the top of the curve adjusted to 1 (maximal growth). The result was a curve that had a max value of 1, and when it crossed the x-axis indicated zero growth. GI_{50} values were then calculated from these curves for the concentration of inhibitor that caused a 50% decrease in cell growth. Combinatorial dose response curves were performed using 2 inhibitors, one of which was held constant throughout all the wells and the other inhibitor having varying concentrations (performed in triplicate).

2.4.4. Cluster Analysis and Cell Line Grouping

A cluster analysis on the cell lines was performed to separate them into sensitive and resistant groups. Using the cell line dose responses to AZD6244 (12 doses per cell line), we input every cell line into Multi-experiment Viewer (MeV) software (187). We performed a sample clustering using the onboard hierarchical clustering analysis software.

2.4.5. In Vivo *Tumor Models*

In vivo models were performed subcutaneously using nude mice. Cells were grown to 90% confluency then lifted with trypsin, resuspended in Hank's Balanced Salt Solution (HBSS) and mixed with Matrigel (BD Biosciences) 1:1. Cells were injected into the back of mice using 150 µL volume at a concentration of 5 million cells/mL. The control and inhibitor suspensions were prepared in a viscous solution of Methocel in DPBS+ (5 mg/mL). After tumors became palpable (~200 mm^3), treatment drug (2.5 mg/kg for AZD6244) or vehicle control was administered *bid*. for up to 4 weeks or until tumor burden reached limit as mandated by the animal care and use committee. Tumor size was measured using calipers.

2.4.6. Receptome and Microarray Data Analyses

Receptome data from our collaborator (178) was used to compare transcript expression levels via RTqPCR between sensitive and resistant cancer lines. The normalized data was converted to a ranked expression level (lower rank corresponding to a higher expression value) and analyzed in MeV software using a rank test, $p \leq 0.05$. Similarly, microarray data from GEO (180) was uploaded into MeV, normalized across cells and genes; sensitive and resistant groups were then compared using a standard t test ($p \leq 0.002$) for differential gene expression. A significance of microarray (SAM) test was also performed for both datasets using the software's built in algorithms.

2.4.7. Ingenuity Analysis

The microarray data files were subsequently uploaded into IPA (Ingenuity Pathway Analysis; Qiagen) to compare sensitive and resistant groups again for differential gene expression as well as for a higher order gene pathway analysis. Using the software's built in algorithms we performed a canonical pathway analysis to identify pathways overexpressed in the sensitive or resistant groups.

Chapter 3

MERTK as a Marker of MEK 1/2 Inhibition Resistance and a Therapeutic Target in PDAC

3.1. Introduction

By comparing pancreatic cell lines that were sensitive and resistant to MEK 1/2 inhibition, we identified differentially expressed genes that had potential to be markers of sensitivity and resistance. Of these, *MERTK* was the top differentially expressed surface receptor transcript. This led us to investigate the potential of MERTK as a protein marker of MEK inhibitor resistance. The MERTK protein is a member of the TAM family of tyrosine kinase receptors that also includes TYRO-3 and AXL. These three receptors share a conserved kinase domain sequence, molecule-like extracellular domains, and the common ligand Gas6 (188). Of the three receptors, MERTK and AXL have the most similar tyrosine kinase domain sequence (189).

In cancer, the TAM family has been reported in a number of different tumor types. The majority of these findings focus on AXL and MERTK. MERTK has been reported in cancers such as melanoma and breast (190), but has yet (as of 2015) to be implicated in pancreatic cancer (188, 191). AXL has gained the most interest and is reported in a myriad of cancers that include breast (192, 193), colon (194, 195), lung (196, 197), liver (198), skin (199) and pancreatic (200, 201). It is typically considered a marker of poor prognosis, tumor cell survival and metastasis (202, 203). It has also been reported as a marker of therapeutic resistance. However, it is interesting that we found *MERTK* and not *AXL* to be differentially expressed between sensitive and resistant groups (Fig. 3.1). Therefore, we hypothesized that the MERTK protein and not AXL will serve as a better marker of MEK inhibition resistance in pancreatic cancer.

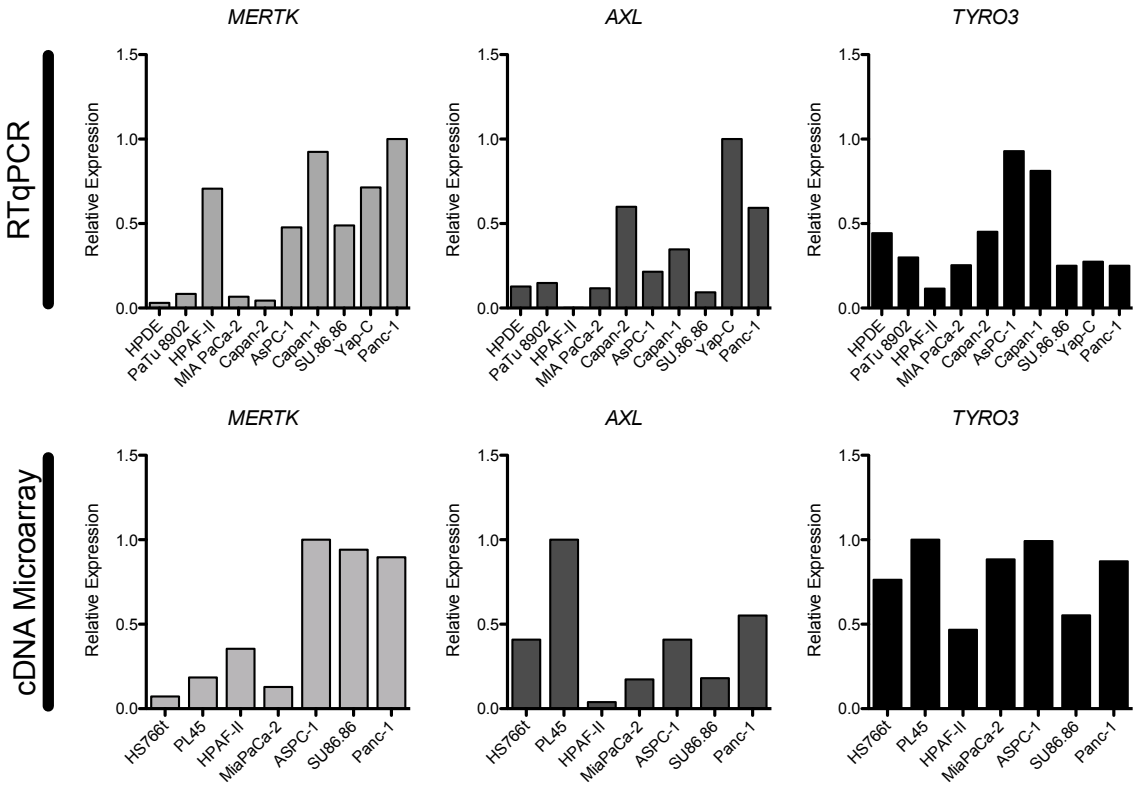

Figure 3.1 TAM family gene expression values from the array datasets. *Top)* Gene expression values from the RTqPCR dataset for *MERTK, AXL* and *TYRO3* in a panel of pancreatic cancer cell lines varying in AZD6244 sensitivity, sensitive (left) to resistant (right). *B)* Gene expression from the cDNA dataset for *MERTK, AXL* and *TYRO3* for a set of cell lines ranging from sensitive (left) to resistant (right).

As receptor tyrosine kinases (RTKs), MERTK and AXL can bind activating ligands such as Gas6 and signal through intracellular pathways. Studies in fibroblasts have shown MERTK to activate three main pathways, PI3K-AKT, MAPK-ERK and PLCγ (204). The end result of these pathways includes growth, proliferation and survival. Studies have found the balance between these pathways to be cell line and context dependent. For example in leukemia cells, the MAPK-ERK and PI3K-AKT pathways converge to decrease apoptosis and serve as redundant pro-survival pathways without increasing proliferation (205). However, in prostate cancer these same pathways have been found to act in opposition on IL-8 - MAPK-ERK stimulated protein production whereas PI3K-AKT suppressed IL-8 expression (206). Further, MERTK has been shown to interact with and activate several other proteins including Shc, Grb2, Vav1, and Ack1, the end result of such interactions also results in pro-growth and pro-survival signals that support tumorgenesis (188).

Similar to MERTK, AXL can be activated by Gas6 to predominantly signal through the RAS-MEK-ERK and PI3K-AKT pathways typically originating with Grb2 activation (207, 208). Differing from MERTK, AXL has a less important role in PLCγ signaling (188) and a different utilization of the PI3K-AKT pathway. AKT activation by MERTK has shown to inhibit IKK, downregulating NFκB-dependent transcription of TNFα (209). Contrary, AXL has been shown to stimulate NFκB activity to result in anti-apoptotic signaling (210). Although MERTK and AXL share many of the same characteristics and downstream effector molecules, it is important to understand the differences between these two receptors and how

each contributes to cancer. Because MERTK's effector pathways can result in growth and survival, we hypothesized that MERTK could not only serve as a marker of resistance, but also as a therapeutic target. Further, despite AXL being more prevalent in cancer literature, we believe MERTK has higher potential as a therapeutic target in PDAC. We specifically wanted to see if therapeutically targeting MERTK could sensitize resistant cell lines to MEK inhibition.

We first examined both MERTK and AXL protein expressions in pancreatic cancer cells. We found that MERTK, but not AXL, correlated with MEK inhibitor resistance. Intriguingly, after conditioning sensitive cells to become resistant to MEK inhibition, we found both MERTK and AXL had increased expression levels, suggesting their utility as markers of acquired resistance. Gas6 was also found to have increased expression with cell conditioning. Knockdown studies using both siRNA and shRNA showed MERTK to be important for cell proliferation especially in the resistant lines. Using a MERTK inhibitor we could inhibit cell growth at similar concentrations to that of AZD6244, but different sets of sensitive and resistant cell lines were found with no correlation to AZD6244 sensitivity. Lastly, when used combinatorially, the MERTK inhibitor did not sensitize cells to MEK 1/2 inhibition.

3.2. Results

3.2.1. Protein Confirmation of Marker Overexpression

Despite finding the *MERTK* transcript elevated in resistant lines, we still needed to validate MERTK as a protein marker. We selected a random subpanel

of 9 pancreatic cancer cell lines of varying resistance and performed quantitative western (qWestern) blots for the MERTK protein, as well as several other key proteins (Fig. 3.2A). As a point of comparison, we also blotted for AXL since it is in the same TAM family of receptors as MERTK but has been reported much more frequently in literature as a poor prognosis marker. ERK 1/2 and P-ERK 1/2, immediately downstream of MEK 1/2, were also selected. It was postulated that resistant lines could simply have increased MEK/ERK activity and that this was the cause of their increased resistance to inhibition. However, the qWestern results found this to not be the case as neither total ERK nor P-ERK correlated with resistance. AXL also had no significant correlation, but MERTK did ($p=0.0186$, $r=0.7551$; Fig 3.2B).

3.2.2. MERTK as a Marker of Acquired Resistance

Hitherto, the work presented has focused on finding innate markers of resistance. One of the leading challenges in utilizing MEK inhibitors is patients will often develop an acquired resistance to the therapy (211). Therefore, we wanted to determine if MERTK could serve as a marker of acquired resistance as well as innate resistance. To do this, we desensitized cells that initially responded well to the inhibitor by growing them under MEK inhibition for a prolonged period of time then examined MERTK and AXL expression changes as a result of the conditioning.

MIA PaCa-2, a sensitive cell line with low MERTK expression, was incubated with a sub-lethal concentration of AZD6244 (2 μM). After 2 months, we

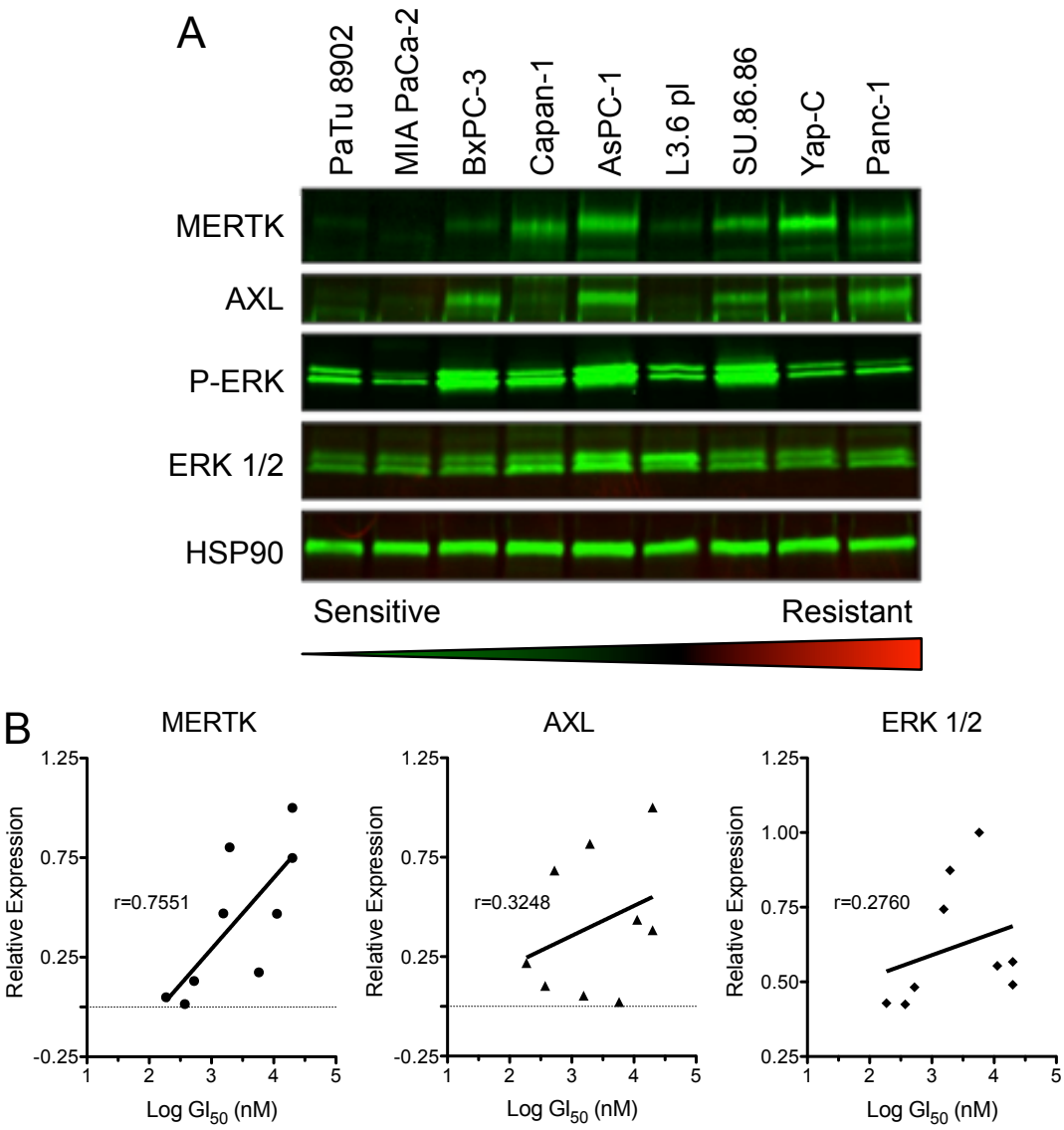

Figure 3.2 Protein Validation of MERTK as a Marker of Resistance. *A)* qWestern blots from 9 randomly selected PDAC cell lines arranged in increasing resistance to AZD6244 based on GI_{50} values. *B)* Quantification of the qWestern blot data reveal the correlation of MERTK (p=0.0186, r=0.7551) with increasing GI_{50} values but no correlation is seen between AXL or ERK 1/2 and GI_{50} values.

treated the conditioned cell line with varying concentrations of AZD6244 and measured cell growth to construct the same dose response curves as in Chapter 2. When plotted against MIA PaCa-2's original inhibition curve, a clear shift in the GI_{50} value is seen. Originally 360 nM, conditioning increases the GI_{50} value over 20-fold to 7.5 μM (Fig. 3.3). qWestern blot analysis compared normal and conditioned MIA PaCa-2 cells with and without drug incubation (3 days with AZD6244) for the effects on MERTK and AXL (Fig. 3.4A). Interestingly, MERTK is upregulated ~2-fold after conditioning, but, more significantly, it is upregulated 3-fold over baseline in the presence of the inhibitor. AXL is upregulated (~3 fold) after acute inhibition of AZD6244 and remains high in the conditioned lines, even without the presence of the inhibitor (Fig. 3.4B). These findings suggest that both MERTK and AXL may be important for acquired resistance to MEK inhibition in MIA PaCa-2 cells.

Several reports indicate that Gas6 may also be important in cancer progression (212, 213). With both MERTK and AXL protein expressions elevated in conditioned cells, we suspected their ligand, Gas6, might be elevated as well. Therefore, qPCR for *GAS6* was performed to compare the 4 different MIA PaCa-2 conditions (Normal, Inhibited, Conditioned, and Conditioned + Inhibited). We found the transcript expression of *GAS6* to be elevated in the presence of the AZD6244 inhibitor for both normal and conditioned cell lysates (Fig. 3.5A). Further, protein expression levels from qWestern blotting showed elevated Gas6 in inhibited, conditioned and inhibited + conditioned cells (Fig. 3.5B).

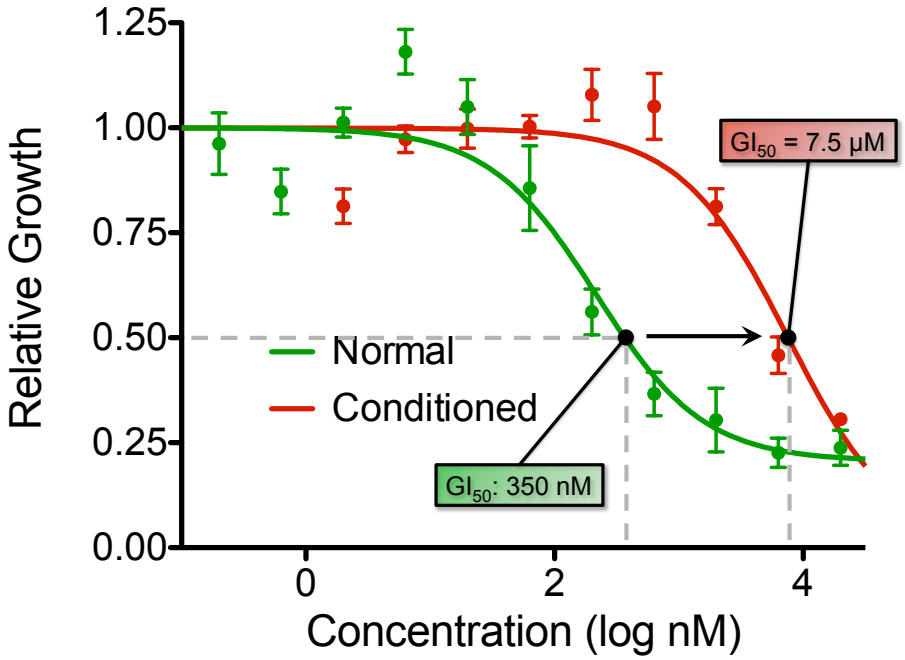

Figure 3.3 MIA PaCa-2 Conditioning. MIA PaCa-2 cells were treated with 2 µM of AZD6244 for 2 months to condition them to the inhibitory effects. Subsequently, the cell line showed a 20 fold increase in resistance to the inhibitor, increasing GI_{50} from 0.35 µM to 7.5 µM.

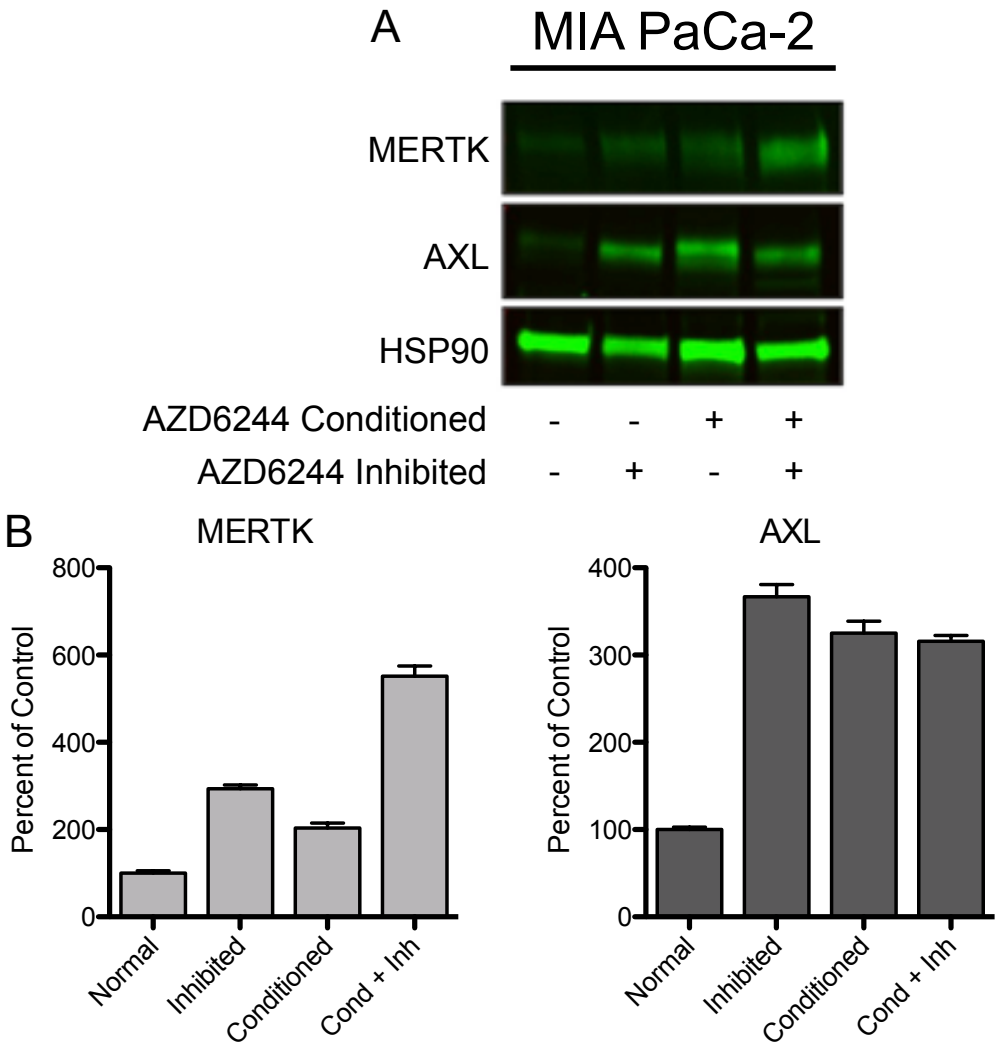

Figure 3.4 Difference in protein expression levels between untreated and conditioned MIA PaCa-2 cells. *A)* qWestern blot showing increased expression of MERTK and AXL when exposed to various conditions of AZD6244. *B)* Quantification of the qWestern blot data.

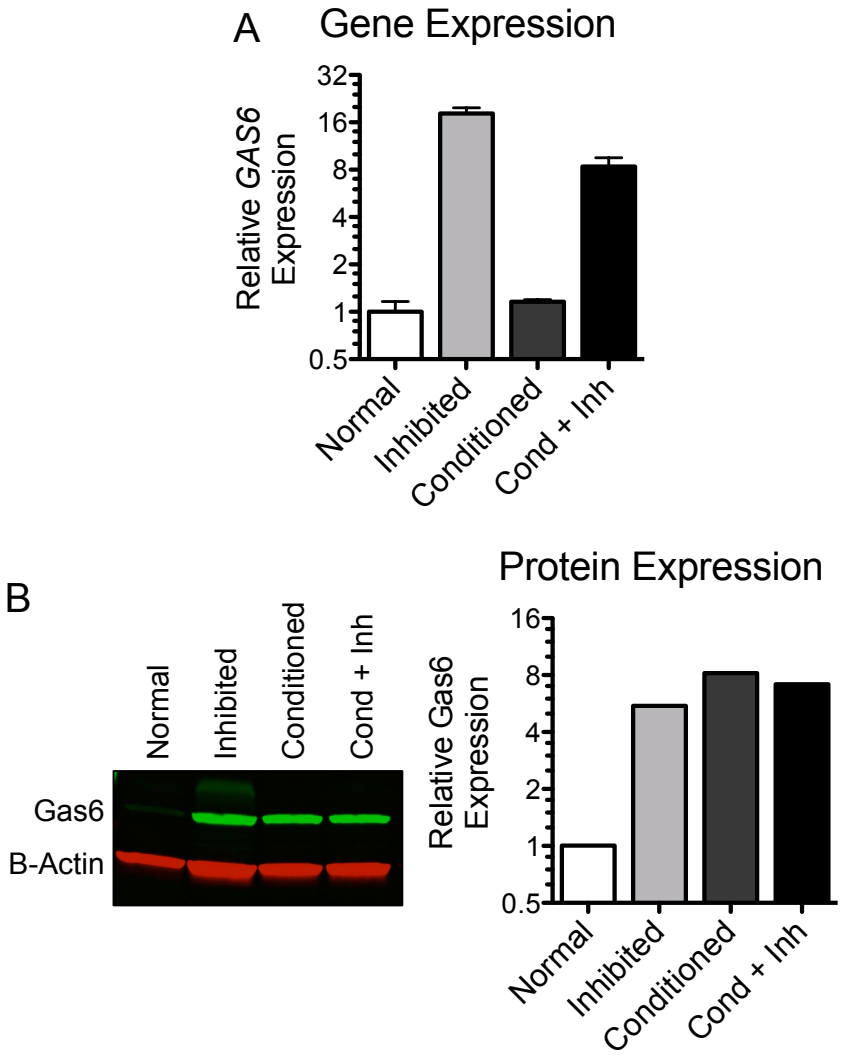

Figure 3.5 Difference in Gas6 expression levels between untreated and conditioned MIA PaCa-2 cells. *A)* qPCR for GAS6 in different conditions (normal, inhibited, conditioned, conditioned + inhibited) of MIA PaCa-2 cells. B) qWestern blotting *(left)* for Gas6 in the various MIA PaCa-2 cell conditions and quantified (*right)*.

3.2.3. MERTK is Important in Cancer Cell Viability

Being a receptor tyrosine kinase that is overexpressed in cell lines with innate resistance to MEK 1/2 inhibition, we hypothesized that MERTK could actively be contributing to the cells' resistance. MERTK can activate a number of effector molecules including the PI3K-AKT pathway (199), which has been reported to contribute to MEK inhibition resistance (142, 214, 215). Further, MERTK becoming upregulated when cells acquired a resistance to AZD6244 supports the theory that the receptor activates compensatory pathways to alleviate the effects of MEK 1/2 inhibition and therefore may serve as a therapeutic target. We further hypothesized that the loss of MERTK signaling, via knockdown or inhibition, would be an effective means of decreasing cancer cell growth and would synergize with MEK 1/2 inhibition.

Stable knockdown lines using shRNA targeted to *MERTK, AXL* (for comparison) and green fluorescent protein *(GFP;* negative control*)* were created in the resistant lines SU.86.86 and Yap-C. Knockdown of MERTK expression in Yap-C cells was lethal and therefore we could not include shMERTK Yap-C cells in these experiments. qWestern blotting confirmed the successful knockdown of each protein (Fig. 3.6A). In cell proliferation studies using a CellTiter-Glo luminescent assay, we found MERTK knockdown to have statistically significant (p=5.01E-5) growth retardation in the SU.86.86 cell line by approximately 25%. AXL knockdown also had an effect in Yap-C (p=3.30E-4, 27% reduction) but no effect in SU.86.86 (Fig. 3.6B).

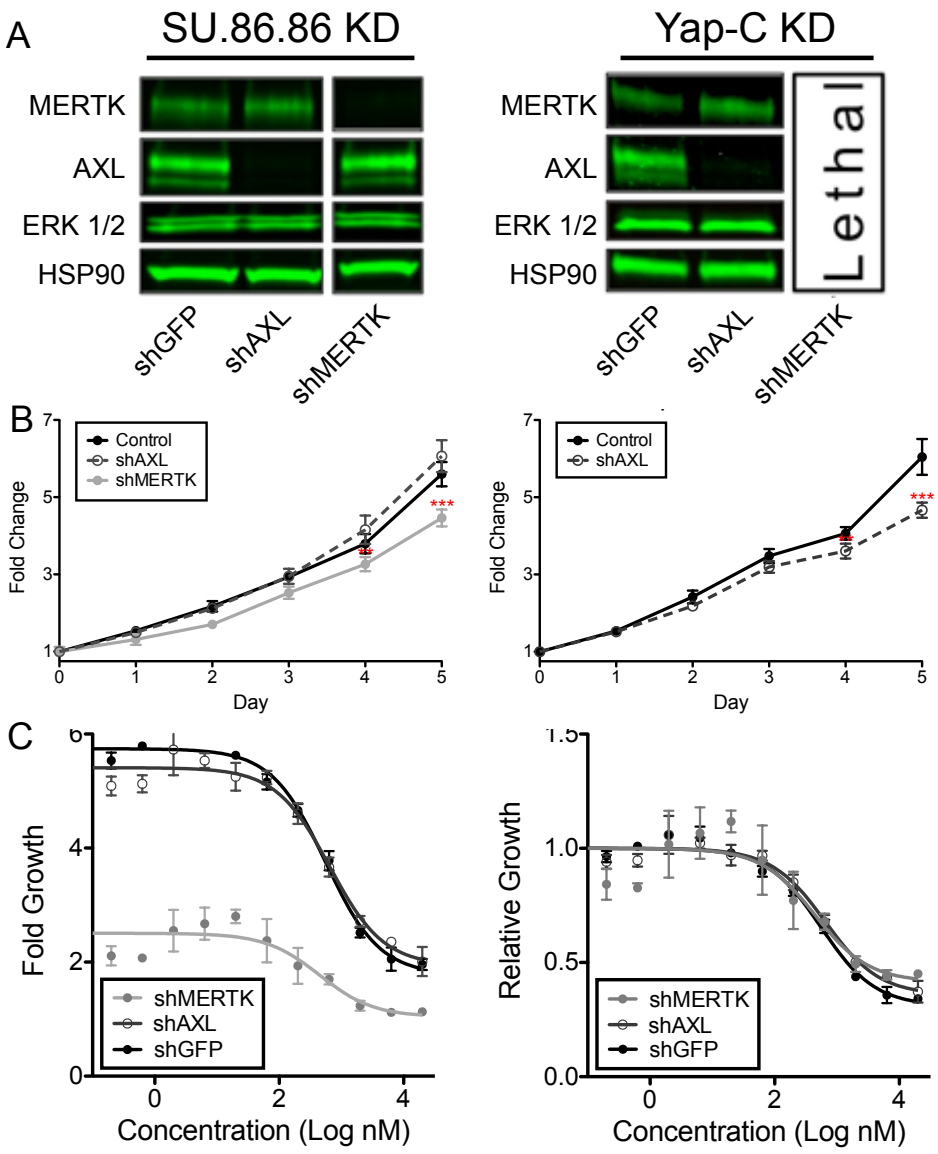

Figure 3.6 *shRNA* growth studies. *A)* Knockdown of MERTK and AXL by *shRNA* for SU.86.86 and Yap-C cell lines – confirmed by qWestern. Knockdown of *MERTK* in Yap-C was found to be lethal. *B)* Growth studies for the SU.86.86 *(left)* and Yap-C *(right)* knockdown lines show shMERTK to significantly slow growth. shAXL slows growth in Yap-C but not SU.86.86. Statistics are shown for days 4 and 5. *C)* AZD6244 inhibition curves *(left)* for SU.86.86 show no decrease in cellular growth with shAXL but slowed growth with shMERTK. Normalization of the inhibition curves *(right)* show no shift in the GI_{50} values. Denotations: * $p \leq 0.05$, ** $p \leq 0.01$, *** $p \leq 0.001$.

We further tested the knockdown lines' dose response to AZD6244. After 3 days of growth under various levels of MEK 1/2 inhibition, shGFP and shAXL SU.86.86 cell lines had very similar response curves, whereas shMERTK has much less growth at all concentrations of the inhibitor. However, when we normalize the curves to max growth, all three curves were essentially the same with no difference in AZD6244 GI_{50} values (Fig. 3.6C). It appears that MERTK is important for cell growth, but knocking down the protein does not sensitize cells to MEK inhibition.

3.2.4. Acute Knockdown of MERTK by siRNA

One observation we noticed when performing the two sets of experiments (growth and inhibition curves) was a discrepancy between overall cell growth with MERTK knockdown between the two assays. Chronologically, the dose response curve experiments were performed first, with the growth assays being conducted a few weeks later. In this time, it appears that the cells might have started to become resistant to the knockdown effects. Therefore, we performed experiments using transient siRNA where we did not need to select for a colony with stable knockdown. This allowed us to study the effects of MERTK knockdown before cells could develop a resistance.

We performed siMERTK transfection in 6 cell lines (HPDE, PaTu 8902, MIA PaCa-2, SU.86.86, Yap-C and Panc-1) with varying degrees of AZD6244 sensitivity. Cell proliferation studies were performed over 6 days, starting on the day of transfection, to compare the effects of siMERTK to siControl. Of the 3

sensitive lines, only MIA PaCa-2 showed significant growth inhibition after treatment with siMERTK, whereas all 3 of the resistant lines had significantly slowed growth rates (Fig. 3.7). Most of the separation in growth curves began after day 3, around the time the siMERTK had maximal effect (Fig 3.7 Inset).

3.2.5. Preliminary Examination of MERTK Signaling

To identify possible signaling pathways that MERTK could be affecting, we wanted to compare the phosphorylation of key signaling proteins with and without MERTK knockdown. From literature, we knew MERTK could activate the PI3K-AKT, MAPK-ERK and PLCγ pathways (204) but as an RTK, the receptor can active a number of other pathways. Through which pathway MERTK was predominantly signaling in PDAC was still unclear. Therefore, we elected to use a Proteome Profiler™ Phospho-Kinase array (R&D Systems) modified for use on a Li-Cor imager for more quantitative results. This assay allowed us to measure the changes in the site-specific phosphorylation of 43 kinases and 2 related total when MERTK was knocked down (Fig. 3.8). Comparing SU.86.86 siMERTK to siControl cells, we found Pyk2 to be the most decreased phospho-protein in the array. PLCγ and AKT (T308) were also less phosphorylated in *siMERTK* cells; as two of MERTK's most prominent effector pathways, it is logical that these would become less active. Interestingly, many MAPK pathway proteins including p38, JNK, and ERK all became more active with the loss of MERTK. The complete list of phospho-protein changes is found in Table 3.1.

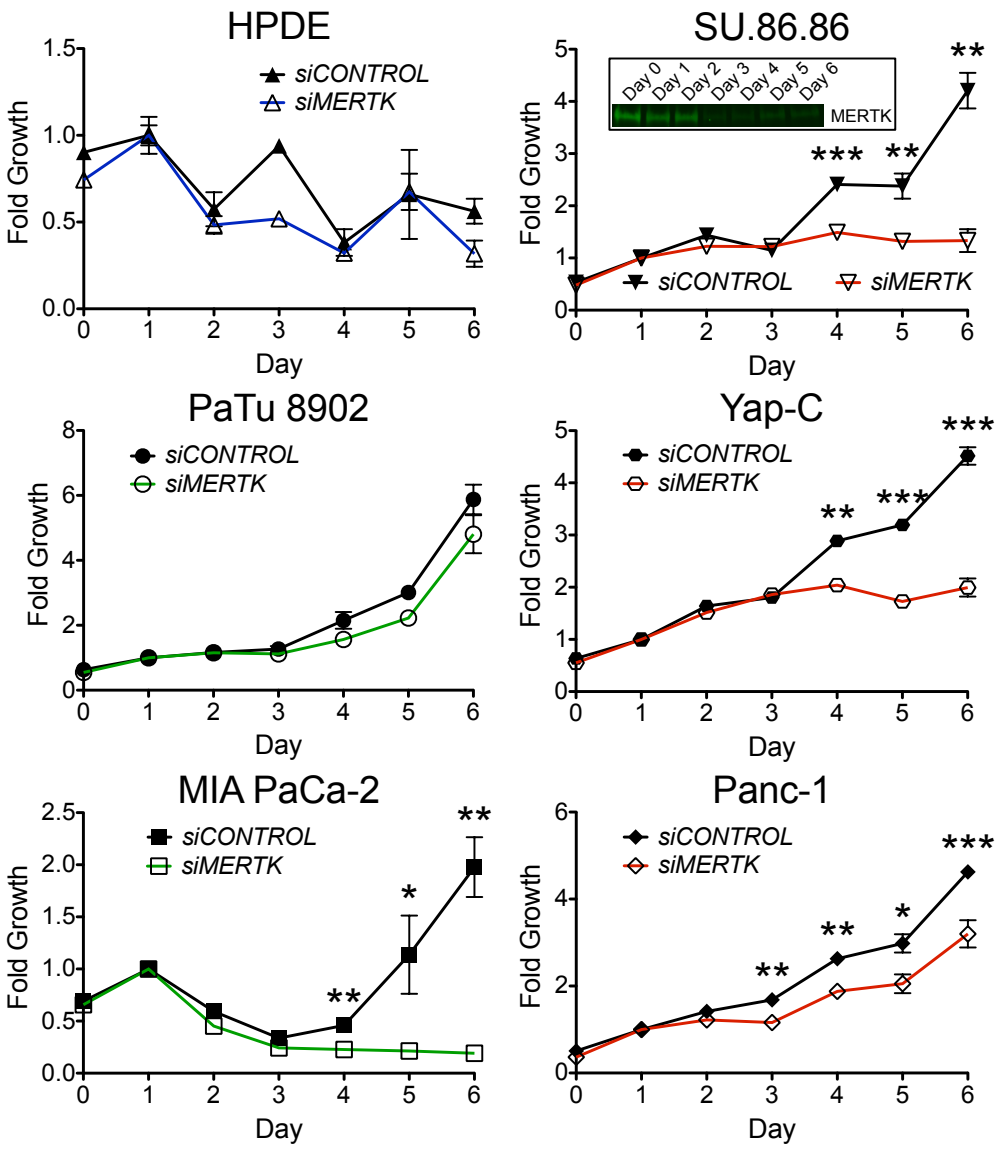

Figure 3.7 Proliferation studies with MERTK knockdown by siRNA. 6 lines were treated with *siMERTK* or *siCONTROL* and cell growth monitored for 6 days. Cell growth was measured by the amount of ATP activity and compared to untreated cells. Denotations: * p≤0.05, ** p≤0.01, *** p≤0.001.

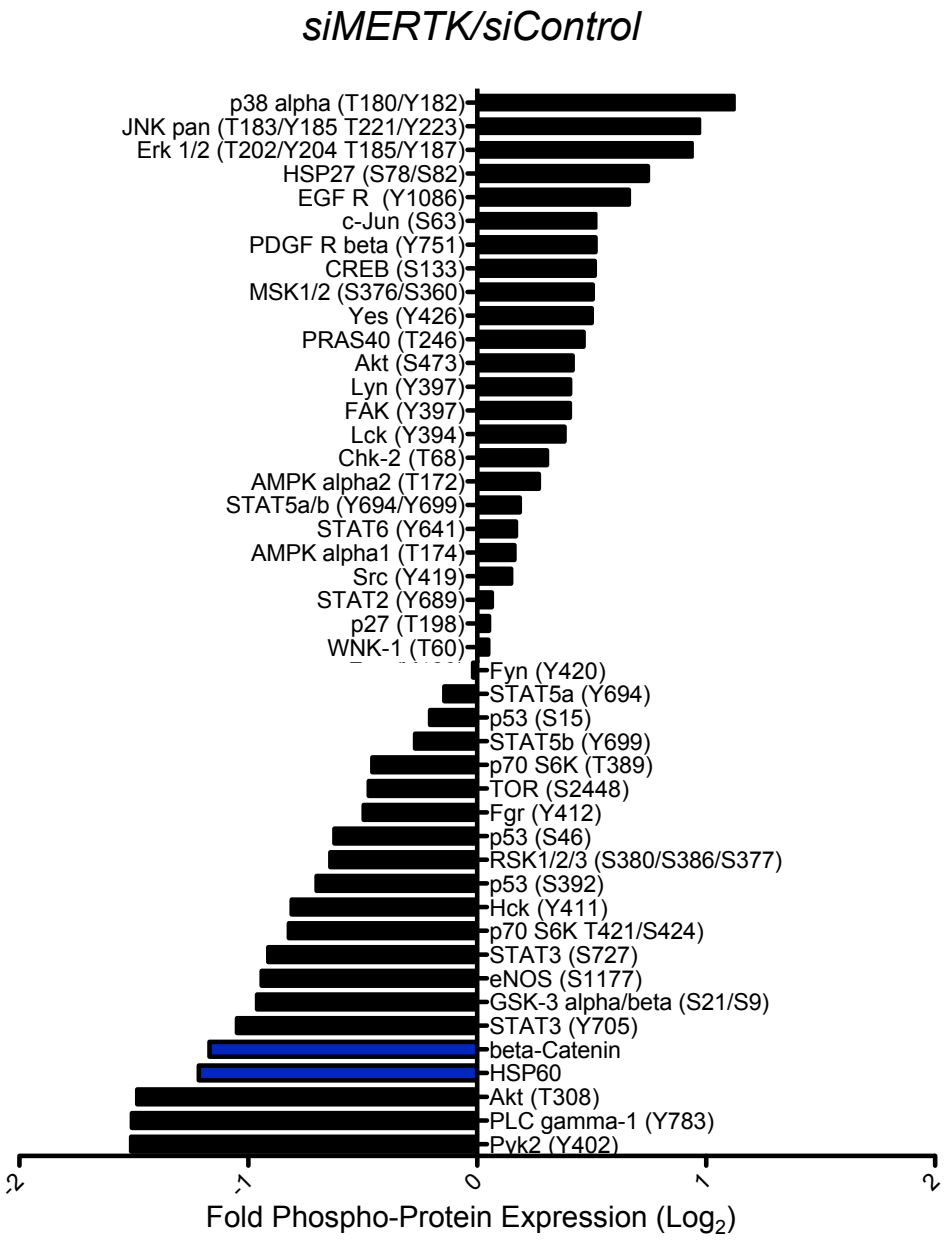

Figure 3.8 Difference in protein phosphorylation between siMERTK and siControl SU.86.86 cells. Phospho-proteome assay results show the changes in kinase activity when *MERTK* is knocked down compared to control. AKT and STAT3 are down regulated while the MAPK proteins become more active with the loss of *MERTK*

Target	Fold Change	Target	Fold Change
Pyk2 (Y402)	0.351	STAT2 (Y689)	1.045
PLC gamma-1 (Y783)	0.352	Src (Y419)	1.108
Akt (T308)	0.357	AMPK alpha1 (T174)	1.120
HSP60	0.431	STAT6 (Y641)	1.125
beta-Catenin	0.445	STAT5a/b (Y694/Y699)	1.138
STAT3 (Y705)	0.483	AMPK alpha2 (T172)	1.205
GSK-3 alpha/beta (S21/S9)	0.514	Chk-2 (T68)	1.235
eNOS (S1177)	0.521	Lck (Y394)	1.303
STAT3 (S727)	0.531	FAK (Y397)	1.325
p70 S6K T421/S424)	0.566	Lyn (Y397)	1.326
Hck (Y411)	0.570	Akt (S473)	1.336
p53 (S392)	0.615	PRAS40 (T246)	1.380
RSK1/2/3 (S380/S386/S377)	0.641	Yes (Y426)	1.415
p53 (S46)	0.649	MSK1/2 (S376/S360)	1.419
Fgr (Y412)	0.709	CREB (S133)	1.429
TOR (S2448)	0.720	PDGF R beta (Y751)	1.432
p70 S6K (T389)	0.728	c-Jun (S63)	1.434
STAT5b (Y699)	0.829	EGF R (Y1086)	1.583
p53 (S15)	0.867	HSP27 (S78/S82)	1.677
STAT5a (Y694)	0.905	Erk 1/2 (T202/Y204 T185/Y187)	1.920
Fyn (Y420)	0.988	JNK pan (T183/Y185 T221/Y223)	1.964
WNK-1 (T60)	1.034	p38 alpha (T180/Y182)	2.180
p27 (T198)	1.037		

Table 3.1 Differential kinase activity between siControl and siMERTK SU.86.86 cells.

3.2.6. UNC569, a MERTK Inhibitor, in Combinatorial Therapies with AZD6244

Lastly, we wanted to determine if the use of a MERTK inhibitor could be used in combination with AZD6244 to enhance the effects of MEK 1/2 inhibition. UNC569 is a pyrazolopyrimidine and the first small molecule inhibitor for MERTK. Although specific for MERTK, it can inhibit all members of the TAM family (MERTK: IC_{50}=2.9 nM, AXL: IC_{50}=37 nM, TYRO-3: IC_{50}=48 nM) (216). Testing the dose response of several cell lines, we found GI_{50} of this inhibitor to be comparable to AZD6244 (Fig. 3.9A), but a different set of lines was sensitive and resistant with no significant correlation (r=0.302, p=0.396) to the MEK 1/2 inhibitor (Fig. 3.9B).

To test the effects of this inhibitor in combination with AZD6244, we selected a single concentration of UNC569 near the GI_{50} of most cell lines, 2 μM, and tested this with varying concentrations of AZD6244. Using 9 different cell lines, we constructed dose response curves under the dual inhibition and compared them to curves of AZD6244 alone (Fig. 3.10A). Using a 1-log unit change in the GI_{50} of AZD6244 as a threshold value for a positive effect, we found only 1 line (Capan-1) to become more sensitive to MEK inhibition with MERTK combinatorial therapy (Fig. 3.10B). Based on these results, targeting MERTK in conjunction with MEK 1/2 does not appear to be a good strategy for therapy.

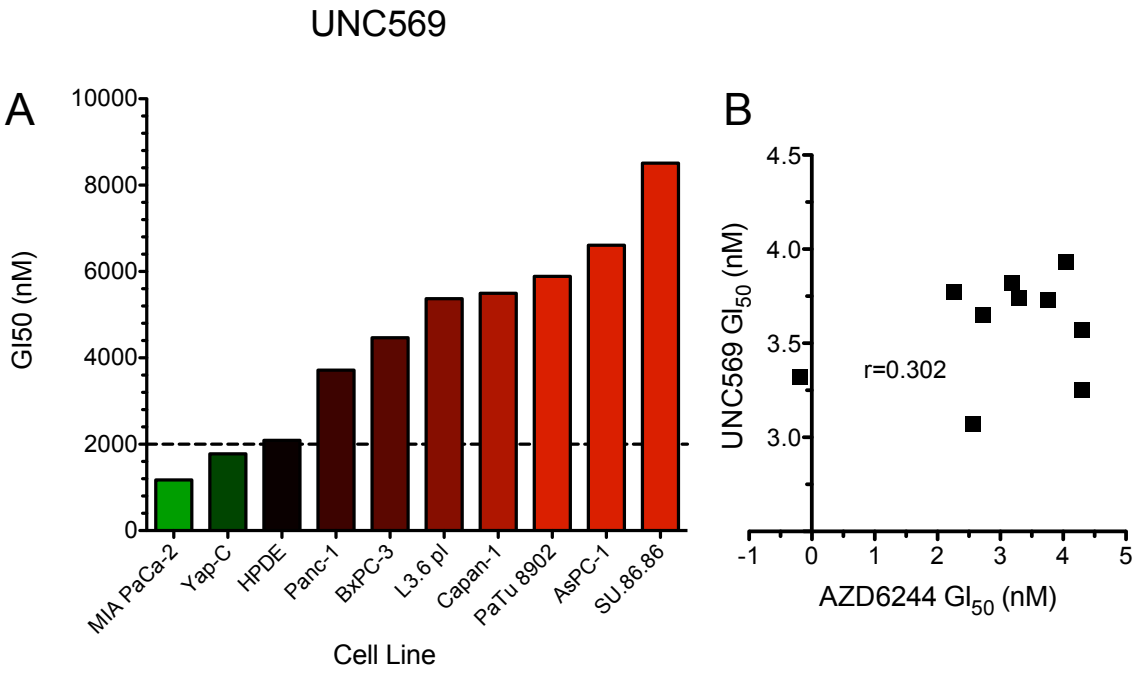

Figure 3.9 Cell line sensitivities in response to the MERTK inhibitor UNC569. *A)* From does response curves using UNC569, GI_{50} values for a panel of cell lines show a low potency of SP600125. *B)* Correlation analyses comparing cell line sensitivities to UNC569 and AZD6244. No correlation was seen between these inhibitors.

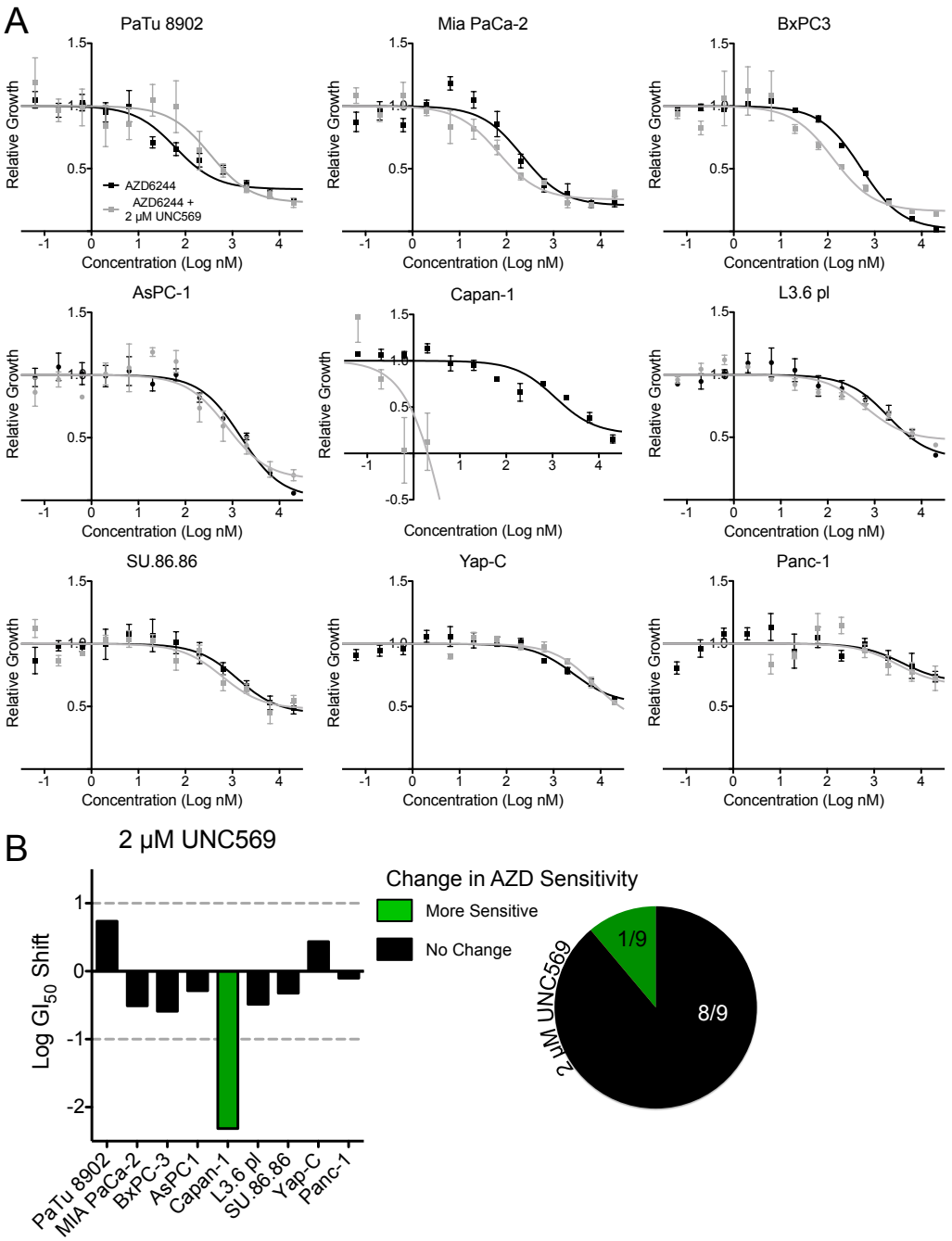

Figure 3.10 Combinatorial therapies using MEK inhibition with the MERTK inhibitor. *A)* 9 Cell lines were tested for inhibition curves using AZD6244 alone or in combination with 2 μM UNC569 (MERTKi). Only Capan-1 shows a combinatorial benefit by a shift in GI_{50}. *B)* Evaluation of the overall combinatorial effects in the 9 lines revealed a >1 log unit shift in GI_{50} value for 1 of the 9 lines.

3.3. Discussion

3.3.1. MERTK, AXL and Gas6 in Acquired Resistance

When we examined MERTK, AXL and Gas6 expression levels in MIA PaCa-2 cells under four different conditions (normal, inhibited, conditioned, conditioned + inhibited) we found all three to increase in expression when the cells are conditioned. Interesting, both Gas6 and AXL had the same elevated expression in any condition that involved the AZD6244 inhibitor whereas MERTK expression was more tied to the duration of which the cells had been exposed to the inhibitor. Because there was no difference between acute exposure and prolonged exposure (and subsequently acquired resistance) to MEK 1/2 inhibition, AXL and Gas6 may not serve as the best marker of acquired resistance. MERTK however continued to increase expression, showing some increase with 3 days of inhibition and maximal expression after conditioning and inhibition.

3.3.2. MERTK Signal Activation

MERTK, AXL and TYRO-3 all share the common ligand Gas6. Gas6 has been shown to have fairly equal affinity for AXL and TRYO-3, but 3-10 fold less for MERTK (217). Gas6's preference to bind AXL might be why AXL is reported more often in cancer literature. Protein S has also been reported as a MERTK ligand; it can bind TYRO-3 as well, but not AXL. Galectin-3 (Gal-3) was recently discovered as a ligand for MERTK that signals "eat-me" for macrophage phagocytosis (218). Two other ligands for MERTK, tubby and tubby-like protein 1

(Tulp1) have also been recently discovered (219). The multiple ligands for MERTK could play a large role in why we see differential overexpression of MERTK and AXL in literature, and why they seem to play slightly different roles in cancer. To add further complexity, both AXL and MERTK can homodimerize and self-activate without the need for a ligand (220, 221). Further understanding of MERTK activation may be key to any use of MERTK as a therapeutic target.

3.3.3. MERTK Signaling

From the siMERTK studies, we found the most decreased phospho-proteins without MERTK to be Pyk2, PLCγ, and AKT. Decreased PLCγ, and AKT phosphorylation with MERTK knockdown makes sense because both are known to be downstream of MERTK. Pyk2 however is less straightforward. Pyk2 is a member of the focal adhesion kinase family and is typically associated with calcium channels, MAPK cascades and apoptosis (222-227). Exactly what role it has in MERTK signaling, or if it's a red herring, still needs to be determined. When we look at the proteins that have increased phosphorylation without MERTK, p38 and JNK top the list. These are both modulators of extracellular stress and can contribute to apoptosis. If the loss of MERTK puts a strain on the cells, it is understandable for these signals to increase.

3.4. Materials and Methods

3.4.1. Antibodies and Drugs

The small molecule inhibitors AZD6244 (MEK 1/2 inhibitor) and UNC569 (MERTK inhibitor) were purchased from Selleck Chemical and Millipore respectively. They were prepared in dimethyl sulfoxide (DMSO) with stock concentrations of 10 mM. Primary antibodies were purchased from Cell Signaling Technology [AXL (C89E7), p44/42 MAPK (Erk1/2) (137F5), P-p44/42 MAPK (Erk1/2) (D13.14.4E), HSP90 (C45G5), β-actin (8H10D10), Mer (D21F11)] and R&D Systems [GAS6 (AF885)]. All secondary antibodies were purchased from Li-Cor [Donkey α-Goat 800CW (926-32214), Donkey α-Mouse 680 (926-32222), Donkey α-Mouse 800CW (926-32212), Donkey α-Rabbit 800CW (926-32213), Streptavidin 800CW (926-32230)].

3.4.2. Cell Culture

9 different PDAC cell lines and one transformed normal pancreatic cell line were used in this study. All cell lines except PaTu 8902, L3.6 pl and HPDE were acquired from American Type Culture Collection (ATCC). The PaTu 8902 line was purchased from the german culture core Deutsche Sammlung von Mikroorganismen und Zellkulturen (DSMZ). L3.6 and HPDE were both obtained from Dr. Craig Logsdon (University of Texas, MD Anderson Cancer Center). AsPC-1, BxPC-3, MIA PaCa-2, PaTu 8902, SU.86.86 and Yap-C were all growth in Roswell Park Memorial Institute (RPMI) medium supplemented with 10% (vol/vol) fetal bovine serum (FBS), 1% penicillin-streptomycin (pen-strep; ATCC

30-2300), and 2mM L-glutamine (L-glut). L3.6 and Panc-1 were grown in Dulbecco's Modified Eagle's Medium (DMEM) supplemented with 10% (vol/vol) FBS, 1% pen-strep, and 2mM L-glut. Capan-1 cells were grown in Iscove's Modified Dulbecco's Medium (IMDM) supplemented with 20% (vol/vol) FBS, 1% pen-strep, and 2 mM L-glut. Lastly, HPDE cells were cultured in Keratinocyte Growth Kit (ATCC PCS-200-040). All cells were incubated at 37°C, 5% CO_2.

MIA PaCa-2 conditioning was performed using the same growth medium as indicated above supplemented with 2 μM AZD6244. After cell culture in this medium occurred for 2 months, the cells were considered "conditioned". From this point forward, they remained in the AZD6244 medium unless otherwise indicated.

3.4.3. Western Blots

All cell lines used for blots were grown to ~90% confluency in 10 cm culture dishes before being lysed in 300 μL of lysis buffer [PBS plus 1% Triton X-100, 1x protease/phosphatase inhibitor (Cell Signaling Technologies)]. Quantification of protein concentrations was performed using a bicinchoninic acid (BCA) assay (Pierce) to ensure even loading between samples. Loading dye (3x) plus Dithiothreitol (DTT, New England Biolabs) was added before heat denaturation and run on 4-15% TGX gels (Bio-Rad). Proteins were transferred to polyvinylidene difluoride (PVDF) membranes and incubated with the appropriate antibodies. Quantitative western (qWestern) blots were performed using fluorescent secondary antibodies (800 and 680 nm, Li-Cor) and a Li-Cor

Odyssey imager. Quantification was performed using the manufacturer's software. Correlation analyses with GI_{50} values were performed by calculating the Pearson product-moment correlation coefficient (r) using the Prism software.

3.4.4. Dose Response Curves

Cell lines were plated in two 96 well plates at a concentration of 2,500 cell/well. After 24 hrs, fresh media containing concentrations of AZD6244 or UNC569 ranging from 20 μM down to 63.2 pM by half-log units were added to each well in triplicate, after which the cells were incubated for three additional days. For combinatorial studies using UNC569, every well had a constant dose of the MERTK inhibitor (2 μM) and the concentration of AZD6244 was varied. The second plate was used for an initial, "Day 0" reading. These cells were washed 3 times with phosphate buffered saline plus calcium and magnesium (PBS+) then fixed with 4% paraformaldehyde (PFA). The cells were again washed then incubated in Syto® 60 dye (Life Technologies) diluted 1:3,000 in PBS+ for 1 hr. Cells were subsequently washed 6 times and imaged using a Li-Cor Odyssey at the 680 wavelength. Quantification was performed using the Li-Cor software. After the three-day incubation the inhibited cells in the first plate were processed the same way and quantified with the imager. Inhibition curves were reconstructed in Prism software using a 3-parameter (Bottom, Top, and IC_{50} with the hill slope constrained to -1) dose response curve. The equation used was $Y=Bottom + (Top-Bottom)/(1+10^{((X-LogIC_{50})))}$. The curves were adjusted by subtracting the Day 0 intensity (therefore y=0 indicates no growth) and the top of the curve adjusted to 1 (maximal growth). The result was a curve that had a

max value of 1, and when it crossed the x-axis indicated zero growth. GI_{50} values were then calculated from these curves for the concentration of inhibitor that caused a 50% decrease in cell growth. Combinatorial dose response curves were performed using 2 inhibitors, one of which was held constant throughout all the wells and the other inhibitor having varying concentrations (performed in triplicate).

3.4.5. qPCR for GAS6

Cells were grown to 90% confluency in 6 well plates. A FastLane cDNA kit (Qiagen) was used to wash, lyse, and extract the RNA from the cells according to the supplied protocol. Reverse transcription was performed at 42°C for 30 minutes to create cDNA. qPCR was performed on the cDNA in triplicate in 96 well plates. A SYBR® Green qPCR kit (Life Technologies) was used to quantify the cDNA expression values. *GAS6* expression was measured and normalized to *GAPDH* for comparison and the experiment performed with three replicates.

3.4.6. shRNA Lentiviral Transduction

Lentivirus pLK0.1 vectors encoding shRNA against human MERTK, AXL and GFP were purchased from Open Biosystems. Cells were seeded on 12-well plates and grown to 50% confluence. The media were replaced by fresh media containing polybrene (4 μg/ml). GFP, MERTK and AXL shRNA lentiviral particles were thawed at room temperature and gently mixed before adding to the cells. Three different ratios of virions to cells were used (1:1, 2:1, and 3:2). The infected cells were incubated overnight and the next morning the media were

replaced to fresh media without polybrene. Stably transfected cells were selected by puromycin treatment (3 µg/mL for SU.86.86 and 2 µg/mL for Yap-C). To further select stable clones, a single colony was isolated using the trypsin method (228). Downregulation of each protein was verified via qWestern.

3.4.7. siRNA Assays

siGENOME pools of four siRNA vectors targeting MERTK were purchased fom GE Healthcare. Cells were seeded in 96 well plates at a concentration of 2,500 cells/well and allowed to adhere overnight. siRNA was prepared as a 5 µM solution in an RNase-free buffer and diluted 1:10 in Opti-MEM (Life Technologies) for a final volume of 10 µL per intended well. DharmaFECT ragent 2 (GE Healthcare) was also diluted 1:50 in a separate tube at a volume of 10 µL/well. Each were allowed to incubate for 5 minutes at room temp. The two tubes were then mixed together and incubated for an additional 20 minutes. 4x the volume of antibiotic-free complete medium was then added to the mixture resulting in a final concentration of 25 nM siRNA. The media on the cells was removed and 100 µL/well of the siRNA medium was added. After 24 hrs, the medium was changed to complete media.

3.4.8. Cell Proliferation Assays

Cells were plated in triplicate using 6 96, opaque walled well plates (one for each day) at a concentration of 2,500 cells/well. After 8 hrs, the number of viable cells in each well of the Day 0 plate was determined by quantifying the ATP presence with a CellTiter-Glo® (Promega) cell viability luminescent assay.

An ATP control (500 nM solution in PBS) was added in triplicate to blank wells, 100 µL/well. 100 µL of CellTiter Glo® reagent, prepared according to protocol, was added to each of the cell and ATP wells. After a 10-minute incubation in the dark, the luminescence of each well was recorded using a FLUOstar OPTIMA microplate reader. Each day the process was repeated using the next cell plate and fresh ATP. Normalization between the days was performed using the ATP well readings.

3.4.9. Phospho-Proteome Analysis

A Human Phospho-Kinase Array Kit (R&D Systems, ARY003B) was used to quantify the activity of 43 kinase phosphorylations and 2 key proteins expression levels. The product protocol was followed with minor alterations. Briefly, siMERTK and siControl cells were lysed with Lysis Buffer 6 (R&D Systems) and agitated for 30 min at 4°C. The array membranes were cut to remove the numbering (they autofluoresce at the 800 wavelength) and blocked with Array Buffer 1 (R&D Systems) for 1 hr then incubated with 350 µg of cell lysates overnight at 4°C under gentle agitation. The membranes were then washed 3 times with the 1x wash buffer (R&D Systems). The membranes were then incubated with biotinylated detection antibodies for 2 hrs at room temperature and washed 3x times with 1x wash buffer. Deviating from the product protocol, we replaced the supplied streptavidin-HRP secondary, with Streptavidin 800CW (diluted in Li-Cor blocking buffer 1:20,000). Membranes were incubated with the secondary for 30 minutes before being washed and

imaged using the Li-Cor imager. Quantification was performed using the Li-Cor software.

Chapter 4

JNK1 as a Marker of MEK 1/2 Inhibition Resistance and a Therapeutic Target in PDAC

4.1. Introduction

Despite MERTK's promise as a marker of MEK 1/2 inhibition resistance, small molecule inhibition studies did not result in sensitization to AZD6244. Therefore, we looked to JNK1 as an alternative therapeutic target. We found *MAPK8*, the gene that codes for JNK1, to be upregulated in resistant pancreatic cancer cell lines. We hypothesized that JNK1 protein expression could serve as both a marker of resistance and a therapeutic target for mono- or combinatorial therapy.

The JNK pathway is predominantly activated by extracellular stress. It is one of the four major MAP kinase pathway, signaling through MLK 2/3 > MEK 4/7 > JNK 1/2/3 > transcriptional factors. The pathway plays an important role in apoptosis, cell growth, differentiation, and immune responses (229-231). The JNK family consists of three different genes (*JNK1, JNK2, JNK3*) with 10 total splice variants (232) and the three proteins act upon multiple different substrates. This creates a complex network and it is difficult to delineate the effects of the pathway's activation (233). JNK is known to interact with and activate over 50 substrates (234), sometimes with converse effects. Such is the case with c-Jun (often pro-apoptotic) and c-Myc (typically pro-growth) but even these molecules can switch function (c-Jun can be pro-survival and c-Myc pro-apoptosis) depending on the cellular context (235). Indeed, the JNK pathway can be difficult to predict and is still an area of active research.

The JNK pathway can also cross talk with other MAPK pathways and shares several effector proteins with the MEK-ERK cascade, potentially creating a redundant pathway that circumvents MEK 1/2 inhibition. Further, negative feedback loops between ERK and JNK are known to exist; inhibiting ERK activity relieves JNK inhibition and vise versa (236). Normally, this might switch a cells signaling from ERK's pro-survival to JNK's pro-apoptotic effects, but in cancer the JNK pathway can be rewired to have pro-survival effects as well – such is the case in melanoma (237). Therefore, we hypothesize that inhibition of JNK will have therapeutic benefits in resistant cell lines and sensitize them to the MEK inhibitor AZD6244.

Similar to MERTK, we first examined JNK1 as a marker resistance. We found JNK1 expression to correlate with innate resistance, but its expression levels were not elevated after acquiring a resistance to the MEK inhibitor. We then evaluated JNK1 as a therapeutic target using knockdown models and small molecule inhibition studies and found significant therapeutic benefits to decreased JNK signaling. Most excitingly, under JNK inhibition, cell lines initially resistant to MEK 1/2 inhibition became sensitive to the AZD6244 inhibitor. These findings support the use of combinatorial therapy targeting both JNK and MEK 1/2 as an avenue of future therapy in pancreatic cancer.

4.2. Results

4.2.1. JNK1 is a Marker of Innate Resistance

As with MERTK, we first examined JNK1 as a marker of resistance in pancreatic cancer. We performed a qWestern blot for JNK1 in the panel of 9 pancreatic cancer lines to get quantitative expression values for JNK1 in each line (Fig. 4.1A). Correlation analysis to GI_{50} values confirmed that elevated JNK1 expression does trend with resistance ($r=0.7832$, $p=0.0107$; Fig 4.1B). To test the proteins utility as a marker of acquired resistance, we used the same conditioned MIA PaCa-2 line as before and blotted for JNK1 in normal, inhibited, conditioned, and conditioned + inhibited cells. Unfortunately, unlike MERTK, which increased in expression level, JNK1 protein levels did not meaningfully change (Fig. 4.1C,D). These findings suggest that JNK1 may serve as a marker of innate resistance, but not acquired resistance.

4.2.2. Altered Pathway Signaling in Acquired Resistant Cells

Despite the total protein level not changing after conditioning, increased JNK1 activity (P-JNK1) could still confer resistance. Furthermore, any number of different pathways could be more active in resistance lines (either innate or acquired) that would not have been detected in the surface receptor dataset or the cDNA microarray. Therefore, we tested normal and conditioned MIA PaCa-2 cell lines in the phospho-kinase array assay to identify signaling molecules that become more active in resistant cells (Fig. 4.2, Table 4.1). We found P-AKT (S473) to be the most increased protein after conditioning. This is

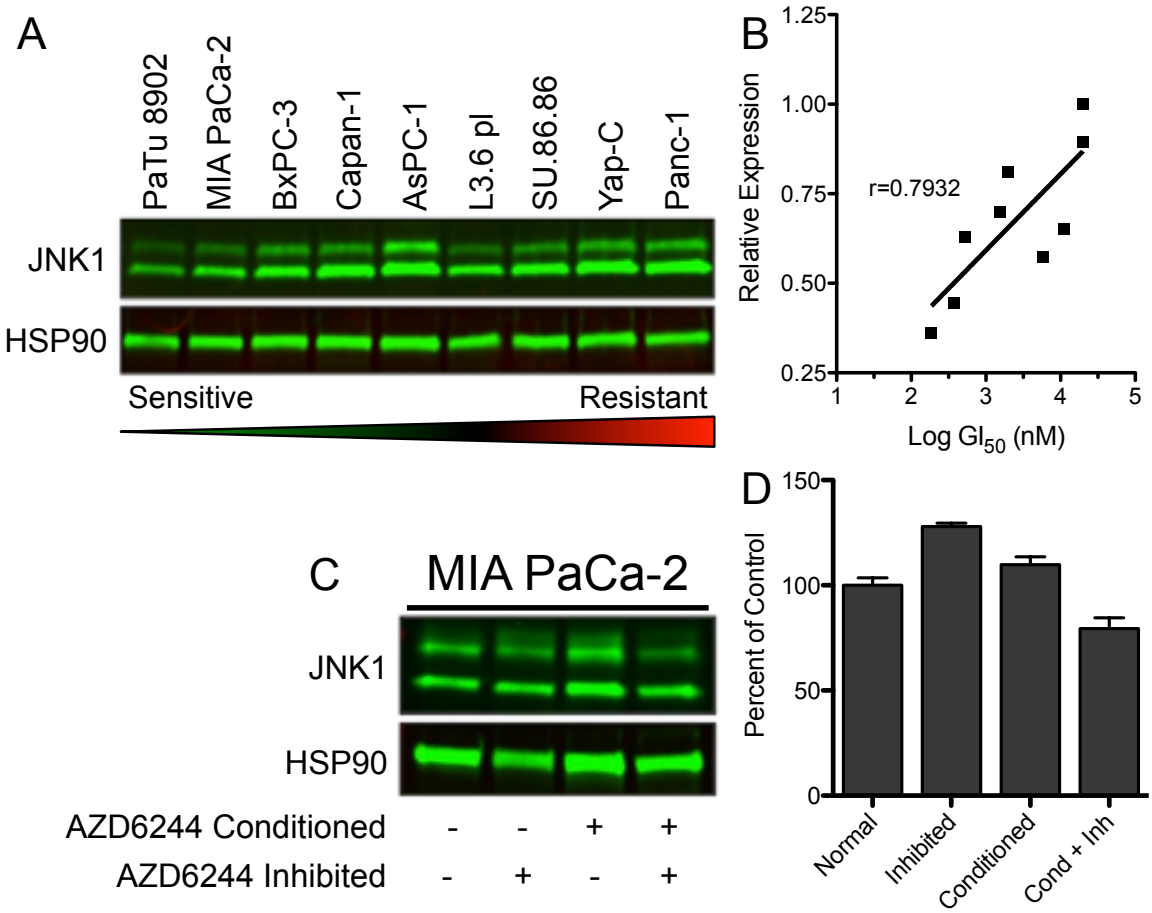

Figure 4.1 Evaluation of JNK1 as a marker of innate and acquired resistance to MEK inhibition. *A)* qWestern blots for JNK1 from 9 PDAC cell lines arranged with increasing resistance to AZD6244 based on GI_{50} values. *B)* Quantification of the qWestern blot data reveal the correlation of JNK1 (p=0.0107, r=0.7932) with increasing GI_{50} values. C*)* qWestern blot showing the protein expression level of JNK1 in the four different conditions of MIA PaCa-2 cells. *D)* Quantification of the qWestern blot data show no increase in JNK1 with acquired resistance.

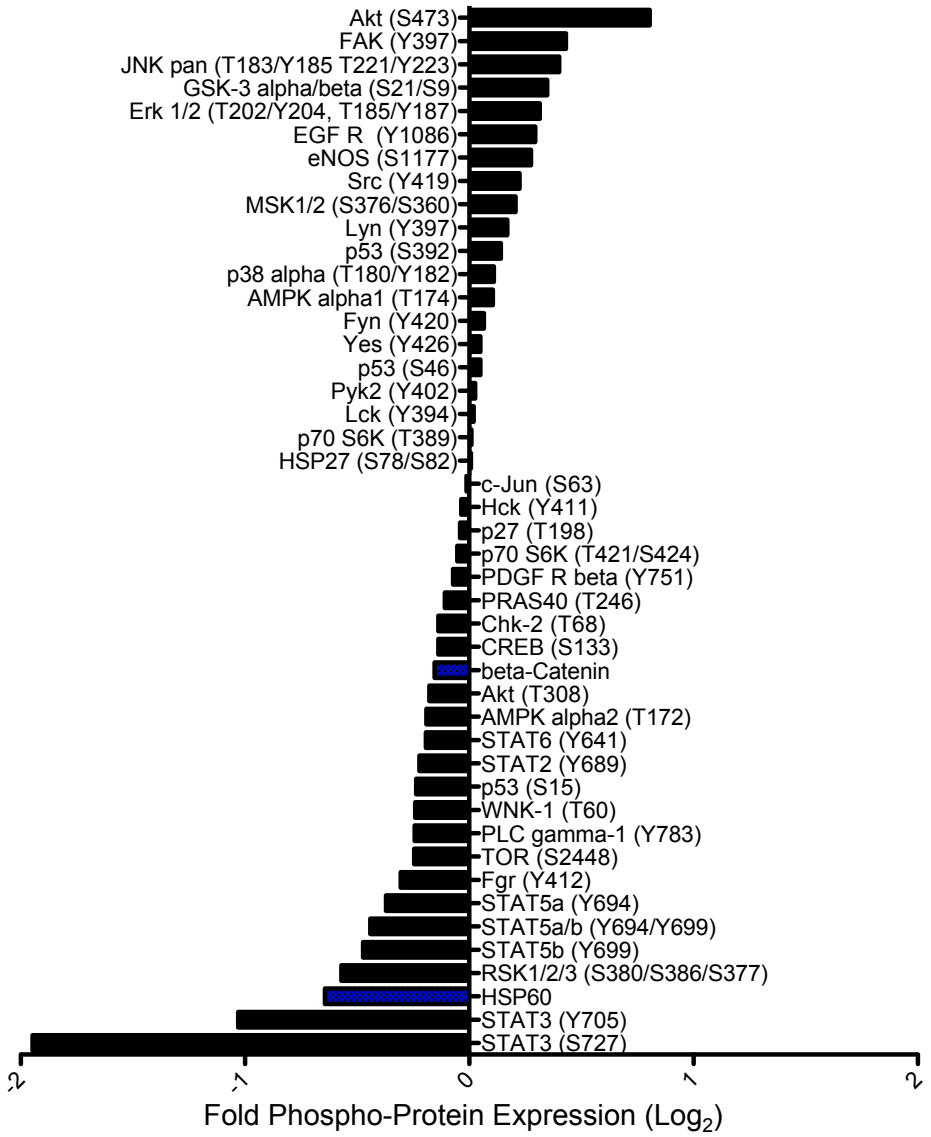

Figure 4.2 Difference in protein phosphorylation between conditioned and normal SU.86.86 cells. Phospho-proteome assay comparing normal to conditioned MIA PaCa-2 cell lines show STAT3 to be less active after conditioning while P-AKT, P-JNK and P-ERK are all upregulated after conditioning.

Target	Fold Change	Target	Fold Change
STAT3 (S727)	0.259	Hck (Y411)	0.976
STAT3 (Y705)	0.490	c-Jun (S63)	0.991
HSP60	0.640	HSP27 (S78/S82)	1.005
RSK1/2/3 (S380/S386/S377)	0.673	p70 S6K (T389)	1.006
STAT5b (Y699)	0.720	Lck (Y394)	1.014
STAT5a/b (Y694/Y699)	0.737	Pyk2 (Y402)	1.018
STAT5a (Y694)	0.773	p53 (S46)	1.035
Fgr (Y412)	0.809	Yes (Y426)	1.035
TOR (S2448)	0.843	Fyn (Y420)	1.046
PLC gamma-1 (Y783)	0.844	AMPK alpha1 (T174)	1.076
WNK-1 (T60)	0.846	p38 alpha (T180/Y182)	1.079
p53 (S15)	0.849	p53 (S392)	1.103
STAT2 (Y689)	0.857	Lyn (Y397)	1.124
STAT6 (Y641)	0.875	MSK1/2 (S376/S360)	1.154
AMPK alpha2 (T172)	0.876	Src (Y419)	1.168
Akt (T308)	0.884	eNOS (S1177)	1.210
beta-Catenin	0.898	EGF R (Y1086)	1.226
CREB (S133)	0.909	Erk 1/2 (T202/Y204 T185/Y187)	1.244
Chk-2 (T68)	0.909	GSK-3 alpha/beta (S21/S9)	1.272
PRAS40 (T246)	0.927	JNK pan (T183/Y185 T221/Y223)	1.320
PDGF R beta (Y751)	0.951	FAK (Y397)	1.348
p70 S6K (T421/S424)	0.964	Akt (S473)	1.747
p27 (T198)	0.972		

Table 4.1 Differential kinase activity between normal and conditioned MIA PaCa-2 cells.

understandable since the AKT cascade is a known compensatory pathway to MEK inhibition. P-JNK (pan) signaling was also increased in conditioned cells, indicating that although total JNK1 protein may not change with conditioning, the pathway might have still become more active. Further exploration into limiting JNK signaling as a therapeutic strategy was needed.

4.2.3. JNK1 Knockdown Greatly Slows Cell Growth

To assess JNK1s importance in cancer cells, we performed stable knockdown lines using shMAPK8 in the resistant lines SU.86.86 and Yap-C. Successful knockdown of JNK1 expression was determined by qWestern blot (Fig. 4.3A). In cell proliferation studies, we found JNK1 knockdown to have profound effect on cell growth. JNK1 knockdown in SU.86.86 and Yap-C resulted in 68% (p=6.6E-9) and 45% (p=2.4E-5) growth reduction respectively (Fig. 4.3B). These results suggest promise for JNK1 as a therapeutic target.

4.2.4. MEK Inhibition In SU.86.86 shMAPK8 Cells

We further tested the SU.86.86 shMAPK8 cells for their response to AZD6244. Using various concentrations of the inhibitor to construct a dose response curve, we found the cells to have very minimal growth at any concentration tested (Fig. 4.4A). This limited growth made it difficult to make any GI_{50} value comparisons. When we normalized the curve to maximal growth, it appears that the response to the MEK 1/2 inhibitor has significantly tempered (Fig 4.4B). We no not believe that this is the case however, rather, knockdown of

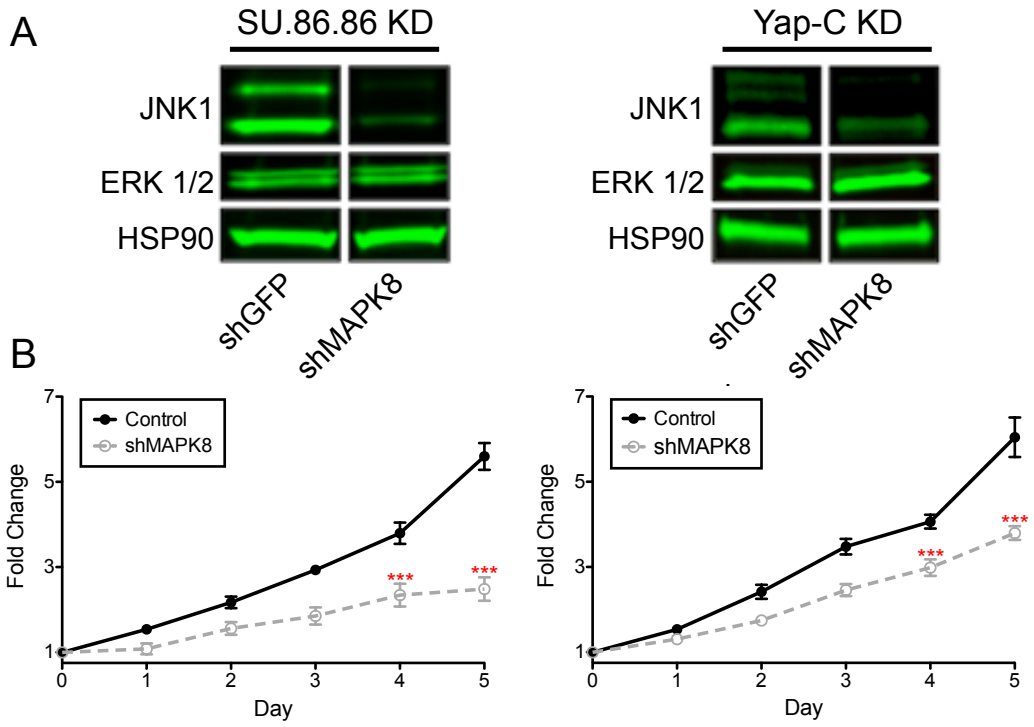

Figure 4.3 *shRNA* growth studies. *A)* Knockdown of JNK1 by *shRNA* for SU.86.86 and Yap-C cell lines – confirmed by qWestern. *B)* Growth studies for the SU.86.86 *(left)* and Yap-C *(right)* knockdown lines show shMMAPK8 to significantly slow growth. Statistics are shown for days 4 and 5. Denotations: * p≤0.05, ** p≤0.01, *** p≤0.001.

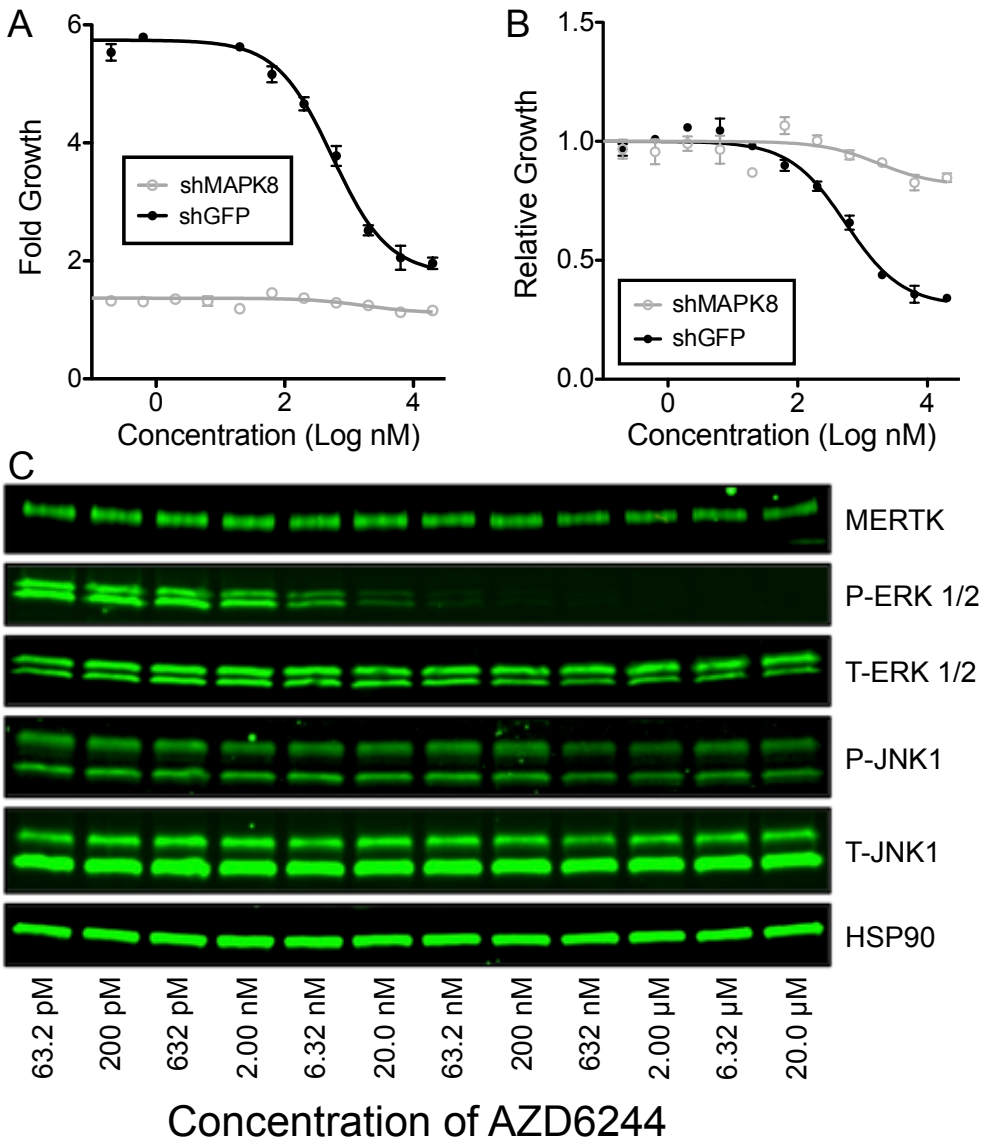

Figure 4.4 JNK1's importance in cellular response to AZD6244 inhibition. *A)* AZD6244 inhibition curves show a sizeable decreased in cellular growth in shMAPK8 cells compared to shGFP cells. *B)* Normalization of the inhibition curves show no positive shift in the GI_{50} value of JNK1 KO cells, but such a small dynamic range of cell growth makes any conclusions difficult. *C)* Protein expression levels with increasing AZD6244 inhibition. Cells were treated with varying concentrations of MEK inhibitor matching those used in the inhibition curves. Protein expression levels for P-ERK show successful inhibition at higher concentrations. No changes in P-JNK were seen at any concentration tested.

JNK1 causes the cells to grow at such a slow rate, accurate results concerning the GI_{50} of AZD6244 cannot be made.

One question we did have from this experiment however was how significant were the effects of off-target inhibition from AZD6244, specifically on MEK 4/7. As a resistant cell line, SU.86.86 required a very high dose of AZD6244 to slow growth (GI_{50}=11.25 μM; Fig. 2.4). At those concentrations, it is reasonable to assume some off target inhibition might be occurring. We were concerned MEK 4/7, being parallel proteins to MEK 1/2, might be the recipients of the off-target inhibition. It follows that because SU.86.86 had substantially slowed in growth with JNK1 KD, the growth reduction in normal SU.86.86 could be from off target effects on MEK 4/7 decreasing JNK1's activity. Therefore, we blotted for P-JNK1 in non-knockdown cells at all concentrations of AZD6244 tested (Fig. 4.4C), but found no effect on JNK1 signaling even at the highest dose tested (20 μM).

4.2.5. The JNK Inhibitor SP600125 Sensitizes Cells to MEK 1/2 Inhibition

As with the MERTK inhibitor UNC569, we tested JNK1 as a therapeutic target by using the JNK inhibitor SP600125. SP600125 is an anthrapyrazolone pan JNK 1/2/3 inhibitor with K_i=190 nM (238). It was selected because of its popularity in literature and medicine for inhibiting JNK proteins. When we tested it on our panel of 9 cell lines, we found it to be less potent than AZD6244 or UNC569 in limiting cell growth (Fig. 4.5A). Therefore, studies using this molecule were performed using 10-fold higher concentrations to account for this. When we

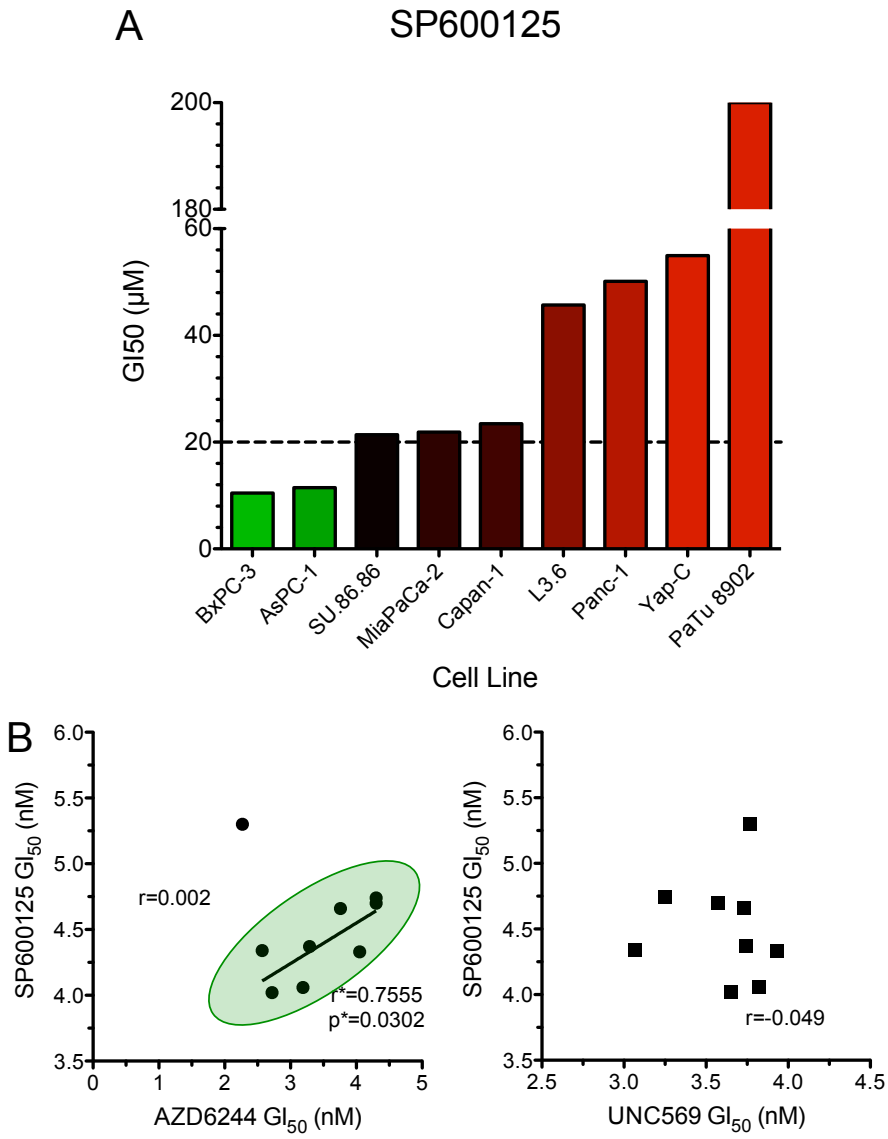

Figure 4.5 Cell line sensitivities in response to the JNK inhibitor SP600125. *A)* From does response curves using SP600125, GI_{50} values for a panel of cell lines show a low potency of SP600125. *B)* Correlation analyses comparing cell line sensitivities to SP600125 and AZD6244 or SP600125 and UNC569. When an outlier is removed, cells resistant to the MEK inhibitor also tend to be resistant to the JNK inhibitor (correlation: p=0.0302, r=0.7555). No correlation was seen between the inhibitors UNC569 and SP600125.

compared the sensitivity of cell lines to JNK inhibition vs. MEK 1/2 we found no correlation (r=0.002), however when the outlier PaTu8902 was removed, we found a significant correlation between cells resistant to MEK 1/2 inhibition and cells resistant to JNK inhibition (r=0.7555, p=0.0302; Fig 4.5B). No correlation was found between the JNK inhibitor and the MERTK inhibitor.

We performed combinatorial studies using 20 μM SP600125 with varying concentrations of AZD6244 to determine if JNK inhibition could sensitize resistant cells to the MEK 1/2 inhibitor (Fig 4.6A). Excitingly of the 9 lines that we tested, 4 showed a positive shift in their GI_{50} value by over 1 log unit. All 4 lines were initially classified as resistant, but when we add the JNK inhibitor their GI_{50} values fell closer to the "sensitive" groups range. Interestingly, 1 sensitive cell line did have a negative shift in GI_{50} from the combinatorial therapy, becoming over a log unit more resistant than monotherapy (Fig. 4.6B). It is unclear why this occurred. Nonetheless, using a combination of JNK and MEK 1/2 inhibitors in cell lines that are resistant to MEK 1/2 inhibition alone appears to be a promising therapeutic strategy.

4.2.6. In Vivo *Use of Combinatorial SP600125-AZD6244 Therapy*

To expand on our *in vitro* findings, we tested the combination of JNK and MEK 1/2 inhibitors in animal tumor models. We created tumors using SU.86.86 cells injected subcutaneously in the backs of mice (2 per mouse). After the tumors became palpable, (approximately 200 mm^3), the mice were broken into four groups: Control, AZD6244, SP600125, or combinatorial therapy. AZD6244

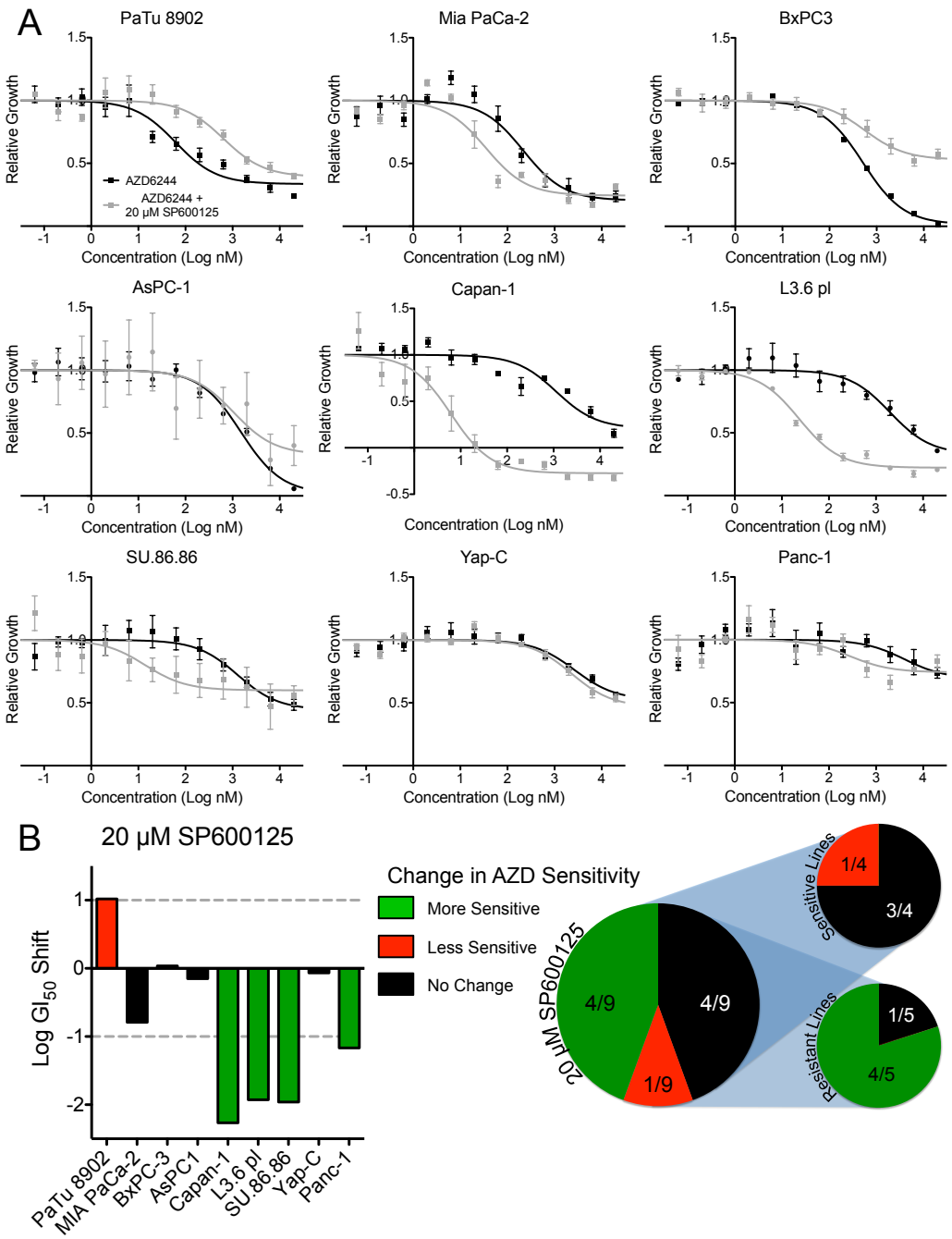

Figure 4.6 Combinatorial therapies using MEK inhibition with the JNK inhibitor. *A)* 9 Cell lines were tested for inhibition curves using AZD6244 alone or in combination with 20 μM SP600125 (JNKi). Several curves show no combinatorial effects and others exhibit a sizeable shift in GI_{50}. *B)* Evaluation of the overall combinatorial effects in the 9 lines revealed a >1 log unit shift in GI_{50} value for 4 of the 9 lines and 1 line became less sensitive by over 1 log unit.

was administered at 2.5 mg/kg *bid* and SP600125 at 12 mg/kg (10 fold higher molar concentration than AZD6244). Treatment was given over a 3-week period, *bid*, and tumors were measured two times per week. Tumors treated with monotherapy showed no difference throughout the study whereas the combinatorial group showed significant improvement in tumor volume (Fig. 4.7). Immunofluorescent imaging of tumor tissue treated with the different drug combinations show enhanced inhibition of P-c-Jun, a downstream protein in both pathways (Fig. 4.8). These findings support the use of combination therapy using JNK and MEK 1/2 inhibitors when pancreatic cancer is resistant to MEK 1/2 inhibition alone.

4.3. Discussion

4.3.1 Phospho-Kinase Activity Changes after Conditioning

From the Phospho-Kinase array comparing normal and conditioned MIA PaCa-2 Cell, the biggest increases in signal were AKT and MAPK pathways. Of the MAPK cascades, JNK had the largest increase in phosphorylation after conditioning. This assay measured pan JNK, which integrates JNK1, JNK2, and JNK3. If only one specific isoform had increased phosphorylation, it would be tempered by the other two remaining stable. Similarly if one decreased in signal and the other increased it might be disguised as well. Teasing apart the isoforms might reveal more information about the pathways involvement in acquired resistance to MEK 1/2 inhibition, particularly if JNK1 is increased more than the other isoforms.

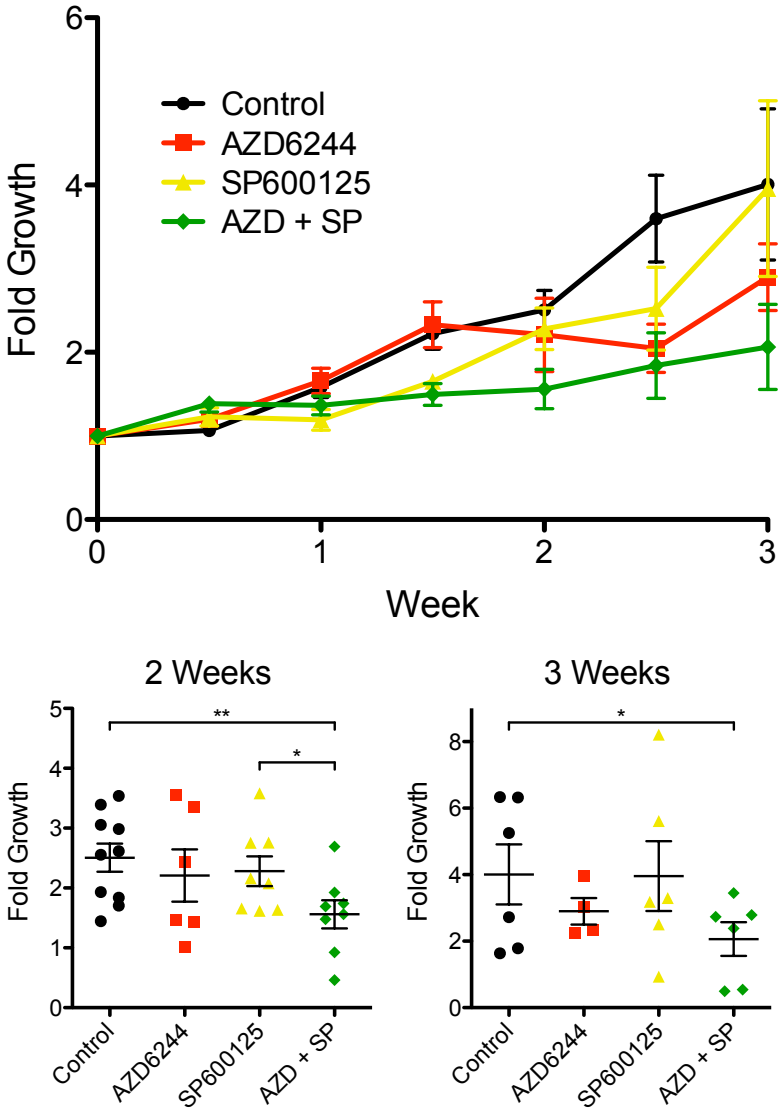

Figure 4.7 Combination therapy in subcutaneous tumor models. ***In vivo*** models using subcutaneous SU.86.86 tumors were treated *bid* with control, 2.5 mg/kg AZD6244, 12 mg/kg SP600125, or both (AZD6244 + SP600125) for 3 weeks. Growth curves (*top*) of tumors receiving each treatment plot average tumor volume. After week 2 and 3 *(bottom)* the combinatorial therapy cohort had significantly reduced tumor growth (p=0.0062 and p=0.0453 respectively). Denotations: * p≤0.05, ** p≤0.01, *** p≤0.001.

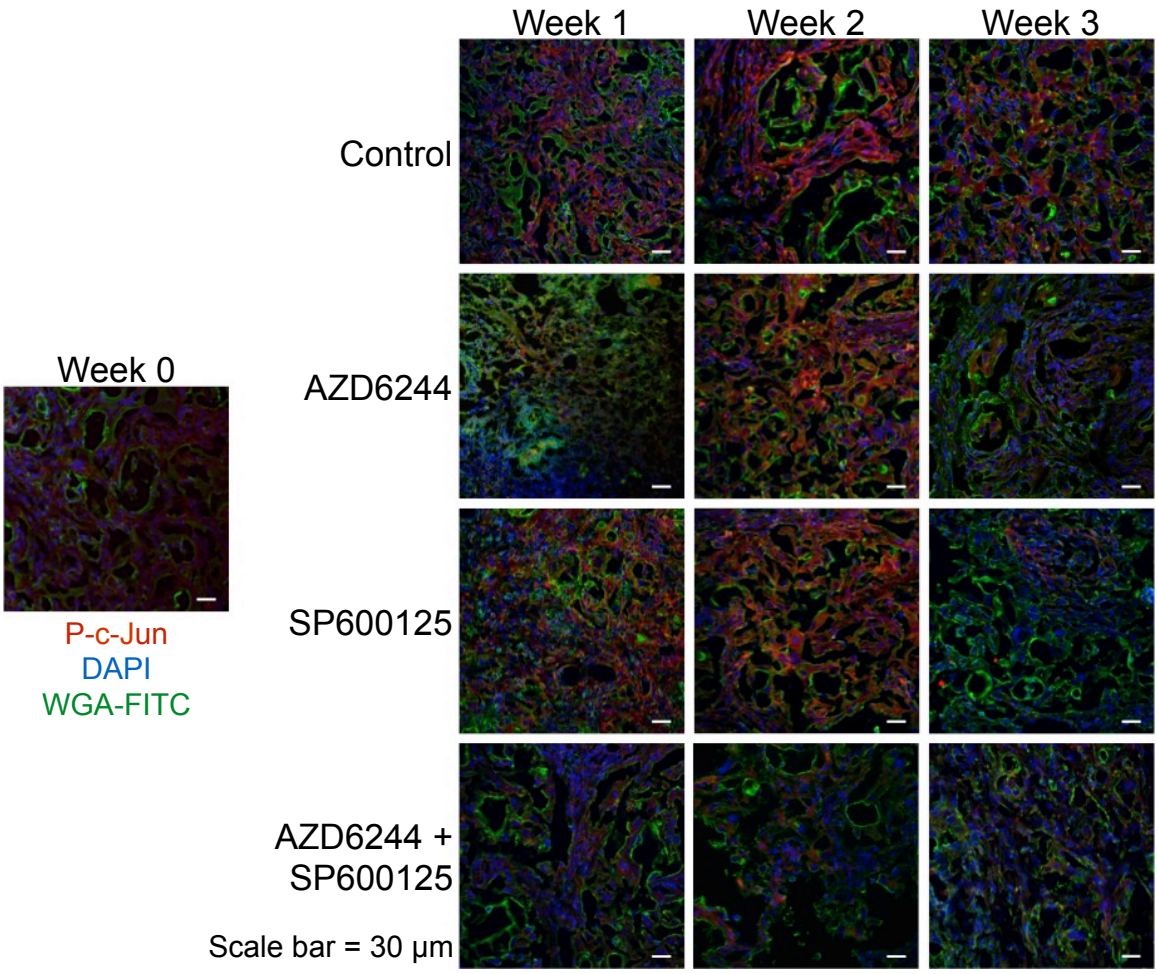

Figure 4.8 Immunofluorescent imaging of tumor tissues treated with different inhibitor combinations. Tumor tissue taken from mice 0, 8,15, and 22 days after treatment began. Immunofluorescent labeling of P-c-Jun (red), wheat germ agglutinin (green) and DAPI staining the efficacy of each therapy to decrease P-c-Jun signaling.

From the Kinase array we also found STAT3 to be heavily downregulated after conditioning. This is particularly interesting because in other forms of cancer such as melanoma and lung, STAT3 has been known to become more active after MEK inhibitor conditioning (239, 240). However, Yoon et al. found that STAT3 activity only increased when PTEN was mutated and not with wild type PTEN (241). According to the catalogue of somatic mutations in cancer (COSMIC), MIA PaCa-2 cells do not have a mutation in PTEN (242); this may partially explain why STAT3 is downregulated and not upregulated, after conditioning.

4.3.2. SP600125 as a JNK Inhibitor

To inhibit JNK1 signaling, we elected to use the inhibitor SP600125. Our choice was largely based on the inhibitor's availability, its popularity in literature for comparisons and the amount of knowledge on the small molecule's effects. However, these criteria do not account for the efficacy or specificity of the inhibitor. SP600125 is known to inhibit a number of proteins other than the JNK family (IC_{50}=40-90 nM). It has an affinity for Aurora A (IC_{50}=60 nM), TrkA (IC_{50}=70nM), FLT3 (IC_{50}=90 nM), MKK4 (IC_{50}=400 nM), among others (238, 243). Having multiple kinases upon which it acts makes it difficult to know if the effects we have seen in this chapter were truly from JNK inhibition or some off target effect. There are other available inhibitors, such as JNK Inhibitor VIII and AS601245, but these are often less potent or just a promiscuous as SP600125 (244, 245). Nonetheless, repeating some of the experiments with a different JNK

inhibitor may help identify some of the true effects of JNK inhibition as opposed to off target inhibition.

4.4. Materials and Methods

4.4.1. Antibodies and Drugs

The small molecule inhibitors AZD6244 (MEK 1/2 inhibitor) and UNC569 (MERTK inhibitor) were purchased from Selleck Chemical and Millipore respectively. They were prepared in dimethyl sulfoxide (DMSO) with stock concentrations of 10 mM. Primary antibodies were purchased from Cell Signaling Technology [JNK1 (2C6), P-SAPK/JNK (81E11), P-c-Jun, p44/42 MAPK (ERK 1/2) (137F5), P-p44/42 MAPK (P-ERK 1/2) (D13.14.4E), HSP90 (C45G5), Mer (D21F11)]. All secondary antibodies were purchased from Li-Cor [Donkey α-Goat 800CW (926-32214), Donkey α-Mouse 680 (926-32222), Donkey α-Mouse 800CW (926-32212), Donkey α-Rabbit 800CW (926-32213), Streptavidin 800CW (926-32230)]. Immunofluorescent antibodies used were goat anti-rabbit Alexa fluor 680 (Abcam), agglutinin Alexa fluor 488 (Life Technologies), donkey anti-goat Alexa fluor 594 (Life Technologies), and DAPI (Life Technologies).

4.4.2. Cell Culture

9 different PDAC cell lines were used in this study. All cell lines except PaTu 8902 and L3.6 pl were acquired from American Type Culture Collection (ATCC). The PaTu 8902 line was purchased from the german culture core Deutsche Sammlung von Mikroorganismen und Zellkulturen (DSMZ). L3.6 cells

were obtained from Dr. Craig Logsdon (University of Texas, MD Anderson Cancer Center). AsPC-1, BxPC-3, MIA PaCa-2, PaTu 8902, SU.86.86 and Yap-C were all growth in Roswell Park Memorial Institute (RPMI) medium supplemented with 10% (vol/vol) fetal bovine serum (FBS), 1% penicillin-streptomycin (pen-strep; ATCC 30-2300), and 2mM L-glutamine (L-glut). L3.6 and Panc-1 were grown in Dulbecco's Modified Eagle's Medium (DMEM) supplemented with 10% (vol/vol) FBS, 1% pen-strep, and 2mM L-glut. Lastly, Capan-1 cells were grown in Iscove's Modified Dulbecco's Medium (IMDM) supplemented with 20% (vol/vol) FBS, 1% pen-strep, and 2 mM L-glut. All cells were incubated at 37°C, 5% CO_2.

MIA PaCa-2 conditioning was performed using the same growth medium as indicated above supplemented with 2 μM AZD6244. After cell culture in this medium occurred for 2 months, the cells were considered "conditioned". From this point forward, they remained in the AZD6244 medium unless otherwise indicated.

4.4.3. Western Blots

All cell lines used for blots were grown to ~90% confluency in 10 cm culture dishes before being lysed in 300 μL of lysis buffer [PBS plus 1% Triton X-100, 1x protease/phosphatase inhibitor (Cell Signaling Technologies)]. Quantification of protein concentrations was performed using a bicinchoninic acid (BCA) assay (Pierce) to ensure even loading between samples. Loading dye (3x) plus Dithiothreitol (DTT, New England Biolabs) was added before heat

denaturation and run on 4-15% TGX gels (Bio-Rad). Proteins were transferred to polyvinylidene difluoride (PVDF) membranes and incubated with the appropriate antibodies. Quantitative western (qWestern) blots were performed using fluorescent secondary antibodies (800 and 680 nm, Li-Cor) and a Li-Cor Odyssey imager. Quantification was performed using the manufacturer's software. Correlation analyses with GI_{50} values were performed by calculating the Pearson product-moment correlation coefficient (r) using the Prism software.

4.4.4. Phospho-Proteome Analysis

A Human Phospho-Kinase Array Kit (R&D Systems, ARY003B) was used to quantify the activity of 43 kinase phosphorylations and 2 key proteins expression levels. The product protocol was followed with minor alterations. Briefly, normal and conditioned MIA PaCa-2 cells were lysed with Lysis Buffer 6 (R&D Systems) and agitated for 30 min at 4°C. The array membranes were cut to remove the numbering (they autofluoresce at the 800 wavelength) and blocked with Array Buffer 1 (R&D Systems) for 1 hr then incubated with 350 µg of cell lysates overnight at 4°C under gentle agitation. The membranes were then washed 3 times with the 1x wash buffer (R&D Systems). The membranes were then incubated with biotinylated detection antibodies for 2 h at room temperature and washed 3x times with 1x wash buffer. Deviating from the product protocol, we replaced the supplied streptavidin-HRP secondary, with Streptavidin 800CW (diluted in Li-Cor blocking buffer 1:20,000). Membranes were incubated with the secondary for 30 minutes before being washed and imaged using the Li-Cor imager. Quantification was performed using the Li-Cor software.

4.4.5. shRNA Lentiviral Transduction

Lentivirus pLK0.1 vectors encoding shRNA against human JNK1 and GFP were purchased from Open Biosystems. Cells were seeded on 12-well plates and grown to 50% confluence. The media were replaced by fresh media containing polybrene (4 µg/ml). GFP, MERTK and AXL shRNA lentiviral particles were thawed at room temperature and gently mixed before adding to the cells. Three different ratios of virions to cells were used (1:1, 2:1, and 3:2). The infected cells were incubated overnight and the next morning the media were replaced to fresh media without polybrene. Stably transfected cells were selected by puromycin treatment (3 µg/mL for SU.86.86 and 2 µg/mL for Yap-C). To further select stable clones, a single colony was isolated using the trypsin method (228). Downregulation of the JNK1 protein was verified via qWestern.

4.4.6. Cell Proliferation Assays

Cells were plated in triplicate using 6 96, opaque walled well plates (one for each day) at a concentration of 2,500 cells/well. After 8 hrs, the number of viable cells in each well of the Day 0 plate was determined by quantifying the ATP presence with a CellTiter-Glo® (Promega) cell viability luminescent assay. An ATP control (500 nM solution in PBS) was added in triplicate to blank wells, 100 µL/well. 100 µL of CellTiter Glo® reagent, prepared according to protocol, was added to each of the cell and ATP wells. After a 10-minute incubation in the dark, the luminescence of each well was recorded using a FLUOstar OPTIMA microplate reader. Each day the process was repeated using the next cell plate

and fresh ATP. Normalization between the days was performed using the ATP well readings.

4.4.7. Dose Response Curves

Cell lines were plated in two 96 well plates at a concentration of 2,500 cell/well. After 24 hrs, fresh media containing concentrations of AZD6244 ranging from 20 μM down to 63.2 pM by half-log units, or from 200 μM to 632 pM for the JNK inhibitor SP600125, were added to each well in triplicate, after which the cells were incubated for three additional days. For combinatorial studies using SP600125, every well had a constant dose of the JNK inhibitor (20 μM) and the concentration of AZD6244 was varied. The second plate was used for an initial, "Day 0" reading. These cells were washed 3 times with phosphate buffered saline plus calcium and magnesium (PBS+) then fixed with 4% paraformaldehyde (PFA). The cells were again washed then incubated in Syto® 60 dye (Life Technologies) diluted 1:3,000 in PBS+ for 1 hr. Cells were subsequently washed 6 times and imaged using a Li-Cor Odyssey at the 680 wavelength. Quantification was performed using the Li-Cor software. After the three-day incubation the inhibited cells in the first plate were processed the same way and quantified with the imager. Inhibition curves were reconstructed in Prism software using a 3-parameter (Bottom, Top, and IC_{50} with the hill slope constrained to -1) dose response curve. The equation used was $Y=Bottom + (Top-Bottom)/(1+10^{((X-LogIC_{50}))})$. The curves were adjusted by subtracting the Day 0 intensity (therefore y=0 indicates no growth) and the top of the curve adjusted to 1 (maximal growth). The result was a curve that had a max

value of 1, and when it crossed the x-axis indicated zero growth. GI_{50} values were then calculated from these curves for the concentration of inhibitor that caused a 50% decrease in cell growth. Combinatorial dose response curves were performed using 2 inhibitors, one of which was held constant throughout all the wells and the other inhibitor having varying concentrations (performed in triplicate).

4.4.8. In Vivo *Tumor Models*

In vivo models were performed subcutaneously using nude mice. Cells were grown to 90% confluency then lifted with trypsin, resuspended in Hank's Balanced Salt Solution (HBSS) and mixed with Matrigel (BD Biosciences) 1:1. Cells were injected into the back of mice using 150 µL volume at a concentration of 5 million cells/mL. The control and inhibitor suspensions were prepared in a viscous solution of Methocel in DPBS+ (5 mg/mL). After tumors became palpable (~200 mm^3), treatment drug (2.5 mg/kg for AZD6244, 12 mg/kg SP600125, or 2.5 mg/kg AZD6244 + 12 mg/kg SP600125) or vehicle control was administered *bid*. for up to 4 weeks or until tumor burden reached limit as mandated by the animal care and use committee. Tumor size was measured using calipers.

4.4.9. Immunofluorescent Imaging

Tumors from the mice under study were fixed in 4% paraformaldehyde for 1 hr, followed by equilibration in 30% sucrose overnight at 4^0C. The tumors were washed 3-4 times in DPBS (Dulbecco's phosphate-buffered saline), placed in OCT medium (Sakura Finetek USA, Inc, Torrance, CA) and frozen by placing

over liquid N_2 vapors. The embedded tumor samples wer then cut into 5-7 μm sections using a cryostat (Leica Microsystems Inc, Buffalo Grove, IL), for subsequent imaging with a fluorescence microscope fitted with appropriate filter sets (Olympus BX41). Antibodies were prepared by diluting P-c-Jun 1:75 (Cell Signaling Technologies) and incubated with the tissues overnight at 4^0C. The next day the appropriate secondary antibodies [goat anti-rabbit Alexa fluor 680 at 1:250 dilution (Abcam) and donkey anti-goat Alexa fluor 594 at 1:200 dilution (Life Technologies)] were applied. After washing, wheat germ agglutinin Alexa fluor 488 (1:500) was applied for 5 minutes. The tumors were washed again and then prepped for imaging by adding mounting medium containing DAPI and sealed with a coverslip. They were imaged using a fluorescence microscope with a 20X objective. Images were processed using image J.

Chapter 5

Developing a Small Molecule-Peptide Screening Technique Using Modified Phage Display

Works from this chapter is published in Multivalent site-specific phage modification enhances the binding affinity of receptor ligands. Beech J, Saleh L, Frentzel J, Figler H, Corrêa Jr IR, Baker B, Ramspacher C, Marshall M, Dasa S, Linden J, Noren CJ, and Kelly KA. 2015. *Bioconjugate Chemistry* (246).

5.1. Introduction

The last few decades have seen enormous progress in proteomic, genomic, and metabolomic understanding and treatment of disease. However, off-target effects of small molecules have hampered drug usage due to toxic side effects resulting in the removal of patients from treatment regimens. Targeting strategies have become a prominent focal point for new drug design with the promise of increasing drug delivery to targeted cells while reducing toxicity. A key component to precision medicine will be more precise targeting of therapeutics to cancer over normal tissue. Unless a drug itself is capable of targeting a desired cell type, such as a therapeutic antibody, hybrid complexes or multifunctional nanoparticles are needed to combine a therapeutic drug with a targeting moiety. Small molecules, aptamers, peptides, and antibodies comprise the most common moieties used in these applications. While each has its benefits, peptides are easy to tether, can be rapidly screened, can be chemically synthesized, and can bind with high affinity and specificity without eliciting an immune response. These qualities make them attractive for targeting.

Of the known ways for producing and screening high affinity peptides, phage display has been one of the most effective and economical. Over the past three decades, phage display has been used to discover thousands of specifically targeted peptides. A common system uses bacteriophage expressing random peptides on the pIII coat protein, resulting in a diverse library, which can contain $\geq 10^9$ different combinations. However, the peptide sequences are limited in the sense that they must be made from the pool of the 20 standard

ribosomally-encoded amino acids. Methods have been developed to expand upon this pool, including the incorporation of phosphorylated proteins (247) or modification with unnatural amino acids such as citrulline (248, 249). However, these expansions have been incremental and any chemically large modification of the pIII protein could compromise the phage coat or more likely decrease the infectivity and expansion of the phage (250). As an alternative, post-biosynthetic modification of the phage would circumvent these limitations and enable the incorporation of rationally selected small molecules. This would involve using a biological linker produced by the phage to enable proteins or synthetic compounds to be tethered selectively to the linker after phage replication. An example of this was described by Barrett et al. in 2007 using icosahedral phage and a streptavidin-biotin linking system in the coat proteins (251).

We sought to create a means of producing targeted incorporation of small molecules onto phage using the previously identified selenocysteine (Sec) insertion sequence (252, 253). Sec, the 21st amino acid, is expressed in a ribosome-mediated protein synthesis manner and the selenol side chain has a pKa of ~5.47, which is lower than that of the chemically related Cysteine (Cys, pKa ~8.0) thus allowing Sec to display stronger nucleophilicity and reactivity than Cys at physiological pH. Therefore, it is possible to tether molecules selectively to Sec and not Cys (254) in a seleno-pIII displaying phage. This method ensures that: 1) no other coat proteins are affected; 2) proper orientation of the phage and small molecule occur when screening; and 3) various flanking peptide sequences can be screened. Furthermore, because Sec is coded for by UGA and requires

opal suppression, a functional pIII protein (required for phage propagation) only occurs upon successful Sec insertion (252, 255).

As a proof of concept, we chose to work with several small molecule ligands that target the adenosine A_1 receptor. The A_1 receptor is one of four G protein-coupled receptors (256) found in many tissues including heart, brain and adipose tissue. The adenosine A1 receptors modify the function of many tissues including cardiac, neuronal, renal and adipose (257). N^6-substituted adenosine analogs have been synthesized that bind with high affinity to the A_1 subtype.

Here, we demonstrate that small molecules that target the adenosine A_1 receptor can be tethered to M13 phage via displayed Sec residues, and that the resulting multivalent constructs enhance the binding of the tethered phage to adenosine A_1 receptor-expressing cells. Using competition assays, we also show that the modified phage is potent and specific for the A_1 receptor and capable of activating the receptor and its downstream signaling pathways. This technology has broad applications and introduces new ways for performing small molecule screens, which serve as platforms for developing improved peptide-drug hybrid compounds.

5.2. Results

5.2.1. Modification of Selenopeptide-Displayed Phage with Adenosine Receptor Ligands

Phage displaying five Sec-pIII peptides, each containing a Sec residue, were produced using a modified *Escherichia coli* strain (ER2738^{selABC}) in the

presence of selenite as previously reported (255). Sec-phage were stored anaerobically to maintain reactivity of the selenol group. The displayed Sec-pIII peptide (SARVSecHGP) is not known to have any specific targets and is thus treated as an inert sequence. A schematic of the insertion of Sec into the peptide and subsequent modification is depicted in Figure 5.1. The small molecules were incorporated specifically into the pIII peptide sequence as visualized by Western blotting, demonstrating the specificity of the approach (Fig 5.2). N6-octylaminoadenosine (NOAM), a small molecule adenosine A_1 agonist specifically designed to have selectivity for the A_1 receptor (K_D=2.4±0.3 nM) over the A_{2A} receptor (K_D=1.9±0.2 μM), was modified via its primary amine to include an iodoacetyl group for tethering to the Sec and a biotin for detection (NOAMI-Bt). Incubation of the s12d phage and NOAMI-Bt in a 1:167,000 molar ratio of phage to small molecule at room temperature for 1 h resulted in the modification of pIII-Sec only with NOAMI-Bt as only one band was present corresponding to the pIII coat protein molecular weight (Fig. 5.2A). As a control, an iodoacetyl-PEG_2-biotin (Bt) was reacted with the phage in the same ratio. A summary of all the phage-small molecule combinations can be found in Table 5.1. A set of negative control reactions were performed with M13KE phage (no Sec) or s12d and vehicle only. M13KE phage did not react with the small molecules under these conditions. Quantitative Western blotting (qWestern) revealed that the Bt reaction is 2-fold less efficient than that of NOAMI-Bt (Fig. 5.2B). Therefore for all subsequent experiments, a 1:333,000 ratio of phage to Bt was used to have equivalent tethering between the Bt and NOAMI-Bt molecules (Fig. 5.2C).

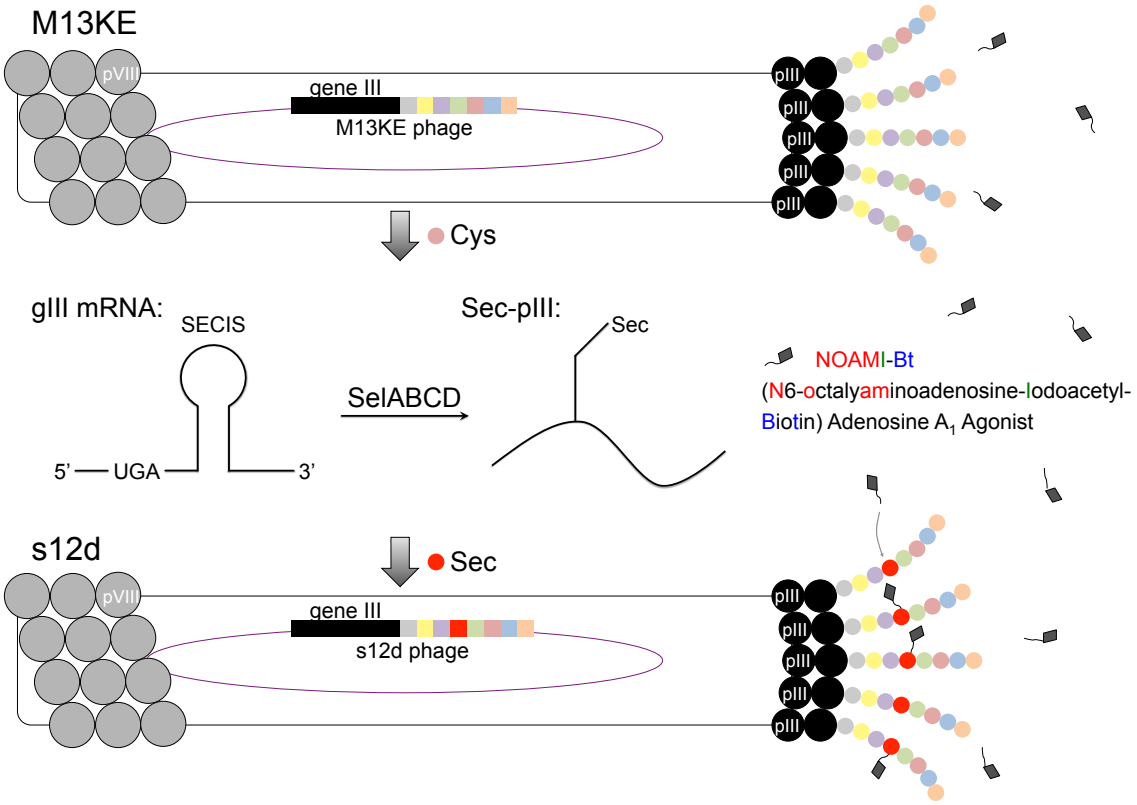

Figure 5.1 Schematic of the M13KE bacteriophage with incorporation of selenocysteine for site-specific modification. A Sec insertion sequence and UGA codon were inserted at the 5' end of M13 gIII, which encodes for the pIII coat protein, providing five Sec residues for small molecule tethering under appropriate conditions (246).

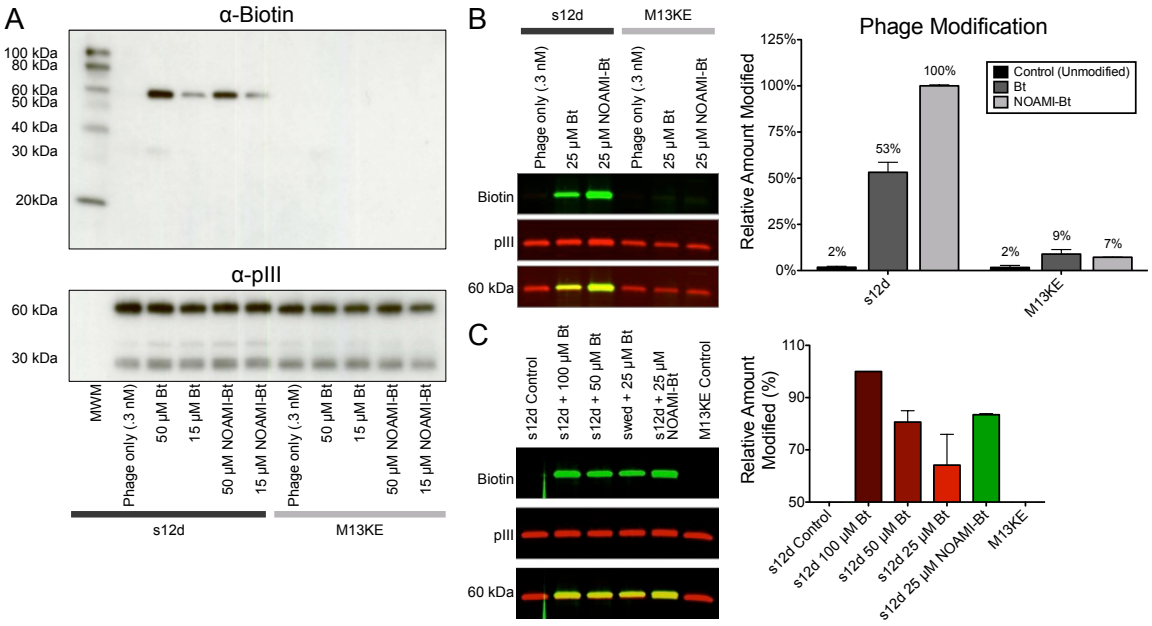

Figure 5.2 Site-specific modification of seleno-pIII coat protein of s12d phage. *A)* Phage modified with the indicated reagents were analyzed via Western blotting for the presence of biotin (*top*) and the pIII coat protein (*bottom*). Bands are seen at molecular masses near 60 kDa (the apparent molecular weight of the pIII protein) for biotin tethered and NOAMI-Bt tethered s12d phage but not for negative control, Sec-free M13KE phage. *B)* Phage-small molecule complexes were reacted and quantified using qWestern blotting (*left*) to determine the relative efficiency of small molecule tethering (*right*). *C)* Small molecule tethering efficiency. *Left)* qWestern blots for Biotin and pIII using different phage-small molecule reaction conditions (100 μM, 50 μM and 25 μM small molecule and 0.3 nM s12d phage). Control and NOAB-Bt reactions are also shown. *Right)* Quantification of the biotin bands normalized to pIII show the efficiencies of the labeling reactions (246).

Phage-Small Molecule	Tethered Molecule	Function	Chemical Structure
s12d-BW4133I	BW4133I	Non-selective adenosine receptor antagonist	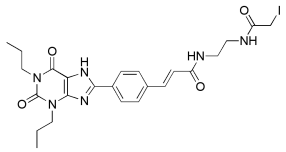
s12d-Bt	Bt	Negative control	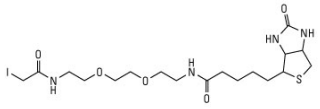
s12d-NOAMI	NOAMI	Selective adenosine A_1 agonist	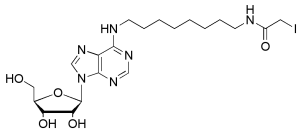
s12d-NOAMI-Bt	NOAMI-Bt	Selective adenosine A_1 agonist	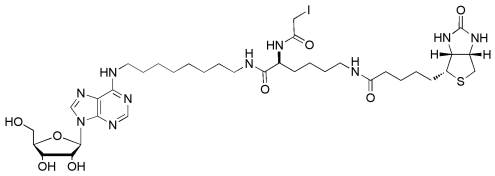
s12d-XACI	XACI	Non-selective adenosine receptor antagonist	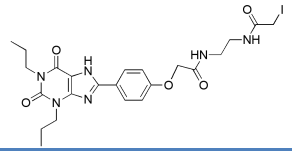

Table 5.1 Modified Phage Molecules. A summary of the 5 molecules used in this chapter, the tethered small molecule functions, modifications, and chemical structures. The chemical structures are those of the tethered molecule (246).

To demonstrate the versatility of the Sec-phage system, additional molecules were tethered to the s12d phage. Two non-selective adenosine A_1 antagonists, Xanthine Amine Congener (XAC) and BW1433, were functionalized as iodoacetamides, forming the reactive molecules XACI and BW1433I, respectively. These modified molecules, as well as a functionalized NOAM without Bt (NOAMI), were reacted with the phage for 1 h then chased with the Bt molecule. Detection of effective modification was observed by a lack of Bt binding in Western blots. As with Bt and NOAMI-Bt, site-specific modification of the pIII coat protein was observed (Fig. 5.3).

5.2.2. NOAMI-Bt-Modified s12d Specifically Targets the A_1 Receptor

To determine if NOAMI-Bt still binds to the adenosine A_1 receptor when conjugated to s12d phage, CHO-K1 cells were stably transformed to express the human adenosine A_1 receptor (hA_1-CHO). Presence of the receptor protein was validated via Western blot (Fig. 5.4 Inset). Enzyme-linked immunosorbent *assays* (ELISAs) were then performed to assess the modified phage's ability to bind the cells. Three different phage species were tested: unmodified s12d, Bt modified (s12d-Bt) and NOAMI-Bt modified (s12d-NOAMI-Bt). Increasing concentrations of phage were incubated with the cells for 1 h. After removing the excess phage by repeated wash steps, the cells were incubated with horseradish peroxidase (HRP) labeled anti-pVIII antibody (α-pVIII-HRP) and the phage bound to cell receptors were quantified by absorbance at 652 nm using a colorimetric substrate to HRP, 3,3',5,5'-tetramethylbenzidine (TMB) (Pierce). The phage modified with the NOAMI-Bt molecule exhibited high binding affinity with a

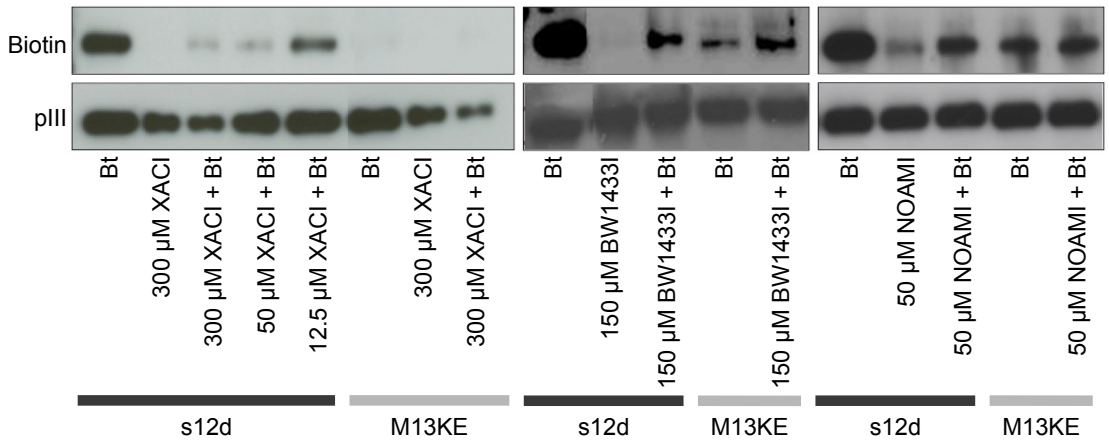

Figure 5.3 Successful modification of sec-phage with additional small molecules. Conjugation of additional small molecules to s12d or M13KE phage. Phage were incubated with the indicated molecules and subsequently incubated with Bt. As the small molecules did not contain a biotin group, the decrease in a band corresponding to the presence of biotin indicates successful tethering of small molecules (246).

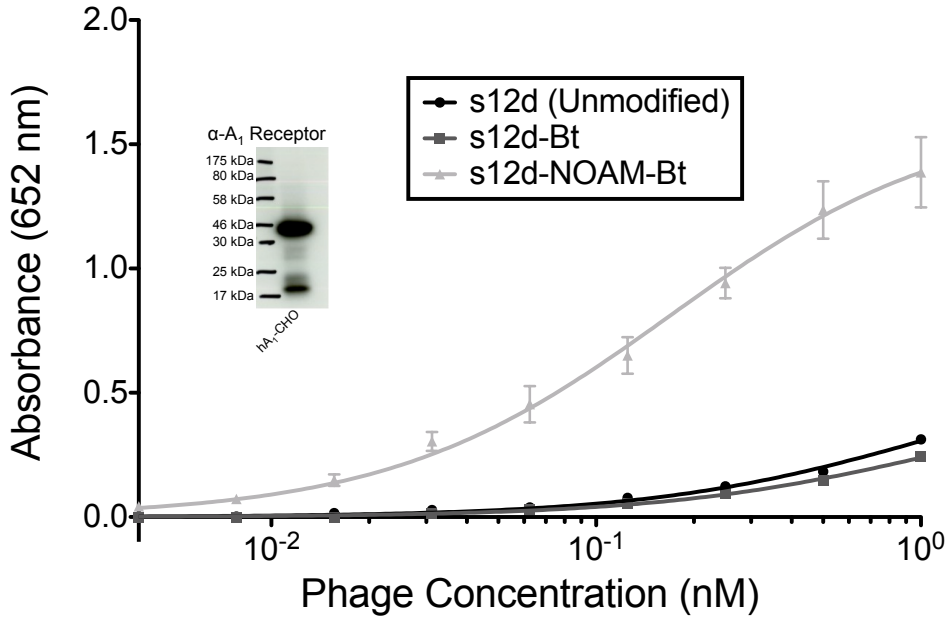

Figure 5.4 NOAMI-Bt conjugated phage bind hA_1-CHO cells with high affinity. Cell binding assays using human adenosine A_1 receptor-expressing CHO cells and modified s12d phage. Cells were incubated with NOAMI-Bt modified phage in the presence of phage detected via ELISA. NOAMI-Bt modified phage bind with high affinity (ED_{50} = 0.17 nM) whereas control phage (unmodified or Biotin conjugated only) demonstrated negligible binding. *Inset)* Western blot of hA_1-CHO cells for the human Adenosine A_1 receptor reveals a strong band at approximately 36 kDa, the reported molecular weight of the A_1 receptor (246).

ED_{50}=0.17 nM, 14 fold lower than the ED_{50} of the free molecule, indicating a possible increased affinity due to multivalency and avidity effects. In contrast, both unmodified s12d and s12d-Bt exhibited negligible binding (Fig. 5.4).

Competition experiments were performed to further validate the specificity of NOAMI-Bt for the A_1 receptor. hA_1-CHO cells were pre-blocked for 1 h using free NOAM molecule at varying concentrations before s12d-NOAMI-Bt phage were added at 0.5 nM. After 1 h of incubation, residual bound phage were detected by absorbance as previously described (Fig. 5.5A). As expected, the small molecule competed s12d-NOAMI-Bt away from the A_1 receptor (final ED_{50}=577 μM).

Competition assays with radiolabeled [^{125}I]-aminobenzyladenosine (^{125}I-ABA), an adenosine A_1 receptor agonist (73), were performed to further validate the specificity and affinity of s12d-NOAMI-Bt phage for the A_1 receptor. ^{125}I-ABA was applied for 1 h to hA_1-CHO membranes. Membranes were used because they bind agonists such as ^{125}I-ABA with high affinity through receptor-G protein complexes. Modified phage were used at increasing concentrations to compete with the bound ^{125}I-ABA. At all concentrations of the s12d-NOAMI-Bt phage tested, a significant decrease in the bound ^{125}I-ABA was detected. Specific ^{125}I-ABA binding after 1 h of incubation with 0.02, 0.2, and 2.0 nM phage was reduced by 18%, 54% and 77%, respectively. The control phage (s12d-Bt) even at the highest concentration competed negligibly (<10%) for ^{125}I-ABA, confirming the specificity of the modified phage for the A_1 receptor (Fig. 5.5B). Taken

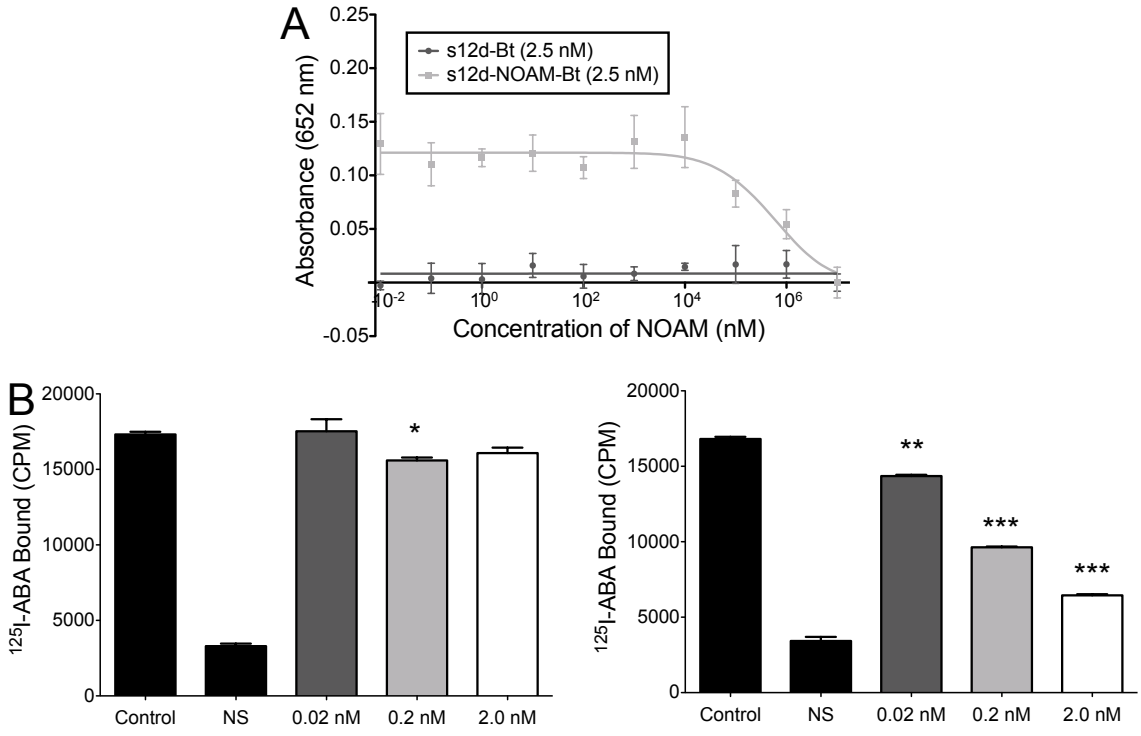

Figure 5.5 NOAMI-Bt conjugated to phage retain specificity for A_1. *A)* Competition assays. hA_1-CHO cells were incubated with increasing concentrations of free NOAM followed by 0.5 nM NOAMI-Bt or Bt modified phage. As in *A*, phage binding were detected via ELISA. *B)* Radioligand competition assays. ^{125}I-ABA incubated with hA_1-CHO membrane was reduced by 18%, 54% and 77% with increasing concentrations of s12d-NOAMI-Bt *(right)* but not s12d-Bt *(left)* (246).

together, these experiments demonstrate that specificity of the conjugated molecule for the A_1 receptor is retained.

5.2.3. Phage-Binding Kinetics

s12d-NOAMI-Bt, s12-Bt, and unmodified s12d phage were added to hA_1-CHO cells for different time periods and the binding kinetics of the phage to hA_1-CHO cells were determined. As can be seen from the graph in Figure 5.6, association kinetics past 10 min conformed to standard exponential binding kinetics with $k_{on}=1.98x10^6$ $M^{-1}s^{-1}$. However, during the first 10 min, phage binding was minimal, suggesting that phage are not freely accessible to cell receptor or that binding is cooperative. Similarly for s12d-NOAMI-Bt dissociation kinetics, a 45-minute lag is seen where the data deviates from typical exponential decay. Beyond 45 min, however, the data can be fit to an exponential equation with a $k_{off}=2.02 \times 10^{-4}$ s^{-1} ($t_{1/2}$=57 min). Combining observed apparent k_{on} and k_{off} values assessed at long incubation times, we can calculate an apparent K_D=0.10 nM.

5.2.4. NOAM Retains Its Agonist Function when Tethered to s12d Phage

In addition to binding to the A_1 receptor, we wanted to determine if the tethered molecule retains its agonistic function. Active human adenosine A_1 receptors expressed in CHO-K1 cells have previously been reported to signal through the AKT pathway. Cheng et al. were able to use the small molecule agonist N^6-cyclohexyladenosine (CHA) to stimulate the receptor and increase P-ATK within 2 minutes and found peak activation around 5 min (258). We were able to reproduce this observation using CHA in our hA_1-CHO cells (Fig. 5.7A).

.

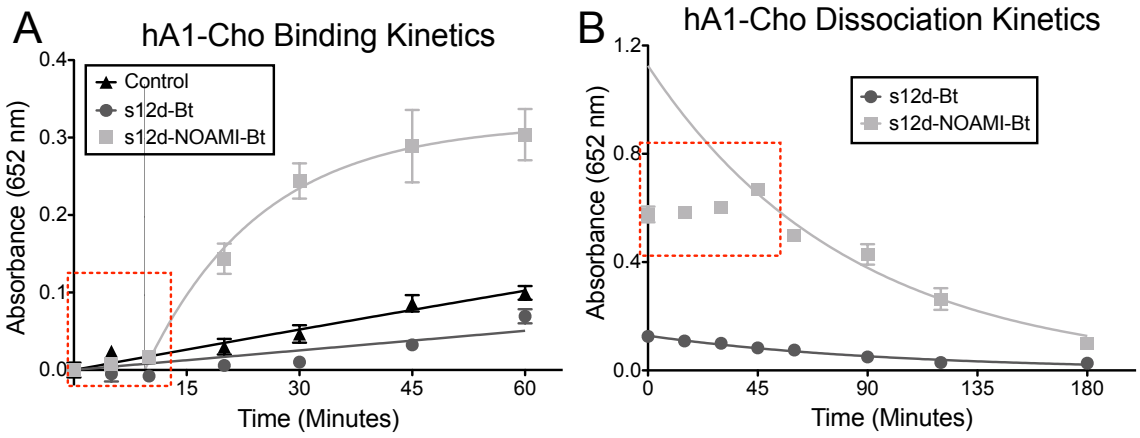

Figure 5.6 Binding kinetics of modified s12d phage. *A)* Aliquots containing 0.5 nM of phage were incubated with hA_1-CHO cells at 4°C for the indicated times. Due to deviation from standard binding kinetics (red box), association kinetic curve fits of s12d-NOAMI-Bt binding (squares) excluded the first 10 min were fit with a R^2=0.868. Unmodified (triangles) and Bt modified (circles) phage are fit without omission. *B)* Phage were incubated for 1 h with hA_1-CHO cells and then removed. The cells washed at various time and remaining phage was quantified via ELISA. Data beyond 45 min were fit to a single exponential decay curve (R^2=0.879) as illustrated for s12d-NOAMI-Bt (246).

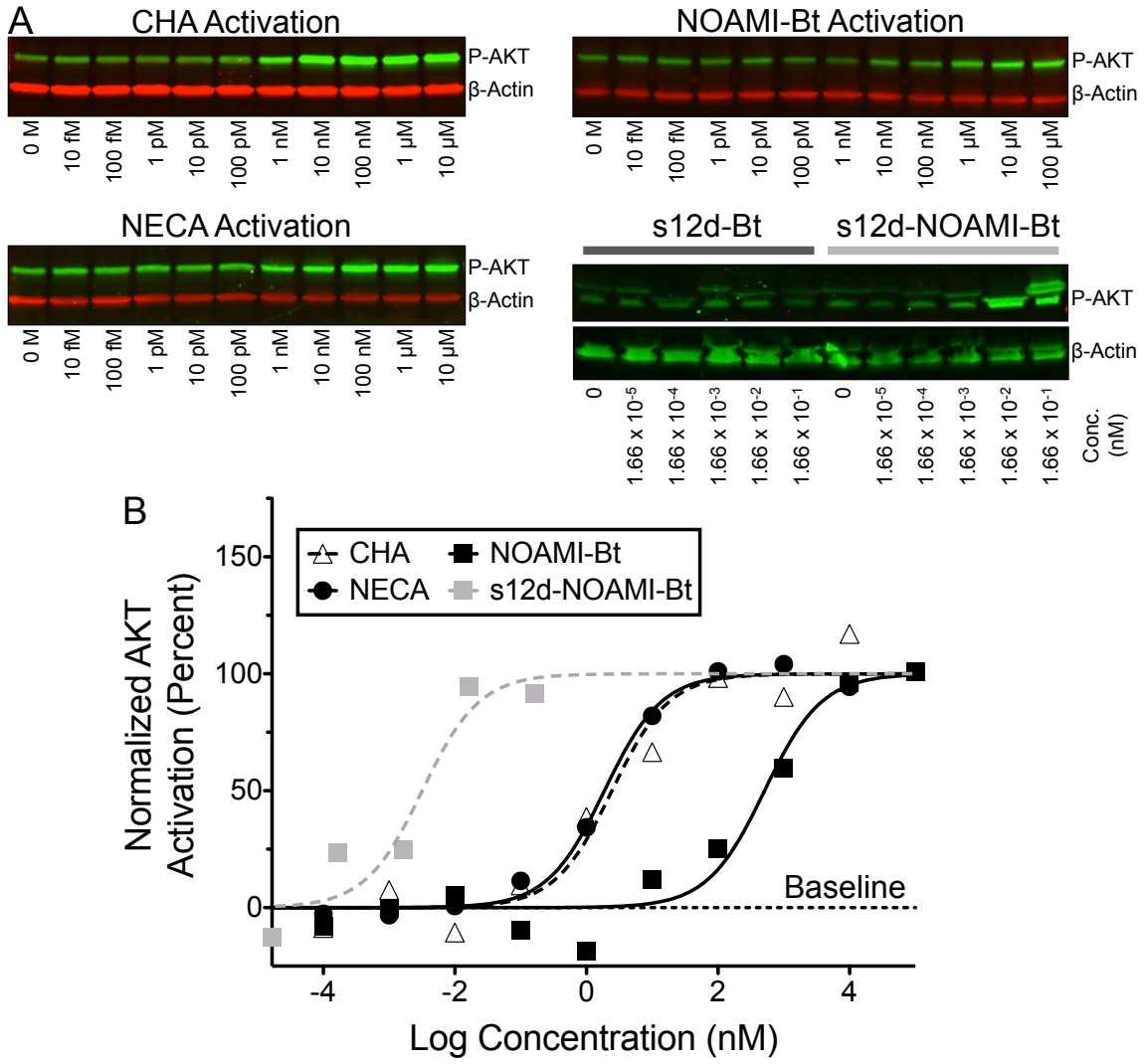

Figure 5.7 NOAMI-Bt is functional when tethered to s12d phage. *A)* AKT pathway activation by small molecules and modified phage. hA_1-CHO cells were incubated with the indicated concentrations of CHA, NECA, and NOAMI-Bt molecules or modified phage for 15 min. Activation of AKT was analyzed by qWestern blotting for phospho-AKT and normalized to β-actin. *B)* Activation plot fits based on the qWestern blots and normalized to baseline for AKT in response to increasing concentrations of s12d-NOAMI-Bt (gray squares, EC_{50}=3.20 pM), free NOAMI-Bt (black squares, EC_{50}=510 nM), CHA (triangles, EC_{50}=2.44 nM), or NECA (circles, EC_{50}=1.88 nM) (246).

Therefore, we used this pathway to determine the receptor activation potency in hA_1-CHO cells. The presence of a doublet in the Western blot for T-AKT or P-AKT was consistent with previously published reports (259). Various concentrations of s12d-NOAMI-Bt phage were incubated with cells and the extent of AKT activation was compared to that of s12d-Bt and several free A_1 agonists, CHA, N^5-ethylcarboxamido-adenosine (NECA), and NOAMI-Bt. To assess extent of AKT activation, the 15 min time point was chosen to account for the 10-min delay of phage binding to cells as observed in the phage binding kinetics (Fig. 5.6A). Remarkably, the NOAMI-Bt modified phage were able to very potently stimulate a response in the AKT pathway (EC_{50}=3.20 pM), whereas s12d-Bt control phage were unable to elicit a response (Fig. 5.7A). Interestingly, conjugated NOAMI-Bt invoked a response at a concentration of ~5 orders of magnitude lower than that of free NOAMI-Bt (EC_{50}=5.11x10^5 pM) (Fig. 5.7B). When compared to free CHA (EC_{50}=2.44x10^3 pM) and NECA (EC_{50}=1.88x10^3 pM), s12d-NOAMI-Bt activation of AKT was 3 fold greater.

5.3. Discussion

5.3.1. Small Molecule Tethering Efficiency

Throughout this chapter, we had worked with the assumption that 5 small molecules were tethered to each phage. Although 100% efficiency is not plausible, we do believe that we had >90% tethering efficiency, based on our findings in Fig. 5.2 and Fig. 5.3. After the s12d phage were reacted with XACI, BW1433I or NOAMI (none of which have a biotin group), excess Bt was added to

react with any remaining Sec groups. The lack of strong biotin bands in the Western blots, <10% of the s12d-Bt control, implies a high small molecule tethering efficiency. Probabilistically, a 90% tethering efficiency would result in 59% of the phage having all 5 Sec residues tethered (0.9^5) and 92% having at least 4 small molecules tethered ($0.9^5+5\cdot0.9^4\cdot0.1^1$). Only 0.001% of phage (0.1^5) would not have a small molecule bound.

5.3.2. Enhanced Binding Affinity through Pentavalancy

The modification of the pentavalently-displayed pIII-Sec with NOAMI-Bt results in a striking increase in the affinity of the tethered NOAMI-Bt molecule compared to the free form. Although the kinetics of phage binding to adenosine receptors on CHO-A1 cells suggest that the phage is not as accessible to receptors as small molecules, a shift of ~5 orders of magnitude in the EC_{50} of NOAMI-Bt compared to free small molecule for activation of AKT is observed when the molecule is tethered to s12d. This is a remarkable difference that we attribute largely to an avidity effect in binding due to the pentavalent display of the NOAMI-Bt-modified pIII-Sec phage coat protein. It has been reported that the covalent linking of two or more ligands within physical proximity to target molecules results in affinity enhancement that is primarily manifested as a result of a slowed dissociation (260). Therefore, the tethering of 5 NOAMI-Bt molecules to the surface of the phage was expected to exhibit a very high apparent binding affinity. If all or most of the closely spaced tethered ligands are capable of binding receptors simultaneously, it is unlikely that all of the tethered ligands will dissociate simultaneously, resulting in very slow dissociation kinetics. Also, the

local concentration of tethered agonists in the region of the A_1 receptor is effectively high due to the closely packed selenocysteines displayed on the tip of the phage; one tethered molecule bound to a receptor keeps four other tethered molecules in very close proximity to other receptors.

5.3.3. Delayed Binding Kinetics

Compared to the unconjugated small molecule radioligands, we did notice deviations in both association and dissociation kinetics of tethered phage. There are a number of factors that may contribute to this phenomenon. Since phage are large molecules, it may take time for them to diffuse and orient to enable productive binding to receptors. Also, their multivalency likely contributes to changing effective affinity, that is, as phage bind the local concentration increases; thus the overall effective concentration increases driving the process forward. Multivalency could also account for the delayed release of phage; if a single phage is bound to multiple receptors, keeping it bound to the surface even when one receptor-agonist bond breaks. Phage dissociation may appear to accelerate as a consequence of receptors being taken up into cells and possibly uncoupled from G proteins that favor high affinity binding. Another possibility is that a change in receptor conformation is needed to switch from a low affinity to a high affinity state for binding and the reverse for dissociation. This may result from the formation of R-G complexes.

5.4. Materials and Methods

5.4.1. Antibodies and Materials

Antibodies were purchased from Abcam [Adenosine A_1 Receptor (EPR6179)], Cell Signaling Technology (CST) [AKT (C67E7), P-AKT (Ser473 9271), β-Actin (8H10D10), Streptavidin-HRP (3999)], GE Healthcare [M13-HRP (27-9421-01)], and Li-Cor [Rabbit-800CW (926-32213), Mouse-800CW (926-32212), Mouse-680LT (926-68022), Streptavidin-800CW (926-32230)]. CHA and NECA were purchased from Abcam and prepared in dimethyl sulfoxide (DMSO).

N^6-octylamineadenosine (NOAM) and N^6-aminobenzyladenosine (ABA) were gifts from Dr. Susan M. Daluge of GlaxoSmithKline PLC. ABA was radio-iodinated and purified as described previously (261). The K_i of NAOM for binding to the human A_1 receptor was determined by competition for radioligand binding as described previously (256, 261).

5.4.2. Preparation of hA_1-CHO Cells

An expression plasmid for the human A_1 receptor in the CLDN10B mammalian expression vector was prepared as described (261). The adenosine receptor was introduced into CHO-K1 cells by means of Lipofectin (Life Technologies) and colonies were selected by growth in 1 mg/mL G418 (Life Technologies) and maintained in 0.5 mg/mL G418. The agonist radioligand ^{125}I-ABA was found to bind to a total of 3.5 pmol/mg recombinant human A_1 receptors on hA1-CHO cell membranes with a K_D of 1.02 nM (261).

5.4.3. Preparation of Modifying s12d Phage

Selenocysteine phage were amplified using ER2738^{SelABC} *E. coli* in the presence of selenite and quantified as described previously (255). The phage were resuspended in Tris-buffered saline (TBS; 50 mM Tris-HCl, pH 7.5 and 150 mM *sodium chloride (*NaCl)*)* with 50% glycerol and stored at -20°C under anaerobic conditions (95% N_2, 5% H_2, and O_2 <1 ppm) to prevent oxidation of selenocysteine to unreactive species.

Tethering of all small molecules was performed in either small (40 µL) or large (250 µL) reaction volumes in Glycine Buffered Saline (GBS) pH 2.5. Small reactions used a phage concentration of 0.3 pM and the large reactions, 30 nM with small molecules at final concentrations for the desired ratio. The reactions were performed for 1 h at room temperature in the dark with the large reactions performed using a stir bar for constant mixing. For molecules without a biotin incorporated (XACI, BW1433I, and NOAMI) a second reaction step where Bt was added at a final concentration of 50 µM for 30 min was performed to react with any unmodified phage. All reactions were subsequently quenched using 40 mM DTT (Thermo Sci). Overnight dialysis was performed in TBS to remove the excess, untethered small molecules before use.

5.4.4. Immunoblotting for the Detection of s12d Modification and Cho Cell Activity

Phage were denatured via heating in SDS sample buffer containing 3x loading dye and DTT (NEB). Equivalent amounts of protein were resolved on

20% Tris Glycine Gels (Novex) and transferred onto PVDF membranes (Millipore) for immunoblot analysis.

All CHO cell blots used cells grown to ~90% confluency in 6 well plates, treated with the indicated testing conditions and lysed in 150 µL of lysis buffer (PBS plus 1% Triton X-100, 1x protease/phosphatase inhibitor (CST). Loading dye (3x) plus DTT (NEB) was added before heat denaturation and run on 4-15% TGX gels (Bio-Rad). Proteins were transferred to polyvinylidene difluoride (PVDF) membranes and incubated with the appropriate antibodies. Quantitative Western blots were performed using fluorescent secondary antibodies (800 and 680 nm, Li-Cor) and a Li-Cor Odyssey imager. Quantification was performed using the manufacturer's software.

5.4.5. Enzyme Linked Immunosorbant Assays (ELISAs)

hA_1-CHO cells were grown to ~90% confluency in 96 well plates. Cells were washed with phosphate buffered saline plus calcium and magnesium (PBS+) containing 1% BSA and 0.1% Tween-20 3 times before the addition of phage in 20 µL PBS+. After 1 h incubation at 4°C (to minimize phage internalization), unbound phage were removed and the cells washed 3 times. The cells were then fixed in 4% paraformaldehyde for 10 min. The cells were washed 3 more times before incubation with anti-M13-HRP (1:3,000 dilution in PBS+ 2% BSA, GE Healthcare) for 1 h. The cells were then washed 5 times and Ultra-TMB (Thermo Sci) added for 10 min before the absorbance was measured at 652 nm.

Kinetic assays were performed in a 96 well plate using reverse order of phage addition, that is, all phage incubations were designed to finish at the same time with their initial addition point being variable. Three wells were washed per condition and the phage, 0.5 nM, were added for the longest time point. After a certain period of incubation at 4°C, the next set of wells were washed and the second longest time point phage were added and the same procedure was repeated until the shortest time point phage were added followed by the appropriate incubation time. The plate was then processed as detailed above. All curve fits were performed using Prism software.

5.4.6. Competition Binding Assays

hA_1-CHO cells grown in 96 well plates were washed with PBS+ 3 times before adding varying concentrations of NOAMI-Bt in 20 µL PBS. After 1 h incubation at 4°C, unbound NOAMI-Bt was removed and the cells were washed again 3 times in PBS+. 20 µL of phage were then added at a concentration of 0.5 nM and incubated with cells for 1 h at 4°C. The cells were then fixed and processed the same as described for the ELISAs.

For the radiolabeled competition assays, hA_1-CHO cells were washed with PBS and harvested in buffer A (10 mM HEPES, 20 mM EDTA, pH 7.4), supplemented with protease inhibitors (20 pg/mL benzamidine, 100 pM phenylmethylsulfonyl fluoride, and 2 pg/mL of aprotinin pepstatin, and leupeptin). The cells were homogenized in a Polytron (Brinkmann) for 20 s, centrifuged at 30,000 g, and the pellet was washed twice with buffer HE (10 mM HEPES, 1 mM

EDTA, pH 7.4, containing protease inhibitors). The pellet was resuspended in buffer HE, supplemented with 10% sucrose, and frozen in aliquots at -80°C.

Binding assays for human A_1 adenosine receptors were performed with the agonist [^{125}I]-aminobenzyladenosine (^{125}I-ABA). Experiments were performed in triplicate using 96 well GF/C filter plates (Millipore). To each well, 10 µg hA_1-CHO membrane protein, 0.5 U/mL adenosine deaminase, Hepes buffer + 5 mM MgCl, and various concentration of phage or competing ligands were added, followed by 0.1 - 0.2 nM of carrier free ^{125}I-ABA, resulting in a total volume of 100 µL. After a 1-hr incubation at room temperature, the liquid in the wells was drawn through the filters under vacuum, and the filters washed by vacuum filtration 3 times with 200 µL ice cold buffer. The filters were removed with a filter punch and the ^{125}I-ABA bound to receptors in the membranes was retained on the filters and counted in a gamma counter. Nonspecific binding was measured in the presence of 10 µM *N*-ethylcarboxamidoadenosine.

5.4.7. AKT Activation Assays

hA_1-CHO cells were grown in 96 well plates until ~90% confluency. The media was removed, the cells washed once with PBS+, and then fresh media with varying concentrations of small molecule or phage added. After a 15 min incubation at 37°C, the media was removed and the cells washed 3 times with PBS+. Cells were lysed in 150 µL of lysis buffer and immunoblotting was performed as indicated above.

Chapter 6

Future Directions and Impact

6.1. Future Directions

6.1.1. MERTK and JNK1 in Lung Cancer

RAS mutations occur not just in PDAC but are seen in many forms of cancer. In lung cancer, RAS is mutated in 15%-20% of tumors (71). Although not a RAS mutation, BRAF (downstream of RAS but upstream of MEK) is known to be mutated in 2/3 of skin cancer, and subsequently the clinical use of MEK inhibitors has been a fruitful strategy in melanoma where Trametinib has gained FDA approval (262). The two proteins identified through this work, MERTK and JNK1, may be important either as markers of resistance or targets for combinatorial therapies so that other cancers with similar genetic mutations or MEK pathway dependence can share this success.

Because many of the same aberrant pathways in PDAC occur in RAS-mutant lung cancer, NSCLC lines are ideal for determining if MERTK or JNK1 has utility in other cancers. We performed a preliminary analysis using a small panel of lung lines to evaluate the correlation of MERTK and JNK1 expression levels to AZD6244 resistance. Six NSCLC cell lines were chosen with a broad range in sensitivity to the inhibitor (263, 264) to get a representative panel for lung cancer (Fig. 6.1A). Our GI_{50} values (Fig. 6.1B,C) were consistent with the findings of Davies et al. Western blots showed a strong trend of MERTK expression with resistance (correlation $p=0.0228$, $r=0.8740$; Fig. 6.1D); however, neither AXL nor JNK1 was seen to be an effective marker in lung cancer (Fig. 6.1E).

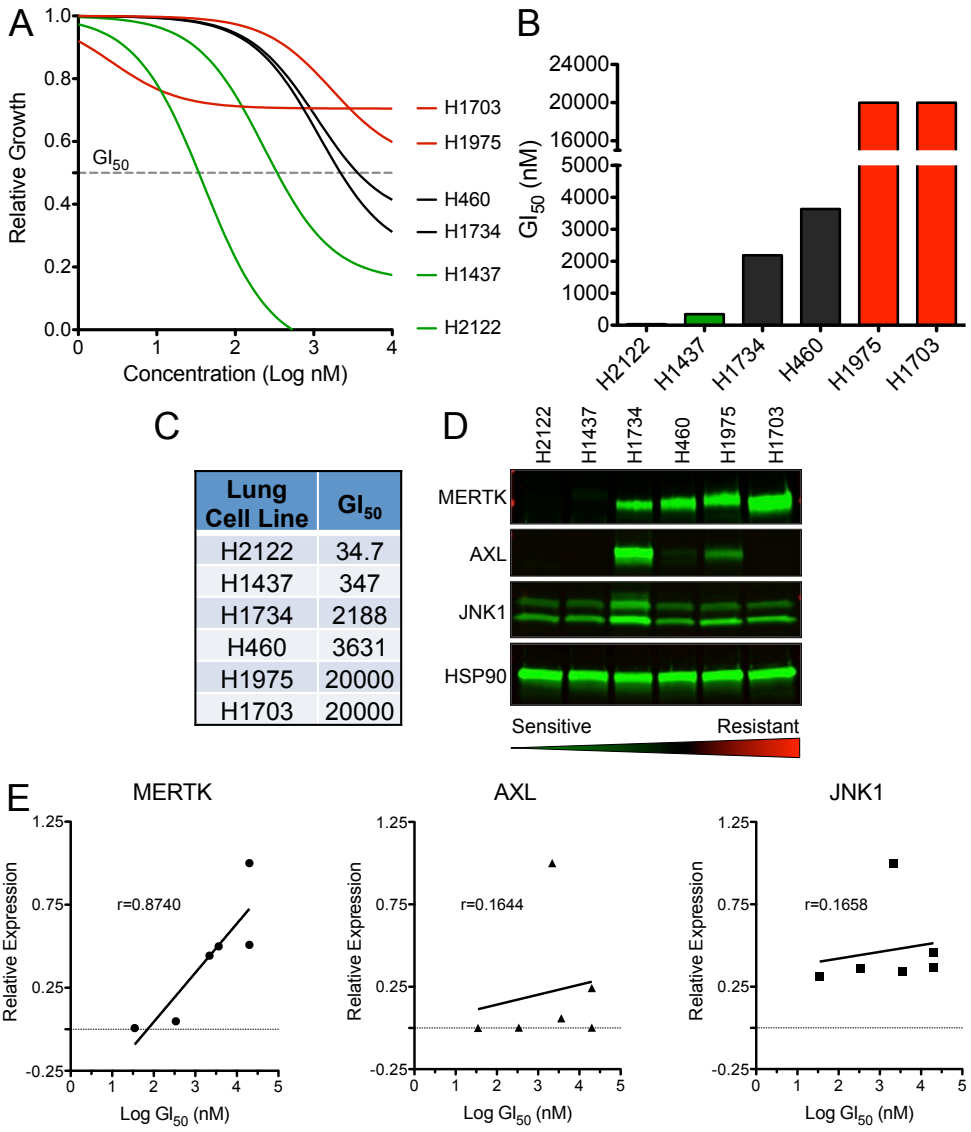

Figure 6.1 MERTK and JNK1 as Markers in Lung Cancer Cell Lines. *A)* AZD6244 inhibition curves for 6 NSCLC lines with varying degrees of sensitivity *B)* GI_{50} values for the cell lines *C)* Table of the GI_{50} Values *D)* qWestern blotting for the key proteins MERTK, AXL, and JNK1 *E)* Correlation analysis for MERTK, AXL and JNK1 to GI_{50} values reveal a significant correlation for MERTK (p=0.0228, r=0.8740) bot not for AXL or JNK1.

To further examine the utility of MERTK in RAS-mutant lung cancer, an expanded set of cell lines should be used to confirm the findings. One exciting finding in PDAC is the increase in MERTK protein expression after acquired resistance to AZD6244. Similar conditioning with the H2122 or H1437 lines would be useful to determine if MERTK can be used as a dual marker of innate and acquired resistance in NSCLC as with PDAC. These studies will help us understand how to best use MERTK as a marker in cancer. Furthermore, if JNK inhibitors can sensitize NSCLC cell lines to AZD6244, as in PDAC, our original observations would extend beyond pancreatic cancer and delineate common pathways in the two cancers.

6.1.2. Clinical Translation

The studies used to identify MERTK and JNK1 have all been in vitro with a few in vivo studies using the JNK inhibitor SP600125. The path from the bench to the bedside is arduous and many laboratory findings do not translate to clinical success. An advantage of using the AZD6244 inhibitor is that several clinical trials have already been performed and have demonstrated success in a subset of patients (171, 265-267). Obtaining tissue samples from patients that underwent these trials could prove valuable in determining MERTK's use as a prognostic marker. Since these trials have concluded, the patients' responses to MEK inhibition are known. Staining the tissue for MERTK expression and having it scored by a pathologist would allow determination of the extent of correlation between MERTK expression and tumor response to the therapy. A significant

correlation would indicate that the use of MERTK as a marker of resistance might be clinically relevant.

6.1.3. Development of a MERTK Probe

One of the challenges of PDAC is the location of the pancreas. Unlike colon cancer, which can be detected with a colonoscopy, or breast cancer that can be detected by a mammogram, no screening technique exists to detect or classify pancreatic cancer. Further, biopsies are difficult and invasive and not routinely performed on the pancreas because of the significant risk of provoking pancreatitis. Our lab has been working to develop a non-invasive imaging agent for the early detection of pancreatic cancer using the biomarker plectin; a similar probe could be designed to detect MERTK as a further diagnostic for predicted therapeutic response.

One of the benefits of MERTK being a surface receptor is its accessibility to molecules that cannot pass through the cell membrane. Our RTqPCR surface receptor transcriptome analysis was designed for this function. This allows for the use of phage display to screen for a targeting peptide that can be incorporated into an image probe. Phage display can be performed on purified MERTK or a cell line such as CHO transfected with a vector to overexpress MERTK on the surface. Our lab has been developing a technique to incorporate the external portion of MERTK into a cleavable “guillotine” construct that will allow for very selective peptide identification and eliminate the non-specific phage that bind to other receptors and proteins in the cell membrane. A depiction of the construct

can be seen in Fig. 6.2. From this screen, peptides that are identified to bind MERTK can be conjugated to radionuclides that allow positron emission tomography (PET) for *in vivo* imaging. Using mouse models, we can evaluate the probe's ability to distinguish between tumors expected to be sensitive or resistant to MEK inhibition. With the Kelly laboratory already performing radiotracer clinical trials, the path to clinical translation is understood for a peptide-based radiotracer.

6.1.4. Downstream Integration of JNK/ERK Signaling

JNK and ERK are parallel proteins in two separate MAPK pathways. Although ERK is pro-survival and JNK is typically associated with pro-apoptosis, these definitions are more fluid in cancer. A study in melanoma found that re-wiring of the ERK-JNK pathways to promote c-Jun and the protein's activity through positive feedback loops promoting the transcription of RACK1 and cyclin D1 (237). In our combinatorial therapy mouse models, we found c-Jun to have the least activity when AZD6244 and SP600125 were used together. c-Jun, a protein in the AP-1 family, is often regarded as the key molecule downstream of JNK and ERK for pro-oncogenic signaling (268-270), but other members of the AP-1 family may be important integrators of these two pathways.

In addition to c-Jun, the AP-1 family and its subfamilies of JUN, FOS, ATF, and MAF consist of proteins that are pro-oncogenic (ex. c-Fos and FOSB) and pro-apoptotic (ex JUNB and JUND). Adding to the complexity, these proteins work in complexes of homodimers and heterodimers to activate different genes

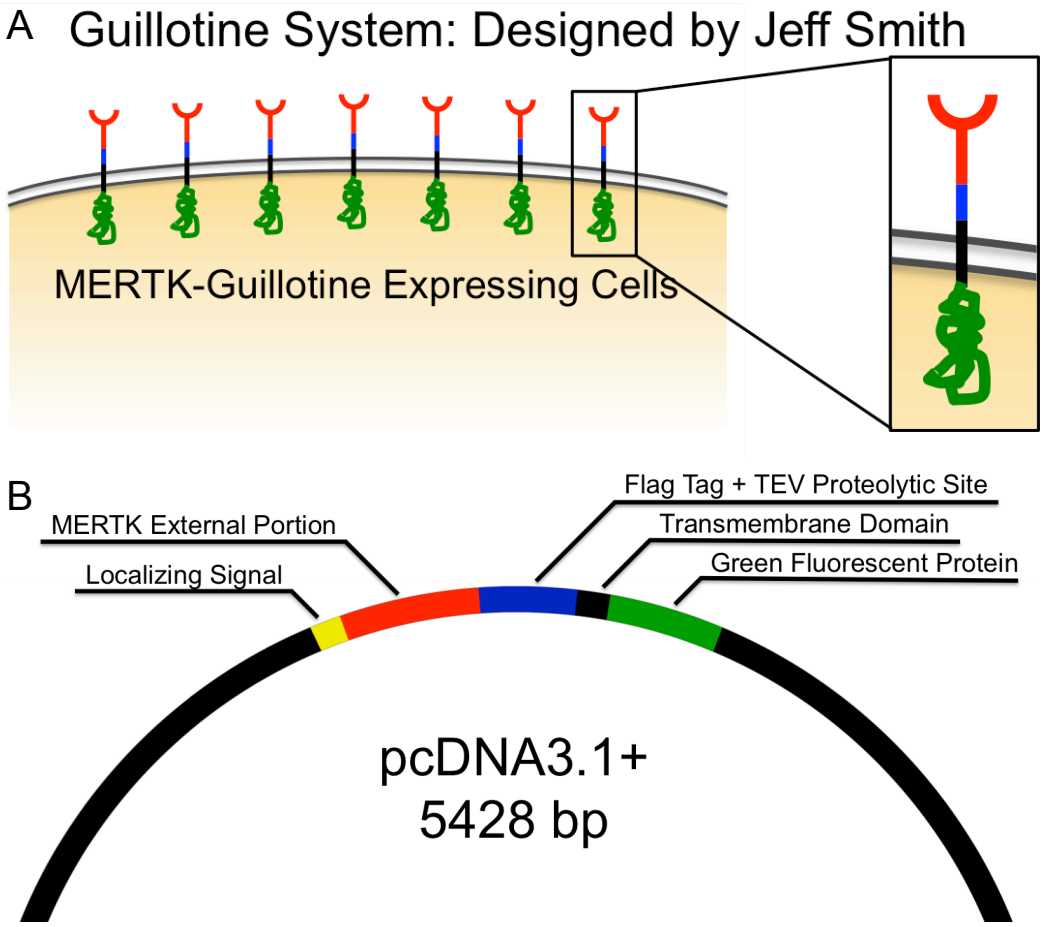

Figure 6.2 Guillotine phage screen design. *A)* Cleavable MERTK cell designs to allow simultaneous selection and subtraction during a phage screen *B)* Vector used to express the MERTK-Guillotine protein for phage screening

based on their pairing (271). To investigate which proteins are playing a key role in MEK inhibitor resistance, we would first look at their phosphorylation levels under MEK, JNK and dually inhibited cells. Important proteins to test in addition to c-Jun include c-Fos, FOSB, and AP-1. Proteins that only become deactivated with dual inhibition should be examined further in knockdown models for their contribution to MEK inhibitor insensitivity. Jiao et al. have studied the effects of c-Jun in cancer using murine cells and a Cre system with floxed c-*JUN* (272). Following this model, vectors with a Cre/LoxP system could conditionally knockdown proteins and allow for the study of the acute effects from protein loss and identify which proteins are necessary for cancer cell survival.

6.1.5. DUSP Proteins as Regulators of the MAPK Pathways

The DUSP family contains 10 different protein phosphatases that can dephosphorylate MAPK proteins, each with different substrate specificity. Specifically the subgroup of DUSP proteins known as MKPs is known to regulate the dephosphorylation of MAPK pathway proteins (273). From the phospho-kinase array comparing siMERTK and siControl cell lines, p38, JNK, and ERK all became more active with the loss of MERTK. This could indicate that MERTK activates a member of the DUSP family that would inhibit MAPK signaling. From Patterson et al. we know that DUSP1, DUSP8 and DUSP10 inhibit p38 and JNK equally well and ERK with slightly less affinity (273). Based on the phospho-kinase results, these are the most likely proteins to play a role in MEK inhibitor resistance. It has been reported that DUSP10 is not strongly expressed in the

pancreas (274); therefore DUSP1 and DUSP8 are the likeliest candidates to investigate.

Likewise, from the kinase array comparing normal to conditioned MIA PaCa-2 cell lines, we saw an increase in JNK and ERK signaling, and a moderate (if any) increase in p38 activity. This could indicate the decrease of DUSP4, which inhibits JNK and ERK equally and only moderately p38. Further, this protein is known to be expressed in the pancreas (275). Western blotting and siRNA assays targeting these proteins in MERTK knockdown (DUSP1 and DUSP8) or conditioned cells (DUSP4) compared to control could indicate if they play a role in MERTK signaling or resistance respectively.

6.1.6. Enhanced Small Molecule Screens

Applications of the enhanced small molecule-peptide phage system extend beyond just a larger library. The most apparent application would start with a small molecule of interest and tethering it to a pool of selenocysteine phage. The ideal small molecule would have high efficacy, but lack the proper specificity to distinguish between the target of interest and similar proteins (ex. distinguishing between MERTK and AXL). Screening of this library could be done to identify enhancing peptides that change the way the small molecule performs. This may cause the small molecules to become more specific, selective, or potent. Most likely, a peptide could be identified that allows the small molecule to still bind the target of interest, but prevents it from binding similar proteins. In

essence, it would be a peptide screen, but with a single, specific small molecule in the center of the peptide.

Development of such a screen could be performed for the matrix metalloproteinase (MMP) inhibitor *SB-3CT.* Inhibition of MMPs is known to have tumor suppression and anti-metastatic effects (276). The SB-3CT inhibitor targets MMP 2 and MMP 9 with nanomolar affinity. Although MMP-2 and MMP-9 are similar MMPs, they do have some different roles in cancer (277). It has been shown that tethering SB-3CT does not alter its inhibitory abilities (278). Tethering the SB-3CT to a full selenocysteine library with billions of unique peptides would allow for the screening of MMP-9 and subtraction on MMP-2. Phage that bind MMP-9, but not MMP-2 would be eluted and the targeting peptide identified by sequencing. If successful, this peptide-small molecule construct would target MMP-9 and not MMP-2.

6.1.7. A Barcode System for Screening Small Molecules

Another application of the system that could be developed would change the way small molecule screens are performed. First, each functionalized small molecule would need to be paired with a unique "barcode" peptide sequence. For example, peptide XXXX(Sec)XXX would be paired with molecule x, peptide YYYY(sec)YYY would be paired with molecule y, and so on. Once modified, the phage could be pooled and subsequently used in a screen. This would allow for all tethered molecules to be screened together as a single pool of phage and performed without the need for very large number of wells, making the screen

much more efficient and economical. The high affinity molecules could later be identified via their tethered, barcode peptides/phage. Sequencing of the phage DNA would indicate the specific peptide, and subsequently the specific molecule that bound the target.

A proof of concept could be performed on a small scale by selecting half a dozen small molecules to be tethered. Ideal molecules would have a well-known binding partner (ex. biotin and streptavidin, FITC and a FITC antibody, etc.). Each small molecule would be paired with a pre-determined phage peptide, specifically a peptide that is benign and will not contribute to the target binding. Once the six small molecule-phage pairs have been made, they can be pooled and applied to a substrate. To validate the system, a substrate that binds one of the molecules (ex. streptavidin) could be used. After a screen with the pooled phage, bound phage-small molecule complexes could be eluted, and the phage DNA sequenced to identify the peptide barcode and subsequently the small molecule. The system would be successful if the majority of phage identified were those tethering biotin. On a large scale, the number of tethered molecules could be extended to hundreds or thousands. Packaged into pools for laboratory screening and eliminate the first round of a small molecule screens.

6.2. Materials and Methods

6.2.1. Antibodies and Drugs

The small molecule inhibitor AZD6244 was purchased from Selleck Chemical and prepared in dimethyl sulfoxide (DMSO) with a stock concentration

of 10 mM. Primary antibodies were purchased from Cell Signaling Technology [JNK1 (2C6), HSP90 (C45G5), Mer (D21F11), AXL (C89E7)]. All secondary antibodies were purchased from Li-Cor [Donkey α-Goat 800CW (926-32214), Donkey α-Mouse 800CW (926-32212), Donkey α-Rabbit 800CW (926-32213), Streptavidin 800CW (926-32230)].

6.2.2. Cell Culture

6 different lung cancer cell lines were used in this study. All cell lines were acquired from American Type Culture Collection (ATCC). H460, H1437, H1703, H1734, H1975, and H2122 were all growth in Roswell Park Memorial Institute (RPMI) medium supplemented with 10% (vol/vol) fetal bovine serum (FBS), 1% penicillin-streptomycin (pen-strep; ATCC 30-2300), and 2mM L-glutamine (L-glut). All cells were incubated at 37°C, 5% CO_2.

6.2.3. Dose Response Curves

Cell lines were plated in two 96 well plates at a concentration of 2,500 cell/well. After 24 hrs, fresh media containing concentrations of AZD6244 ranging from 20 μM down to 63.2 pM by half-log units were added to each well in triplicate, after which the cells were incubated for three additional days. The second plate was used for an initial, “Day 0” reading. These cells were washed 3 times with phosphate buffered saline plus calcium and magnesium (PBS+) then fixed with 4% paraformaldehyde (PFA). The cells were again washed then incubated in Syto® 60 dye (Life Technologies) diluted 1:3,000 in PBS+ for 1 hr. Cells were subsequently washed 6 times and imaged using a Li-Cor Odyssey at

the 680 wavelength. Quantification was performed using the Li-Cor software. After the three-day incubation the inhibited cells in the first plate were processed the same way and quantified with the imager. Inhibition curves were reconstructed in Prism software using a 3-parameter (Bottom, Top, and IC_{50} with the hill slope constrained to -1) dose response curve. The equation used was $Y=Bottom + (Top-Bottom)/(1+10^{((X-LogIC_{50})))}$. The curves were adjusted by subtracting the Day 0 intensity (therefore y=0 indicates no growth) and the top of the curve adjusted to 1 (maximal growth). The result was a curve that had a max value of 1, and when it crossed the x-axis indicated zero growth. GI_{50} values were then calculated from these curves for the concentration of inhibitor that caused a 50% decrease in cell growth. Combinatorial dose response curves were performed using 2 inhibitors, one of which was held constant throughout all the wells and the other inhibitor having varying concentrations (performed in triplicate).

6.2.4. Western Blots

All cell lines used for blots were grown to ~90% confluency in 10 cm culture dishes before being lysed in 300 µL of lysis buffer [PBS plus 1% Triton X-100, 1x protease/phosphatase inhibitor (Cell Signaling Technologies)]. Quantification of protein concentrations was performed using a bicinchoninic acid (BCA) assay (Pierce) to ensure even loading between samples. Loading dye (3x) plus Dithiothreitol (DTT, New England Biolabs) was added before heat denaturation and run on 4-15% TGX gels (Bio-Rad). Proteins were transferred to polyvinylidene difluoride (PVDF) membranes and incubated with the appropriate

antibodies. Quantitative western (qWestern) blots were performed using fluorescent secondary antibodies (800 and 680 nm, Li-Cor) and a Li-Cor Odyssey imager. Quantification was performed using the manufacturer's software. Correlation analyses with GI_{50} values were performed by calculating the Pearson product-moment correlation coefficient (r) using the Prism software.

6.2.5. Phospho-Proteome Analysis

A Human Phospho-Kinase Array Kit (R&D Systems, ARY003B) was used to quantify the activity of 43 kinase phosphorylations and 2 key proteins expression levels. The product protocol was followed with minor alterations. Briefly, normal and inhibited MIA PaCa-2 cells were lysed with Lysis Buffer 6 (R&D Systems) and agitated for 30 min at 4°C. The array membranes were cut to remove the numbering (they autofluoresce at the 800 wavelength) and blocked with Array Buffer 1 (R&D Systems) for 1 hr then incubated with 350 µg of cell lysates overnight at 4°C under gentle agitation. The membranes were then washed 3 times with the 1x wash buffer (R&D Systems). The membranes were then incubated with biotinylated detection antibodies for 2 h at room temperature and washed 3x times with 1x wash buffer. Deviating from the product protocol, we replaced the supplied streptavidin-HRP secondary, with Streptavidin 800CW (diluted in Li-Cor blocking buffer 1:20,000). Membranes were incubated with the secondary for 30 minutes before being washed and imaged using the Li-Cor imager. Quantification was performed using the Li-Cor software.

6.3. Impact

Wistuba et al. in a *Nature* review recognize two critical components to precision medicine: 1) a comprehensive understanding of tumor biology in patients and 2) mechanisms to identify and classify patients into proper subgroups that will benefit from a specific therapy (279). I find this definition of precision medicine to be insufficient, and that a third component is needed. Understanding cancer biology and identifying a tumor's weaknesses is only beneficial if we can target and exploit those weaknesses. Therefore, I believe the development of treatment strategies with specific targeting ability is also needed in precision medicine - therapeutics that can selectively target tumor over normal tissue, inhibit a key oncogenic protein, etc. In the above example of RAF inhibitors, these strategies appeared doomed until the development of inhibitors that could selectively target mutant BRAF and not wild type, such as vemurafenib and dabrafenib. These molecules have since seen great clinical success in melanoma because of their precision (124). Targeting mutant proteins over wild type, targeting therapeutics to cancer and not normal tissue – it is abilities like these, that increase selectivity and specificity, that will be key in future medicine.

In the work presented here, we address all three components of precision medicine. We discovered markers to help predict tumor response to MEK inhibition, expanded our knowledge on the mechanisms of MEK inhibitor resistance, and developed a new small molecule-peptide screening technique for the development of future targeting moieties. Because RAS is mutated in >90 of pancreatic cancers (54), causing overactivation of growth and proliferation

pathways, developing therapeutics that limit the oncoprotein's signaling could be instrumental in combating the disease. Unfortunately, despite decades of research, RAS largely remains an "undruggable" target. As an alternative, efforts have pursued targeting the downstream pathway of RAS, usually with small molecule inhibitors, with the hopes of achieving the same end result. In some instances, these molecules have proven to be effective therapeutic strategies. In May, 2013 the FDA approved Trametinib as the first MEK inhibitor for cancer therapy. Approval was for patients with melanoma harboring a BRAF mutation; this narrowing of the inhibitors use, to a subpopulation most likely to respond, was key to successful clinical trials (280).

Using this as a model, this work takes the first steps to subtyping pancreatic cancers based on their expected response to MEK inhibition to help design therapies that can achieve clinical success as well. By identifying groups of pancreatic cancer cell lines that are sensitive and resistant to MEK inhibition, we were able to compare mRNA transcript differences between these two groups and identify potential markers indicative of sensitivity and resistance. We focused on the only transcript that emerged from two different arrays, *MERTK*. MERTK has been implicated in a number of different cancers, but its importance in PDAC had yet to be examined. We found MERTK to be overexpressed in cell lines resistant to MEK inhibition, both in PDAC as well as NSCLC. High expression of this receptor in tumors could be exploited in clinical applications to help clinicians decide whom to give MEK inhibitor therapies to in the future.

We further explored the differences between the sensitive and resistant groups to identify JNK1 as another protein overexpressed in resistant cell lines. As a member of a parallel MAPK cascade to that of MEK/ERK, JNK1 can activate several of the same effector molecules as ERK. However the JNK pathway is often associated with apoptosis. There are many conflicting reports of the JNK and the effects it has in cancer (281). This leads one to the conclusion that it is very context dependent. Here we found JNK1 signaling to be pro-oncogenic. Inhibiting the JNK1 pathway in conjunction with MEK had a favorable response, especially in cell lines resistant to MEK inhibition alone. These findings support the use of combination therapy when monotherapy alone is insufficient.

Lastly, a key component to future medicine will be the ability to target cancer with high precision. This is important for both diagnostic and therapeutic design. Finding way to discriminate normal tissue from cancer is a huge challenge in the clinic today. High therapeutic precision minimizes patient toxicity and allows for a tighter control of the effects of the therapy. To design such medicine, new targeting techniques are required. Since the development of phage display in 1985, thousands of targeting peptides have been discovered and used to create better imaging agents and therapeutics (282). One of the largest limitations of phage display however is the requirement that peptides be formed from the pool of 20 naturally occurring amino acids. We developed a way to significantly expand the diversity of phage display by the addition of small molecules to the screening peptides. This can open many new avenues for phage applications. Now, peptide-small molecule hybrids can be screened for

enhanced affinity or specificity compared to either component alone. This new technique will be greatly beneficial in designing tomorrow's medicine.

Chapter 7

References

1. 2014. SEER Cancer Statistics Factsheets: Pancreas Cancer.
2. Howlader, N., A. M. Noone, M. Krapcho, J. Garshell, N. Neyman, S. F. Altekruse, C. L. Kosary, M. Yu, J. Ruhl, Z. Tatalovich, H. Cho, A. Mariotto, D. R. Lewis, H. S. Chen, E. J. Feuer, and K. A. Cronin. 2014. SEER Cancer Statistics Review, 1975-2011.
3. Rahib, L., B. D. Smith, R. Aizenberg, A. B. Rosenzweig, J. M. Fleshman, and L. M. Matrisian. 2014. Projecting cancer incidence and deaths to 2030: the unexpected burden of thyroid, liver, and pancreas cancers in the United States. *Cancer Res* 74: 2913-2921.
4. Goggins, M. 2007. Identifying molecular markers for the early detection of pancreatic neoplasia. *Semin Oncol* 34: 303-310.
5. Hassan, M. M., M. L. Bondy, R. A. Wolff, J. L. Abbruzzese, J. N. Vauthey, P. W. Pisters, D. B. Evans, R. Khan, T. H. Chou, R. Lenzi, L. Jiao, and D. Li. 2007. Risk factors for pancreatic cancer: case-control study. *Am J Gastroenterol* 102: 2696-2707.
6. Bulajic, M., N. Panic, and J. M. Lohr. 2014. Helicobacter pylori and pancreatic diseases. *World J Gastrointest Pathophysiol* 5: 380-383.
7. Talamini, G., M. Falconi, C. Bassi, N. Sartori, R. Salvia, E. Caldiron, L. Frulloni, V. Di Francesco, B. Vaona, P. Bovo, I. Vantini, P. Pederzoli, and G. Cavallini. 1999. Incidence of cancer in the course of chronic pancreatitis. *Am J Gastroenterol* 94: 1253-1260.
8. Ekoe, J. M., P. Ghadirian, A. Simard, J. Baillargeon, and C. Perret. 1992. [Diabetes mellitus and pancreatic cancer: a case-control study in greater Montreal, Quebec, Canada]. *Rev Epidemiol Sante Publique* 40: 447-453.
9. Everhart, J., and D. Wright. 1995. Diabetes mellitus as a risk factor for pancreatic cancer. A meta-analysis. *JAMA* 273: 1605-1609.
10. Ghadirian, P., H. T. Lynch, and D. Krewski. 2003. Epidemiology of pancreatic cancer: an overview. *Cancer Detect Prev* 27: 87-93.
11. Wolpin, B. M., A. T. Chan, P. Hartge, S. J. Chanock, P. Kraft, D. J. Hunter, E. L. Giovannucci, and C. S. Fuchs. 2009. ABO blood group and the risk of pancreatic cancer. *J Natl Cancer Inst* 101: 424-431.
12. Tersmette, A. C., G. M. Petersen, G. J. Offerhaus, F. C. Falatko, K. A. Brune, M. Goggins, E. Rozenblum, R. E. Wilentz, C. J. Yeo, J. L. Cameron, S. E. Kern, and R. H. Hruban. 2001. Increased risk of incident pancreatic cancer among first-degree relatives of patients with familial pancreatic cancer. *Clin Cancer Res* 7: 738-744.
13. Shi, C., R. H. Hruban, and A. P. Klein. 2009. Familial pancreatic cancer. *Arch Pathol Lab Med* 133: 365-374.
14. Zhen, D. B., K. G. Rabe, S. Gallinger, S. Syngal, A. G. Schwartz, M. G. Goggins, R. H. Hruban, M. L. Cote, R. R. McWilliams, N. J. Roberts, L. A. Cannon-Albright, D. Li, K. Moyes, R. J. Wenstrup, A. R. Hartman, D. Seminara, A. P. Klein, and G. M. Petersen. 2014. BRCA1, BRCA2, PALB2, and CDKN2A mutations in familial pancreatic cancer: a PACGENE study. *Genet Med*
15. Couch, F. J., M. R. Johnson, K. G. Rabe, K. Brune, M. de Andrade, M. Goggins, H. Rothenmund, S. Gallinger, A. Klein, G. M. Petersen, and R. H.

Hruban. 2007. The prevalence of BRCA2 mutations in familial pancreatic cancer. *Cancer Epidemiol Biomarkers Prev* 16: 342-346.
16. Jones, S., R. H. Hruban, M. Kamiyama, M. Borges, X. Zhang, D. W. Parsons, J. C. Lin, E. Palmisano, K. Brune, E. M. Jaffee, C. A. Iacobuzio-Donahue, A. Maitra, G. Parmigiani, S. E. Kern, V. E. Velculescu, K. W. Kinzler, B. Vogelstein, J. R. Eshleman, M. Goggins, and A. P. Klein. 2009. Exomic sequencing identifies PALB2 as a pancreatic cancer susceptibility gene. *Science* 324: 217.
17. Sinilnikova, O. M., S. Mazoyer, C. Bonnardel, H. T. Lynch, S. A. Narod, and G. M. Lenoir. 2006. BRCA1 and BRCA2 mutations in breast and ovarian cancer syndrome: reflection on the Creighton University historical series of high risk families. *Fam Cancer* 5: 15-20.
18. Goggins, M., M. Schutte, J. Lu, C. A. Moskaluk, C. L. Weinstein, G. M. Petersen, C. J. Yeo, C. E. Jackson, H. T. Lynch, R. H. Hruban, and S. E. Kern. 1996. Germline BRCA2 gene mutations in patients with apparently sporadic pancreatic carcinomas. *Cancer Res* 56: 5360-5364.
19. Landi, S. 2009. Genetic predisposition and environmental risk factors to pancreatic cancer: A review of the literature. *Mutat Res* 681: 299-307.
20. Witt, H., W. Luck, H. C. Hennies, M. Classen, A. Kage, U. Lass, O. Landt, and M. Becker. 2000. Mutations in the gene encoding the serine protease inhibitor, Kazal type 1 are associated with chronic pancreatitis. *Nat Genet* 25: 213-216.
21. Lynch, H. T., R. M. Fusaro, J. F. Lynch, and R. Brand. 2008. Pancreatic cancer and the FAMMM syndrome. *Fam Cancer* 7: 103-112.
22. Zbuk, K. M., and C. Eng. 2007. Hamartomatous polyposis syndromes. *Nat Clin Pract Gastroenterol Hepatol* 4: 492-502.
23. Rustgi, A. K. 2007. The genetics of hereditary colon cancer. *Genes Dev* 21: 2525-2538.
24. Groden, J., A. Thliveris, W. Samowitz, M. Carlson, L. Gelbert, H. Albertsen, G. Joslyn, J. Stevens, L. Spirio, M. Robertson, and A. et. 1991. Identification and characterization of the familial adenomatous polyposis coli gene. *Cell* 66: 589-600.
25. Bartsch, D. K., T. M. Gress, and P. Langer. 2012. Familial pancreatic cancer--current knowledge. *Nat Rev Gastroenterol Hepatol* 9: 445-453.
26. Hidalgo, M. 2010. Pancreatic cancer. *N Engl J Med* 362: 1605-1617.
27. Miura, F., T. Takada, H. Amano, M. Yoshida, S. Furui, and K. Takeshita. 2006. Diagnosis of pancreatic cancer. *HPB (Oxford)* 8: 337-342.
28. Karmazanovsky, G., V. Fedorov, V. Kubyshkin, and A. Kotchatkov. 2005. Pancreatic head cancer: accuracy of CT in determination of resectability. *Abdom Imaging* 30: 488-500.
29. Ito, Y., T. Kenmochi, T. Irino, T. Egawa, S. Hayashi, A. Nagashima, N. Hiroe, M. Kitano, and Y. Kitagawa. 2012. Endoscopic management of pancreatic duct injury by endoscopic stent placement: a case report and literature review. *World J Emerg Surg* 7: 21.
30. Harsha, H. C., K. Kandasamy, P. Ranganathan, S. Rani, S. Ramabadran, S. Gollapudi, L. Balakrishnan, S. B. Dwivedi, D. Telikicherla, L. D. Selvan,

R. Goel, S. Mathivanan, A. Marimuthu, M. Kashyap, R. F. Vizza, R. J. Mayer, J. A. Decaprio, S. Srivastava, S. M. Hanash, R. H. Hruban, and A. Pandey. 2009. A compendium of potential biomarkers of pancreatic cancer. *PLoS Med* 6: e1000046.

31. Humphris, J. L., D. K. Chang, A. L. Johns, C. J. Scarlett, M. Pajic, M. D. Jones, E. K. Colvin, A. Nagrial, V. T. Chin, L. A. Chantrill, J. S. Samra, A. J. Gill, J. G. Kench, N. D. Merrett, A. Das, E. A. Musgrove, R. L. Sutherland, and A. V. Biankin. 2012. The prognostic and predictive value of serum CA19.9 in pancreatic cancer. *Ann Oncol* 23: 1713-1722.
32. Locker, G. Y., S. Hamilton, J. Harris, J. M. Jessup, N. Kemeny, J. S. Macdonald, M. R. Somerfield, D. F. Hayes, and R. C. J. Bast. 2006. ASCO 2006 update of recommendations for the use of tumor markers in gastrointestinal cancer. *J Clin Oncol* 24: 5313-5327.
33. Hawes, R. H., Q. Xiong, I. Waxman, K. J. Chang, D. B. Evans, and J. L. Abbruzzese. 2000. A multispecialty approach to the diagnosis and management of pancreatic cancer. *Am J Gastroenterol* 95: 17-31.
34. reprint from UpToDate, O., D. P. Ryan, H. Mamon, R. M. Goldberg, S. W. Ashley, C. G. Willett, and D. M. F. Savarese. Initial chemotherapy and radiation for nonmetastatic locally advanced unresectable, borderline resectable, and potentially resectable exocrine pancreatic cancer.
35. Cameron, J. L., T. S. Riall, J. Coleman, and K. A. Belcher. 2006. One thousand consecutive pancreaticoduodenectomies. *Ann Surg* 244: 10-15.
36. Herman, J. M., M. J. Swartz, C. C. Hsu, J. Winter, T. M. Pawlik, E. Sugar, R. Robinson, D. A. Laheru, E. Jaffee, R. H. Hruban, K. A. Campbell, C. L. Wolfgang, F. Asrari, R. Donehower, M. Hidalgo, L. A. J. Diaz, C. Yeo, J. L. Cameron, R. D. Schulick, and R. Abrams. 2008. Analysis of fluorouracil-based adjuvant chemotherapy and radiation after pancreaticoduodenectomy for ductal adenocarcinoma of the pancreas: results of a large, prospectively collected database at the Johns Hopkins Hospital. *J Clin Oncol* 26: 3503-3510.
37. Katz, M. H., P. W. Pisters, D. B. Evans, C. C. Sun, J. E. Lee, J. B. Fleming, J. N. Vauthey, E. K. Abdalla, C. H. Crane, R. A. Wolff, G. R. Varadhachary, and R. F. Hwang. 2008. Borderline resectable pancreatic cancer: the importance of this emerging stage of disease. *J Am Coll Surg* 206: 833-46; discussion 846.
38. Burris, H. A., M. J. Moore, J. Andersen, M. R. Green, M. L. Rothenberg, M. R. Modiano, M. C. Cripps, R. K. Portenoy, A. M. Storniolo, P. Tarassoff, R. Nelson, F. A. Dorr, C. D. Stephens, and D. D. Von Hoff. 1997. Improvements in survival and clinical benefit with gemcitabine as first-line therapy for patients with advanced pancreas cancer: a randomized trial. *J Clin Oncol* 15: 2403-2413.
39. Ryan, D. P., M. H. Kulke, C. S. Fuchs, M. L. Grossbard, S. R. Grossman, J. A. Morgan, C. C. Earle, R. Shivdasani, H. Kim, R. J. Mayer, and J. W. Clark. 2002. A Phase II study of gemcitabine and docetaxel in patients with metastatic pancreatic carcinoma. *Cancer* 94: 97-103.

40. Philip, P. A., M. M. Zalupski, V. K. Vaitkevicius, P. Arlauskas, R. Chaplen, L. K. Heilbrun, V. Adsay, D. Weaver, and A. F. Shields. 2001. Phase II study of gemcitabine and cisplatin in the treatment of patients with advanced pancreatic carcinoma. *Cancer* 92: 569-577.
41. Louvet, C., R. Labianca, P. Hammel, G. Lledo, M. G. Zampino, T. Andre, A. Zaniboni, M. Ducreux, E. Aitini, J. Taieb, R. Faroux, C. Lepere, and A. de Gramont. 2005. Gemcitabine in combination with oxaliplatin compared with gemcitabine alone in locally advanced or metastatic pancreatic cancer: results of a GERCOR and GISCAD phase III trial. *J Clin Oncol* 23: 3509-3516.
42. Berlin, J. D., P. Catalano, J. P. Thomas, J. W. Kugler, D. G. Haller, and A. B. Benson. 2002. Phase III study of gemcitabine in combination with fluorouracil versus gemcitabine alone in patients with advanced pancreatic carcinoma: Eastern Cooperative Oncology Group Trial E2297. *J Clin Oncol* 20: 3270-3275.
43. Stathopoulos, G. P., K. Syrigos, G. Aravantinos, A. Polyzos, P. Papakotoulas, G. Fountzilas, A. Potamianou, N. Ziras, J. Boukovinas, J. Varthalitis, N. Androulakis, A. Kotsakis, G. Samonis, and V. Georgoulias. 2006. A multicenter phase III trial comparing irinotecan-gemcitabine (IG) with gemcitabine (G) monotherapy as first-line treatment in patients with locally advanced or metastatic pancreatic cancer. *Br J Cancer* 95: 587-592.
44. Singhal, M. K., A. Kapoor, P. K. Bagri, S. Narayan, D. Singh, R. K. Nirban, G. Singh, S. Maharia, P. Kumari, and S. L. Jakhar. 2014. 617PDA PHASE III TRIAL COMPARING FOLFIRINOX VERSUS GEMCITABINE FOR METASTATIC PANCREATIC CANCER. *Annals of Oncology* 25: iv210-iv211.
45. Valsecchi, M. E., E. D?az-Cant?n, M. de la Vega, and S. J. Littman. 2014. Recent treatment advances and novel therapies in pancreas cancer: a review. *Journal of gastrointestinal cancer* 45: 190-201.
46. Von Hoff, D. D., T. Ervin, F. P. Arena, E. G. Chiorean, J. Infante, M. Moore, T. Seay, S. A. Tjulandin, W. W. Ma, M. N. Saleh, M. Harris, M. Reni, S. Dowden, D. Laheru, N. Bahary, R. K. Ramanathan, J. Tabernero, M. Hidalgo, D. Goldstein, E. Van Cutsem, X. Wei, J. Iglesias, and M. F. Renschler. 2013. Increased survival in pancreatic cancer with nab-paclitaxel plus gemcitabine. *N Engl J Med* 369: 1691-1703.
47. Lurje, G., and H. J. Lenz. 2009. EGFR signaling and drug discovery. *Oncology* 77: 400-410.
48. Heinemann, V., S. Boeck, A. Hinke, R. Labianca, and C. Louvet. 2008. Meta-analysis of randomized trials: evaluation of benefit from gemcitabine-based combination chemotherapy applied in advanced pancreatic cancer. *BMC Cancer* 8: 82.
49. Moore, M. J., D. Goldstein, J. Hamm, A. Figer, J. R. Hecht, S. Gallinger, H. J. Au, P. Murawa, D. Walde, R. A. Wolff, D. Campos, R. Lim, K. Ding, G. Clark, T. Voskoglou-Nomikos, M. Ptasynski, and W. Parulekar. 2007. Erlotinib plus gemcitabine compared with gemcitabine alone in patients with

advanced pancreatic cancer: a phase III trial of the National Cancer Institute of Canada Clinical Trials Group. *J Clin Oncol* 25: 1960-1966.
50. Miyabayashi, K., H. Ijichi, D. Mohri, M. Tada, K. Yamamoto, Y. Asaoka, T. Ikenoue, K. Tateishi, Y. Nakai, H. Isayama, Y. Morishita, M. Omata, H. L. Moses, and K. Koike. 2013. Erlotinib prolongs survival in pancreatic cancer by blocking gemcitabine-induced MAPK signals. *Cancer Res* 73: 2221-2234.
51. Hezel, A. F., A. C. Kimmelman, B. Z. Stanger, N. Bardeesy, and R. A. Depinho. 2006. Genetics and biology of pancreatic ductal adenocarcinoma. *Genes Dev* 20: 1218-1249.
52. Eser, S., A. Schnieke, G. Schneider, and D. Saur. 2014. Oncogenic KRAS signalling in pancreatic cancer. *Br J Cancer* 111: 817-822.
53. Basturk, O., A. B. Farris III, and N. V. Adsay. 2009. Immunohistochemistry of pancreas, biliary tract and liver. *Diagnostic immunohistochemistry. New York: Churchill Livingstone* 541-593.
54. Kanda, M., H. Matthaei, J. Wu, S. M. Hong, J. Yu, M. Borges, R. H. Hruban, A. Maitra, K. Kinzler, B. Vogelstein, and M. Goggins. 2012. Presence of somatic mutations in most early-stage pancreatic intraepithelial neoplasia. *Gastroenterology* 142: 730-733.e9.
55. Lohr, M., G. Kloppel, P. Maisonneuve, A. B. Lowenfels, and J. Luttges. 2005. Frequency of K-ras mutations in pancreatic intraductal neoplasias associated with pancreatic ductal adenocarcinoma and chronic pancreatitis: a meta-analysis. *Neoplasia* 7: 17-23.
56. Neumann, J., E. Zeindl-Eberhart, T. Kirchner, and A. Jung. 2009. Frequency and type of KRAS mutations in routine diagnostic analysis of metastatic colorectal cancer. *Pathol Res Pract* 205: 858-862.
57. Morris, J. P., S. C. Wang, and M. Hebrok. 2010. KRAS, Hedgehog, Wnt and the twisted developmental biology of pancreatic ductal adenocarcinoma. *Nat Rev Cancer* 10: 683-695.
58. Rozenblum, E., M. Schutte, M. Goggins, S. A. Hahn, S. Panzer, M. Zahurak, S. N. Goodman, T. A. Sohn, R. H. Hruban, C. J. Yeo, and S. E. Kern. 1997. Tumor-suppressive pathways in pancreatic carcinoma. *Cancer Res* 57: 1731-1734.
59. Hustinx, S. R., L. M. Leoni, C. J. Yeo, P. N. Brown, M. Goggins, S. E. Kern, R. H. Hruban, and A. Maitra. 2005. Concordant loss of MTAP and p16/CDKN2A expression in pancreatic intraepithelial neoplasia: evidence of homozygous deletion in a noninvasive precursor lesion. *Mod Pathol* 18: 959-963.
60. Honda, R., and H. Yasuda. 1999. Association of p19(ARF) with Mdm2 inhibits ubiquitin ligase activity of Mdm2 for tumor suppressor p53. *EMBO J* 18: 22-27.
61. Moll, U. M., and O. Petrenko. 2003. The MDM2-p53 interaction. *Mol Cancer Res* 1: 1001-1008.
62. Morton, J. P., P. Timpson, S. A. Karim, R. A. Ridgway, D. Athineos, B. Doyle, N. B. Jamieson, K. A. Oien, A. M. Lowy, V. G. Brunton, M. C. Frame, T. R. Evans, and O. J. Sansom. 2010. Mutant p53 drives metastasis and

overcomes growth arrest/senescence in pancreatic cancer. *Proc Natl Acad Sci U S A* 107: 246-251.
63. Maitra, A., N. V. Adsay, P. Argani, C. Iacobuzio-Donahue, A. De Marzo, J. L. Cameron, C. J. Yeo, and R. H. Hruban. 2003. Multicomponent analysis of the pancreatic adenocarcinoma progression model using a pancreatic intraepithelial neoplasia tissue microarray. *Mod Pathol* 16: 902-912.
64. Hahn, S. A., M. Schutte, A. T. Hoque, C. A. Moskaluk, L. T. da Costa, E. Rozenblum, C. L. Weinstein, A. Fischer, C. J. Yeo, R. H. Hruban, and S. E. Kern. 1996. DPC4, a candidate tumor suppressor gene at human chromosome 18q21.1. *Science* 271: 350-353.
65. Hasegawa, Y., S. Takanashi, Y. Kanehira, T. Tsushima, T. Imai, and K. Okumura. 2001. Transforming growth factor-beta1 level correlates with angiogenesis, tumor progression, and prognosis in patients with nonsmall cell lung carcinoma. *Cancer* 91: 964-971.
66. Rich, J. N., M. Zhang, M. B. Datto, D. D. Bigner, and X. F. Wang. 1999. Transforming growth factor-beta-mediated p15(INK4B) induction and growth inhibition in astrocytes is SMAD3-dependent and a pathway prominently altered in human glioma cell lines. *J Biol Chem* 274: 35053-35058.
67. Colicelli, J. 2004. Human RAS superfamily proteins and related GTPases. *Sci STKE* 2004: RE13.
68. Lodish, H. F., A. Berk, S. L. Zipursky, P. Matsudaira, D. Baltimore, and J. Darnell. 2000. *Molecular cell biology*. WH Freeman New York,
69. Rudack, T., F. Xia, J. Schlitter, C. Kotting, and K. Gerwert. 2012. Ras and GTPase-activating protein (GAP) drive GTP into a precatalytic state as revealed by combining FTIR and biomolecular simulations. *Proc Natl Acad Sci U S A* 109: 15295-15300.
70. Grady, W. M., and S. D. Markowitz. 2002. Genetic and epigenetic alterations in colon cancer. *Annu Rev Genomics Hum Genet* 3: 101-128.
71. Mitsuuchi, Y., and J. R. Testa. 2002. Cytogenetics and molecular genetics of lung cancer. *Am J Med Genet* 115: 183-188.
72. Jaffee, E. M., R. H. Hruban, M. Canto, and S. E. Kern. 2002. Focus on pancreas cancer. *Cancer Cell* 2: 25-28.
73. Prior, I. A., P. D. Lewis, and C. Mattos. 2012. A comprehensive survey of Ras mutations in cancer. *Cancer Res* 72: 2457-2467.
74. Zhang, K., J. E. DeClue, W. C. Vass, A. G. Papageorge, F. McCormick, and D. R. Lowy. 1990. Suppression of c-ras transformation by GTPase-activating protein. *Nature* 346: 754-756.
75. Goitre, L., E. Trapani, L. Trabalzini, and S. F. Retta. 2014. The Ras superfamily of small GTPases: the unlocked secrets. *Methods Mol Biol* 1120: 1-18.
76. Feig, L. A., and G. M. Cooper. 1988. Relationship among guanine nucleotide exchange, GTP hydrolysis, and transforming potential of mutated ras proteins. *Mol Cell Biol* 8: 2472-2478.
77. von Lintig, F. C., A. D. Dreilinger, N. M. Varki, A. M. Wallace, D. E. Casteel, and G. R. Boss. 2000. Ras activation in human breast cancer. *Breast Cancer Res Treat* 62: 51-62.

78. Wilentz, R. E., C. A. Iacobuzio-Donahue, P. Argani, D. M. McCarthy, J. L. Parsons, C. J. Yeo, S. E. Kern, and R. H. Hruban. 2000. Loss of expression of Dpc4 in pancreatic intraepithelial neoplasia: evidence that DPC4 inactivation occurs late in neoplastic progression. *Cancer Res* 60: 2002-2006.
79. Lim, K. H., K. O'Hayer, S. J. Adam, S. D. Kendall, P. M. Campbell, C. J. Der, and C. M. Counter. 2006. Divergent roles for RalA and RalB in malignant growth of human pancreatic carcinoma cells. *Curr Biol* 16: 2385-2394.
80. Feldmann, G., A. Mishra, S. M. Hong, S. Bisht, C. J. Strock, D. W. Ball, M. Goggins, A. Maitra, and B. D. Nelkin. 2010. Inhibiting the cyclin-dependent kinase CDK5 blocks pancreatic cancer formation and progression through the suppression of Ras-Ral signaling. *Cancer Res* 70: 4460-4469.
81. Carpenter, C. L., B. C. Duckworth, K. R. Auger, B. Cohen, B. S. Schaffhausen, and L. C. Cantley. 1990. Purification and characterization of phosphoinositide 3-kinase from rat liver. *J Biol Chem* 265: 19704-19711.
82. Berndt, N., A. D. Hamilton, and S. M. Sebti. 2011. Targeting protein prenylation for cancer therapy. *Nat Rev Cancer* 11: 775-791.
83. Karakas, B., K. E. Bachman, and B. H. Park. 2006. Mutation of the PIK3CA oncogene in human cancers. *Br J Cancer* 94: 455-459.
84. Holmes, D. 2011. PI3K pathway inhibitors approach junction. *Nat Rev Drug Discov* 10: 563-564.
85. Chen, Z., L. C. Trotman, D. Shaffer, H. K. Lin, Z. A. Dotan, M. Niki, J. A. Koutcher, H. I. Scher, T. Ludwig, W. Gerald, C. Cordon-Cardo, and P. P. Pandolfi. 2005. Crucial role of p53-dependent cellular senescence in suppression of Pten-deficient tumorigenesis. *Nature* 436: 725-730.
86. Samuels, Y., and T. Waldman. 2010. Oncogenic mutations of PIK3CA in human cancers. *Curr Top Microbiol Immunol* 347: 21-41.
87. Asano, T., Y. Yao, J. Zhu, D. Li, J. L. Abbruzzese, and S. A. Reddy. 2004. The PI 3-kinase/Akt signaling pathway is activated due to aberrant Pten expression and targets transcription factors NF-kappaB and c-Myc in pancreatic cancer cells. *Oncogene* 23: 8571-8580.
88. Lim, K. H., and C. M. Counter. 2005. Reduction in the requirement of oncogenic Ras signaling to activation of PI3K/AKT pathway during tumor maintenance. *Cancer Cell* 8: 381-392.
89. Pearson, G., F. Robinson, T. Beers Gibson, B. E. Xu, M. Karandikar, K. Berman, and M. H. Cobb. 2001. Mitogen-activated protein (MAP) kinase pathways: regulation and physiological functions. *Endocr Rev* 22: 153-183.
90. Davies, H., G. R. Bignell, C. Cox, P. Stephens, S. Edkins, S. Clegg, J. Teague, H. Woffendin, M. J. Garnett, W. Bottomley, N. Davis, E. Dicks, R. Ewing, Y. Floyd, K. Gray, S. Hall, R. Hawes, J. Hughes, V. Kosmidou, A. Menzies, C. Mould, A. Parker, C. Stevens, S. Watt, S. Hooper, R. Wilson, H. Jayatilake, B. A. Gusterson, C. Cooper, J. Shipley, D. Hargrave, K. Pritchard-Jones, N. Maitland, G. Chenevix-Trench, G. J. Riggins, D. D. Bigner, G. Palmieri, A. Cossu, A. Flanagan, A. Nicholson, J. W. Ho, S. Y. Leung, S. T. Yuen, B. L. Weber, H. F. Seigler, T. L. Darrow, H. Paterson, R.

Marais, C. J. Marshall, R. Wooster, M. R. Stratton, and P. A. Futreal. 2002. Mutations of the BRAF gene in human cancer. *Nature* 417: 949-954.
91. Hirano, T., Y. Shino, T. Saito, F. Komoda, Y. Okutomi, A. Takeda, T. Ishihara, T. Yamaguchi, H. Saisho, and H. Shirasawa. 2002. Dominant negative MEKK1 inhibits survival of pancreatic cancer cells. *Oncogene* 21: 5923-5928.
92. Gysin, S., S. H. Lee, N. M. Dean, and M. McMahon. 2005. Pharmacologic inhibition of RAF-->MEK-->ERK signaling elicits pancreatic cancer cell cycle arrest through induced expression of p27Kip1. *Cancer Res* 65: 4870-4880.
93. Kato, Y., R. I. Tapping, S. Huang, M. H. Watson, R. J. Ulevitch, and J. D. Lee. 1998. Bmk1/Erk5 is required for cell proliferation induced by epidermal growth factor. *Nature* 395: 713-716.
94. Wang, X., and C. Tournier. 2006. Regulation of cellular functions by the ERK5 signalling pathway. *Cell Signal* 18: 753-760.
95. Hu, B., D. Ren, D. Su, H. Lin, Z. Xian, X. Wan, J. Zhang, X. Fu, L. Jiang, D. Diao, X. Fan, L. Wang, and J. Wang. 2012. Expression of the phosphorylated MEK5 protein is associated with TNM staging of colorectal cancer. *BMC Cancer* 12: 127.
96. Esparis-Ogando, A., E. Diaz-Rodriguez, J. C. Montero, L. Yuste, P. Crespo, and A. Pandiella. 2002. Erk5 participates in neuregulin signal transduction and is constitutively active in breast cancer cells overexpressing ErbB2. *Mol Cell Biol* 22: 270-285.
97. Ramos-Nino, M. E., S. R. Blumen, T. Sabo-Attwood, H. Pass, M. Carbone, J. R. Testa, D. A. Altomare, and B. T. Mossman. 2008. HGF mediates cell proliferation of human mesothelioma cells through a PI3K/MEK5/Fra-1 pathway. *Am J Respir Cell Mol Biol* 38: 209-217.
98. Deng, X., L. Xiao, W. Lang, F. Gao, P. Ruvolo, and W. S. J. May. 2001. Novel role for JNK as a stress-activated Bcl2 kinase. *J Biol Chem* 276: 23681-23688.
99. Putcha, G. V., S. Le, S. Frank, C. G. Besirli, K. Clark, B. Chu, S. Alix, R. J. Youle, A. LaMarche, A. C. Maroney, and E. M. J. Johnson. 2003. JNK-mediated BIM phosphorylation potentiates BAX-dependent apoptosis. *Neuron* 38: 899-914.
100. Iyoda, K., Y. Sasaki, M. Horimoto, T. Toyama, T. Yakushijin, M. Sakakibara, T. Takehara, J. Fujimoto, M. Hori, J. R. Wands, and N. Hayashi. 2003. Involvement of the p38 mitogen-activated protein kinase cascade in hepatocellular carcinoma. *Cancer* 97: 3017-3026.
101. Tournier, C., P. Hess, D. D. Yang, J. Xu, T. K. Turner, A. Nimnual, D. Bar-Sagi, S. N. Jones, R. A. Flavell, and R. J. Davis. 2000. Requirement of JNK for stress-induced activation of the cytochrome c-mediated death pathway. *Science* 288: 870-874.
102. Dong, C., S. B. Waters, and K. H. Holt. PessinJE (1996) SOS phosphorylation and disassociation of the Grb2-SOS complex by the ERK and JNK signaling pathways. *J Bioi Chem* 271: 6328-6332.
103. Kwang-Hyun, C., S. Sung-Young, K. Hyun-Woo, O. Wolkenhauer, B. McFerran, and W. Kolch. 2003. Mathematical modeling of the influence of

RKIP on the ERK signaling pathway. Computational methods in systems biology: 127-141.
104. Shin, S. Y., O. Rath, S. M. Choo, F. Fee, B. McFerran, W. Kolch, and K. H. Cho. 2009. Positive- and negative-feedback regulations coordinate the dynamic behavior of the Ras-Raf-MEK-ERK signal transduction pathway. *J Cell Sci* 122: 425-435.
105. Fruman, D. A., and C. Rommel. 2014. PI3K and cancer: lessons, challenges and opportunities. *Nat Rev Drug Discov* 13: 140-156.
106. Aksamitiene, E., A. Kiyatkin, and B. N. Kholodenko. 2012. Cross-talk between mitogenic Ras/MAPK and survival PI3K/Akt pathways: a fine balance. *Biochem Soc Trans* 40: 139-146.
107. Shen, Y. H., J. Godlewski, J. Zhu, P. Sathyanarayana, V. Leaner, M. J. Birrer, A. Rana, and G. Tzivion. 2003. Cross-talk between JNK/SAPK and ERK/MAPK pathways: sustained activation of JNK blocks ERK activation by mitogenic factors. *J Biol Chem* 278: 26715-26721.
108. Gavrin, L., E. Saiah, and T. Waldman. 2012. Approaches to discover non-ATP site kinase inhibitors. *MedChemComm* 1: 41-51.
109. Schirmer, J., and K. Aktories. 2004. Large clostridial cytotoxins: cellular biology of Rho/Ras-glucosylating toxins. *Biochim Biophys Acta* 1673: 66-74.
110. Seabra, M. C. 1998. Membrane association and targeting of prenylated Ras-like GTPases. *Cell Signal* 10: 167-172.
111. Whyte, D. B., P. Kirschmeier, T. N. Hockenberry, I. Nunez-Oliva, L. James, J. J. Catino, W. R. Bishop, and J. K. Pai. 1997. K- and N-Ras are geranylgeranylated in cells treated with farnesyl protein transferase inhibitors. *J Biol Chem* 272: 14459-14464.
112. Zimmermann, G., B. Papke, S. Ismail, N. Vartak, A. Chandra, M. Hoffmann, S. A. Hahn, G. Triola, A. Wittinghofer, P. I. Bastiaens, and H. Waldmann. 2013. Small molecule inhibition of the KRAS-PDEdelta interaction impairs oncogenic KRAS signalling. *Nature* 497: 638-642.
113. Hocker, H. J., K. J. Cho, C. Y. Chen, N. Rambahal, S. R. Sagineedu, K. Shaari, J. Stanslas, J. F. Hancock, and A. A. Gorfe. 2013. Andrographolide derivatives inhibit guanine nucleotide exchange and abrogate oncogenic Ras function. *Proc Natl Acad Sci U S A* 110: 10201-10206.
114. Lim, S. M., K. D. Westover, S. B. Ficarro, R. A. Harrison, H. G. Choi, M. E. Pacold, M. Carrasco, J. Hunter, N. D. Kim, T. Xie, T. Sim, P. A. Janne, M. Meyerson, J. A. Marto, J. R. Engen, and N. S. Gray. 2014. Therapeutic targeting of oncogenic K-Ras by a covalent catalytic site inhibitor. *Angew Chem Int Ed Engl* 53: 199-204.
115. Wu, X., P. Upadhyaya, M. Villalona-Calero, R. Briesewitz, and D. Pei. 2013. Inhibition of Ras–effector interactions by cyclic peptides. *MedChemComm* 2: 378-382.
116. Ying, H., A. C. Kimmelman, C. A. Lyssiotis, S. Hua, G. C. Chu, E. Fletcher-Sananikone, J. W. Locasale, J. Son, H. Zhang, J. L. Coloff, H. Yan, W. Wang, S. Chen, A. Viale, H. Zheng, J. H. Paik, C. Lim, A. R. Guimaraes, E. S. Martin, J. Chang, A. F. Hezel, S. R. Perry, J. Hu, B. Gan, Y. Xiao, J. M. Asara, R. Weissleder, Y. A. Wang, L. Chin, L. C. Cantley, and R. A.

DePinho. 2012. Oncogenic Kras maintains pancreatic tumors through regulation of anabolic glucose metabolism. *Cell* 149: 656-670.
117. Collins, M. A., F. Bednar, Y. Zhang, J. C. Brisset, S. Galban, C. J. Galban, S. Rakshit, K. S. Flannagan, N. V. Adsay, and M. Pasca di Magliano. 2012. Oncogenic Kras is required for both the initiation and maintenance of pancreatic cancer in mice. *J Clin Invest* 122: 639-653.
118. Singh, A., P. Greninger, D. Rhodes, L. Koopman, S. Violette, N. Bardeesy, and J. Settleman. 2009. A gene expression signature associated with "K-Ras addiction" reveals regulators of EMT and tumor cell survival. *Cancer Cell* 15: 489-500.
119. Arcaro, A., and M. P. Wymann. 1993. Wortmannin is a potent phosphatidylinositol 3-kinase inhibitor: the role of phosphatidylinositol 3,4,5-trisphosphate in neutrophil responses. *Biochem J* 296: 297-301.
120. Kwitkowski, V. E., T. M. Prowell, A. Ibrahim, A. T. Farrell, R. Justice, S. S. Mitchell, R. Sridhara, and R. Pazdur. 2010. FDA approval summary: temsirolimus as treatment for advanced renal cell carcinoma. *Oncologist* 15: 428-435.
121. Carew, J. S., K. R. Kelly, and S. T. Nawrocki. 2011. Mechanisms of mTOR inhibitor resistance in cancer therapy. *Target Oncol* 6: 17-27.
122. Dienstmann, R., J. Rodon, V. Serra, and J. Tabernero. 2014. Picking the point of inhibition: a comparative review of PI3K/AKT/mTOR pathway inhibitors. *Mol Cancer Ther* 13: 1021-1031.
123. Eisen, T., T. Ahmad, K. T. Flaherty, M. Gore, S. Kaye, R. Marais, I. Gibbens, S. Hackett, M. James, L. M. Schuchter, K. L. Nathanson, C. Xia, R. Simantov, B. Schwartz, M. Poulin-Costello, P. J. O'Dwyer, and M. J. Ratain. 2006. Sorafenib in advanced melanoma: a Phase II randomised discontinuation trial analysis. *Br J Cancer* 95: 581-586.
124. Chapman, P. B., A. Hauschild, C. Robert, J. B. Haanen, P. Ascierto, J. Larkin, R. Dummer, C. Garbe, A. Testori, M. Maio, D. Hogg, P. Lorigan, C. Lebbe, T. Jouary, D. Schadendorf, A. Ribas, S. J. O'Day, J. A. Sosman, J. M. Kirkwood, A. M. Eggermont, B. Dreno, K. Nolop, J. Li, B. Nelson, J. Hou, R. J. Lee, K. T. Flaherty, and G. A. McArthur. 2011. Improved survival with vemurafenib in melanoma with BRAF V600E mutation. *N Engl J Med* 364: 2507-2516.
125. Su, F., A. Viros, C. Milagre, K. Trunzer, G. Bollag, O. Spleiss, J. S. Reis-Filho, X. Kong, R. C. Koya, K. T. Flaherty, P. B. Chapman, M. J. Kim, R. Hayward, M. Martin, H. Yang, Q. Wang, H. Hilton, J. S. Hang, J. Noe, M. Lambros, F. Geyer, N. Dhomen, I. Niculescu-Duvaz, A. Zambon, D. Niculescu-Duvaz, N. Preece, L. Robert, N. J. Otte, S. Mok, D. Kee, Y. Ma, C. Zhang, G. Habets, E. A. Burton, B. Wong, H. Nguyen, M. Kockx, L. Andries, B. Lestini, K. B. Nolop, R. J. Lee, A. K. Joe, J. L. Troy, R. Gonzalez, T. E. Hutson, I. Puzanov, B. Chmielowski, C. J. Springer, G. A. McArthur, J. A. Sosman, R. S. Lo, A. Ribas, and R. Marais. 2012. RAS mutations in cutaneous squamous-cell carcinomas in patients treated with BRAF inhibitors. *N Engl J Med* 366: 207-215.

126. Poulikakos, P. I., C. Zhang, G. Bollag, K. M. Shokat, and N. Rosen. 2010. RAF inhibitors transactivate RAF dimers and ERK signalling in cells with wild-type BRAF. *Nature* 464: 427-430.
127. Wallace, E. M., J. P. Lyssikatos, T. Yeh, J. D. Winkler, and K. Koch. 2005. Progress towards therapeutic small molecule MEK inhibitors for use in cancer therapy. *Curr Top Med Chem* 5: 215-229.
128. Ohren, J. F., H. Chen, A. Pavlovsky, C. Whitehead, E. Zhang, P. Kuffa, C. Yan, P. McConnell, C. Spessard, C. Banotai, W. T. Mueller, A. Delaney, C. Omer, J. Sebolt-Leopold, D. T. Dudley, I. K. Leung, C. Flamme, J. Warmus, M. Kaufman, S. Barrett, H. Tecle, and C. A. Hasemann. 2004. Structures of human MAP kinase kinase 1 (MEK1) and MEK2 describe novel noncompetitive kinase inhibition. *Nat Struct Mol Biol* 11: 1192-1197.
129. Lee, C.-S., and N. S Duesbery. 2010. Highly selective MEK inhibitors. *Current Enzyme Inhibition* 6: 146-157.
130. Alessi, D. R., A. Cuenda, P. Cohen, D. T. Dudley, and A. R. Saltiel. 1995. PD 098059 is a specific inhibitor of the activation of mitogen-activated protein kinase kinase in vitro and in vivo. *J Biol Chem* 270: 27489-27494.
131. Dudley, D. T., L. Pang, S. J. Decker, A. J. Bridges, and A. R. Saltiel. 1995. A synthetic inhibitor of the mitogen-activated protein kinase cascade. *Proc Natl Acad Sci U S A* 92: 7686-7689.
132. Mody, N., J. Leitch, C. Armstrong, J. Dixon, and P. Cohen. 2001. Effects of MAP kinase cascade inhibitors on the MKK5/ERK5 pathway. *FEBS Lett* 502: 21-24.
133. Wang, D., S. A. Boerner, J. D. Winkler, and P. M. LoRusso. 2007. Clinical experience of MEK inhibitors in cancer therapy. *Biochim Biophys Acta* 1773: 1248-1255.
134. Sebolt-Leopold, J. S., D. T. Dudley, R. Herrera, K. Van Becelaere, A. Wiland, R. C. Gowan, H. Tecle, S. D. Barrett, A. Bridges, S. Przybranowski, W. R. Leopold, and A. R. Saltiel. 1999. Blockade of the MAP kinase pathway suppresses growth of colon tumors in vivo. *Nat Med* 5: 810-816.
135. Lorusso, P. M., A. A. Adjei, M. Varterasian, S. Gadgeel, J. Reid, D. Y. Mitchell, L. Hanson, P. DeLuca, L. Bruzek, J. Piens, P. Asbury, K. Van Becelaere, R. Herrera, J. Sebolt-Leopold, and M. B. Meyer. 2005. Phase I and pharmacodynamic study of the oral MEK inhibitor CI-1040 in patients with advanced malignancies. *J Clin Oncol* 23: 5281-5293.
136. Yeh, T. C., V. Marsh, B. A. Bernat, J. Ballard, H. Colwell, R. J. Evans, J. Parry, D. Smith, B. J. Brandhuber, S. Gross, A. Marlow, B. Hurley, J. Lyssikatos, P. A. Lee, J. D. Winkler, K. Koch, and E. Wallace. 2007. Biological characterization of ARRY-142886 (AZD6244), a potent, highly selective mitogen-activated protein kinase kinase 1/2 inhibitor. *Clin Cancer Res* 13: 1576-1583.
137. Dragovich, T., D. Laheru, F. Dayyani, V. Bolejack, L. Smith, J. Seng, H. Burris, P. Rosen, M. Hidalgo, P. Ritch, A. F. Baker, N. Raghunand, J. Crowley, and D. D. Von Hoff. 2014. Phase II trial of vatalanib in patients with advanced or metastatic pancreatic adenocarcinoma after first-line

gemcitabine therapy (PCRT O4-001). *Cancer Chemother Pharmacol* 74: 379-387.
138. Gilmartin, A. G., M. R. Bleam, A. Groy, K. G. Moss, E. A. Minthorn, S. G. Kulkarni, C. M. Rominger, S. Erskine, K. E. Fisher, J. Yang, F. Zappacosta, R. Annan, D. Sutton, and S. G. Laquerre. 2011. GSK1120212 (JTP-74057) is an inhibitor of MEK activity and activation with favorable pharmacokinetic properties for sustained in vivo pathway inhibition. *Clin Cancer Res* 17: 989-1000.
139. Infante, J. R., B. G. Somer, J. O. Park, C. P. Li, M. E. Scheulen, S. M. Kasubhai, D. Y. Oh, Y. Liu, S. Redhu, K. Steplewski, and N. Le. 2014. A randomised, double-blind, placebo-controlled trial of trametinib, an oral MEK inhibitor, in combination with gemcitabine for patients with untreated metastatic adenocarcinoma of the pancreas. *Eur J Cancer* 50: 2072-2081.
140. Falchook, G. S., K. D. Lewis, J. R. Infante, M. S. Gordon, N. J. Vogelzang, D. J. DeMarini, P. Sun, C. Moy, S. A. Szabo, L. T. Roadcap, V. G. Peddareddigari, P. F. Lebowitz, N. T. Le, H. A. Burris, W. A. Messersmith, P. J. O'Dwyer, K. B. Kim, K. Flaherty, J. C. Bendell, R. Gonzalez, R. Kurzrock, and L. A. Fecher. 2012. Activity of the oral MEK inhibitor trametinib in patients with advanced melanoma: a phase 1 dose-escalation trial. *Lancet Oncol* 13: 782-789.
141. Hainsworth, J. D., C. L. Cebotaru, V. Kanarev, T. E. Ciuleanu, D. Damyanov, P. Stella, H. Ganchev, G. Pover, C. Morris, and V. Tzekova. 2010. A phase II, open-label, randomized study to assess the efficacy and safety of AZD6244 (ARRY-142886) versus pemetrexed in patients with non-small cell lung cancer who have failed one or two prior chemotherapeutic regimens. *J Thorac Oncol* 5: 1630-1636.
142. Shimizu, T., A. W. Tolcher, K. P. Papadopoulos, M. Beeram, D. W. Rasco, L. S. Smith, S. Gunn, L. Smetzer, T. A. Mays, B. Kaiser, M. J. Wick, C. Alvarez, A. Cavazos, G. L. Mangold, and A. Patnaik. 2012. The clinical effect of the dual-targeting strategy involving PI3K/AKT/mTOR and RAS/MEK/ERK pathways in patients with advanced cancer. *Clin Cancer Res* 18: 2316-2325.
143. Akinleye, A., M. Furqan, N. Mukhi, P. Ravella, and D. Liu. 2013. MEK and the inhibitors: from bench to bedside. *J Hematol Oncol* 6: 27.
144. Pao, W., V. A. Miller, K. A. Politi, G. J. Riely, R. Somwar, M. F. Zakowski, M. G. Kris, and H. Varmus. 2005. Acquired resistance of lung adenocarcinomas to gefitinib or erlotinib is associated with a second mutation in the EGFR kinase domain. *PLoS Med* 2: e73.
145. Meng, J., H. Peng, B. Dai, W. Guo, L. Wang, L. Ji, J. D. Minna, C. M. Chresta, P. D. Smith, B. Fang, and J. A. Roth. 2009. High level of AKT activity is associated with resistance to MEK inhibitor AZD6244 (ARRY-142886). *Cancer Biol Ther* 8: 2073-2080.
146. Camidge, D. R., W. Pao, and L. V. Sequist. 2014. Acquired resistance to TKIs in solid tumours: learning from lung cancer. *Nat Rev Clin Oncol* 11: 473-481.

147. Cappuzzo, F., P. A. Janne, M. Skokan, G. Finocchiaro, E. Rossi, C. Ligorio, P. A. Zucali, L. Terracciano, L. Toschi, M. Roncalli, A. Destro, M. Incarbone, M. Alloisio, A. Santoro, and M. Varella-Garcia. 2009. MET increased gene copy number and primary resistance to gefitinib therapy in non-small-cell lung cancer patients. *Ann Oncol* 20: 298-304.
148. Sequist, L. V., B. A. Waltman, D. Dias-Santagata, S. Digumarthy, A. B. Turke, P. Fidias, K. Bergethon, A. T. Shaw, S. Gettinger, A. K. Cosper, S. Akhavanfard, R. S. Heist, J. Temel, J. G. Christensen, J. C. Wain, T. J. Lynch, K. Vernovsky, E. J. Mark, M. Lanuti, A. J. Iafrate, M. Mino-Kenudson, and J. A. Engelman. 2011. Genotypic and histological evolution of lung cancers acquiring resistance to EGFR inhibitors. *Sci Transl Med* 3: 75ra26.
149. Bowlin, S. J., F. Xia, W. Wang, K. D. Robinson, and E. J. Stanek. 2013. Twelve-month frequency of drug-metabolizing enzyme and transporter-based drug-drug interaction potential in patients receiving oral enzyme-targeted kinase inhibitor antineoplastic agents. *Mayo Clin Proc* 88: 139-148.
150. Budha, N. R., A. Frymoyer, G. S. Smelick, J. Y. Jin, M. R. Yago, M. J. Dresser, S. N. Holden, L. Z. Benet, and J. A. Ware. 2012. Drug absorption interactions between oral targeted anticancer agents and PPIs: is pH-dependent solubility the Achilles heel of targeted therapy? *Clin Pharmacol Ther* 92: 203-213.
151. Janne, P. A., A. T. Shaw, J. R. Pereira, G. Jeannin, J. Vansteenkiste, C. Barrios, F. A. Franke, L. Grinsted, V. Zazulina, P. Smith, I. Smith, and L. Crino. 2013. Selumetinib plus docetaxel for KRAS-mutant advanced non-small-cell lung cancer: a randomised, multicentre, placebo-controlled, phase 2 study. *Lancet Oncol* 14: 38-47.
152. Hong, K. W., and B. Oh. 2010. Overview of personalized medicine in the disease genomic era. *BMB Rep* 43: 643-648.
153. Collisson, E. A., A. Sadanandam, P. Olson, W. J. Gibb, M. Truitt, S. Gu, J. Cooc, J. Weinkle, G. E. Kim, L. Jakkula, H. S. Feiler, A. H. Ko, A. B. Olshen, K. L. Danenberg, M. A. Tempero, P. T. Spellman, D. Hanahan, and J. W. Gray. 2011. Subtypes of pancreatic ductal adenocarcinoma and their differing responses to therapy. *Nat Med* 17: 500-503.
154. Ulloa-Montoya, F., J. Louahed, B. Dizier, O. Gruselle, B. Spiessens, F. F. Lehmann, S. Suciu, W. H. Kruit, A. M. Eggermont, J. Vansteenkiste, and V. G. Brichard. 2013. Predictive gene signature in MAGE-A3 antigen-specific cancer immunotherapy. *J Clin Oncol* 31: 2388-2395.
155. Lewis, C. A., C. Brault, B. Peck, K. Bensaad, B. Griffiths, R. Mitter, P. Chakravarty, P. East, B. Dankworth, D. Alibhai, A. L. Harris, and A. Schulze. 2015. SREBP maintains lipid biosynthesis and viability of cancer cells under lipid- and oxygen-deprived conditions and defines a gene signature associated with poor survival in glioblastoma multiforme. *Oncogene*
156. Sergeant, G., R. van Eijsden, T. Roskams, V. Van Duppen, and B. Topal. 2012. Pancreatic cancer circulating tumour cells express a cell motility gene signature that predicts survival after surgery. *BMC Cancer* 12: 527.
157. Byers, L. A., L. Diao, J. Wang, P. Saintigny, L. Girard, M. Peyton, L. Shen, Y. Fan, U. Giri, P. K. Tumula, M. B. Nilsson, J. Gudikote, H. Tran, R. J.

Cardnell, D. J. Bearss, S. L. Warner, J. M. Foulks, S. B. Kanner, V. Gandhi, N. Krett, S. T. Rosen, E. S. Kim, R. S. Herbst, G. R. Blumenschein, J. J. Lee, S. M. Lippman, K. K. Ang, G. B. Mills, W. K. Hong, J. N. Weinstein, I. I. Wistuba, K. R. Coombes, J. D. Minna, and J. V. Heymach. 2013. An epithelial-mesenchymal transition gene signature predicts resistance to EGFR and PI3K inhibitors and identifies Axl as a therapeutic target for overcoming EGFR inhibitor resistance. *Clin Cancer Res* 19: 279-290.

158. Dietel, M., and C. Sers. 2006. Personalized medicine and development of targeted therapies: The upcoming challenge for diagnostic molecular pathology. A review. *Virchows Arch* 448: 744-755.
159. Jones, S., X. Zhang, D. W. Parsons, J. C. Lin, R. J. Leary, P. Angenendt, P. Mankoo, H. Carter, H. Kamiyama, A. Jimeno, S. M. Hong, B. Fu, M. T. Lin, E. S. Calhoun, M. Kamiyama, K. Walter, T. Nikolskaya, Y. Nikolsky, J. Hartigan, D. R. Smith, M. Hidalgo, S. D. Leach, A. P. Klein, E. M. Jaffee, M. Goggins, A. Maitra, C. Iacobuzio-Donahue, J. R. Eshleman, S. E. Kern, R. H. Hruban, R. Karchin, N. Papadopoulos, G. Parmigiani, B. Vogelstein, V. E. Velculescu, and K. W. Kinzler. 2008. Core signaling pathways in human pancreatic cancers revealed by global genomic analyses. *Science* 321: 1801-1806.
160. Montagut, C., and J. Settleman. 2009. Targeting the RAF-MEK-ERK pathway in cancer therapy. *Cancer Lett* 283: 125-134.
161. Torii, S., T. Yamamoto, Y. Tsuchiya, and E. Nishida. 2006. ERK MAP kinase in G cell cycle progression and cancer. *Cancer Sci* 97: 697-702.
162. Malumbres, M., I. Perez De Castro, M. I. Hernandez, M. Jimenez, T. Corral, and A. Pellicer. 2000. Cellular response to oncogenic ras involves induction of the Cdk4 and Cdk6 inhibitor p15(INK4b). *Mol Cell Biol* 20: 2915-2925.
163. Karasarides, M., A. Chiloeches, R. Hayward, D. Niculescu-Duvaz, I. Scanlon, F. Friedlos, L. Ogilvie, D. Hedley, J. Martin, C. J. Marshall, C. J. Springer, and R. Marais. 2004. B-RAF is a therapeutic target in melanoma. *Oncogene* 23: 6292-6298.
164. Ley, R., K. Balmanno, K. Hadfield, C. Weston, and S. J. Cook. 2003. Activation of the ERK1/2 signaling pathway promotes phosphorylation and proteasome-dependent degradation of the BH3-only protein, Bim. *J Biol Chem* 278: 18811-18816.
165. Liu, L., Y. Cao, C. Chen, X. Zhang, A. McNabola, D. Wilkie, S. Wilhelm, M. Lynch, and C. Carter. 2006. Sorafenib blocks the RAF/MEK/ERK pathway, inhibits tumor angiogenesis, and induces tumor cell apoptosis in hepatocellular carcinoma model PLC/PRF/5. *Cancer Res* 66: 11851-11858.
166. Garnett, M. J., and R. Marais. 2004. Guilty as charged: B-RAF is a human oncogene. *Cancer Cell* 6: 313-319.
167. McCubrey, J. A., L. S. Steelman, S. L. Abrams, J. T. Lee, F. Chang, F. E. Bertrand, P. M. Navolanic, D. M. Terrian, R. A. Franklin, A. B. D'Assoro, J. L. Salisbury, M. C. Mazzarino, F. Stivala, and M. Libra. 2006. Roles of the RAF/MEK/ERK and PI3K/PTEN/AKT pathways in malignant transformation and drug resistance. *Adv Enzyme Regul* 46: 249-279.

168. Montagut, C., and J. Settleman. 2009. Targeting the RAF-MEK-ERK pathway in cancer therapy. *Cancer Lett* 283: 125-134.
169. Gioeli, D., J. W. Mandell, G. R. Petroni, H. F. J. Frierson, and M. J. Weber. 1999. Activation of mitogen-activated protein kinase associated with prostate cancer progression. *Cancer Res* 59: 279-284.
170. Flaherty, K. T., C. Robert, P. Hersey, P. Nathan, C. Garbe, M. Milhem, L. V. Demidov, J. C. Hassel, P. Rutkowski, P. Mohr, R. Dummer, U. Trefzer, J. M. Larkin, J. Utikal, B. Dreno, M. Nyakas, M. R. Middleton, J. C. Becker, M. Casey, L. J. Sherman, F. S. Wu, D. Ouellet, A. M. Martin, K. Patel, and D. Schadendorf. 2012. Improved survival with MEK inhibition in BRAF-mutated melanoma. *N Engl J Med* 367: 107-114.
171. Bodoky, G., C. Timcheva, D. R. Spigel, P. J. La Stella, T. E. Ciuleanu, G. Pover, and N. C. Tebbutt. 2012. A phase II open-label randomized study to assess the efficacy and safety of selumetinib (AZD6244 [ARRY-142886]) versus capecitabine in patients with advanced or metastatic pancreatic cancer who have failed first-line gemcitabine therapy. *Invest New Drugs* 30: 1216-1223.
172. Redston, M. S., C. Caldas, A. B. Seymour, R. H. Hruban, L. da Costa, C. J. Yeo, and S. E. Kern. 1994. p53 mutations in pancreatic carcinoma and evidence of common involvement of homocopolymer tracts in DNA microdeletions. *Cancer Res* 54: 3025-3033.
173. Moore, P. S., B. Sipos, S. Orlandini, C. Sorio, F. X. Real, N. R. Lemoine, T. Gress, C. Bassi, G. Kloppel, H. Kalthoff, H. Ungefroren, M. Lohr, and A. Scarpa. 2001. Genetic profile of 22 pancreatic carcinoma cell lines. Analysis of K-ras, p53, p16 and DPC4/Smad4. *Virchows Arch* 439: 798-802.
174. Deer, E. L., J. Gonzalez-Hernandez, J. D. Coursen, J. E. Shea, J. Ngatia, C. L. Scaife, M. A. Firpo, and S. J. Mulvihill. 2010. Phenotype and genotype of pancreatic cancer cell lines. *Pancreas* 39: 425-435.
175. Sipos, B., S. Moser, H. Kalthoff, V. Torok, M. Lohr, and G. Kloppel. 2003. A comprehensive characterization of pancreatic ductal carcinoma cell lines: towards the establishment of an in vitro research platform. *Virchows Arch* 442: 444-452.
176. Ouyang, H., L. Mou, C. Luk, N. Liu, J. Karaskova, J. Squire, and M. S. Tsao. 2000. Immortal human pancreatic duct epithelial cell lines with near normal genotype and phenotype. *Am J Pathol* 157: 1623-1631.
177. Agdeppa, E. D., and M. E. Spilker. 2009. A review of imaging agent development. *AAPS J* 11: 286-299.
178. Kang, B. H., K. J. Jensen, J. A. Hatch, and K. A. Janes. 2013. Simultaneous profiling of 194 distinct receptor transcripts in human cells. *Sci Signal* 6: rs13.
179. Breitling, R., and P. Herzyk. 2005. Rank-based methods as a non-parametric alternative of the T-statistic for the analysis of biological microarray data. *J Bioinform Comput Biol* 3: 1171-1189.
180. Maupin, K. A., A. Sinha, E. Eugster, J. Miller, J. Ross, V. Paulino, V. G. Keshamouni, N. Tran, M. Berens, C. Webb, and B. B. Haab. 2010. Glycogene expression alterations associated with pancreatic cancer

epithelial-mesenchymal transition in complementary model systems. *PLoS One* 5: e13002.
181. Sheet, A. D. 2004. GeneChip Human Genome Arrays.
182. Fallahi-Sichani, M., S. Honarnejad, L. M. Heiser, J. W. Gray, and P. K. Sorger. 2013. Metrics other than potency reveal systematic variation in responses to cancer drugs. *Nat Chem Biol* 9: 708-714.
183. Nakamura, T., I. J. Fidler, and K. R. Coombes. 2007. Gene expression profile of metastatic human pancreatic cancer cells depends on the organ microenvironment. *Cancer Res* 67: 139-148.
184. Bruns, C. J., M. T. Harbison, H. Kuniyasu, I. Eue, and I. J. Fidler. 1999. In vivo selection and characterization of metastatic variants from human pancreatic adenocarcinoma by using orthotopic implantation in nude mice. *Neoplasia* 1: 50-62.
185. Shin, S. J., J. A. Smith, G. A. Rezniczek, S. Pan, R. Chen, T. A. Brentnall, G. Wiche, and K. A. Kelly. 2013. Unexpected gain of function for the scaffolding protein plectin due to mislocalization in pancreatic cancer. *Proceedings of the National Academy of Sciences* 110: 19414-19419.
186. Elnemr, A., T. Ohta, A. Yachie, M. Kayahara, H. Kitagawa, T. Fujimura, I. Ninomiya, S. Fushida, G. I. Nishimura, K. Shimizu, and K. Miwa. 2001. Human pancreatic cancer cells disable function of Fas receptors at several levels in Fas signal transduction pathway. *Int J Oncol* 18: 311-316.
187. Saeed, A. I., V. Sharov, J. White, J. Li, W. Liang, N. Bhagabati, J. Braisted, M. Klapa, T. Currier, M. Thiagarajan, A. Sturn, M. Snuffin, A. Rezantsev, D. Popov, A. Ryltsov, E. Kostukovich, I. Borisovsky, Z. Liu, A. Vinsavich, V. Trush, and J. Quackenbush. 2003. TM4: a free, open-source system for microarray data management and analysis. *Biotechniques* 34: 374-378.
188. Linger, R. M., A. K. Keating, H. S. Earp, and D. K. Graham. 2008. TAM receptor tyrosine kinases: biologic functions, signaling, and potential therapeutic targeting in human cancer. *Adv Cancer Res* 100: 35-83.
189. Graham, D. K., G. W. Bowman, T. L. Dawson, W. L. Stanford, H. S. Earp, and H. R. Snodgrass. 1995. Cloning and developmental expression analysis of the murine c-mer tyrosine kinase. *Oncogene* 10: 2349-2359.
190. Schlegel, J., M. J. Sambade, S. Sather, S. J. Moschos, A. C. Tan, A. Winges, D. DeRyckere, C. C. Carson, D. G. Trembath, J. J. Tentler, S. G. Eckhardt, P. F. Kuan, R. L. Hamilton, L. M. Duncan, C. R. Miller, N. Nikolaishvili-Feinberg, B. R. Midkiff, J. Liu, W. Zhang, C. Yang, X. Wang, S. V. Frye, H. S. Earp, J. M. Shields, and D. K. Graham. 2013. MERTK receptor tyrosine kinase is a therapeutic target in melanoma. *J Clin Invest* 123: 2257-2267.
191. Cummings, C. T., D. Deryckere, H. S. Earp, and D. K. Graham. 2013. Molecular pathways: MERTK signaling in cancer. *Clin Cancer Res* 19: 5275-5280.
192. Gjerdrum, C., C. Tiron, T. Hoiby, I. Stefansson, H. Haugen, T. Sandal, K. Collett, S. Li, E. McCormack, B. T. Gjertsen, D. R. Micklem, L. A. Akslen, C. Glackin, and J. B. Lorens. 2010. Axl is an essential epithelial-to-

mesenchymal transition-induced regulator of breast cancer metastasis and patient survival. *Proc Natl Acad Sci U S A* 107: 1124-1129.
193. Zhang, Y. X., P. G. Knyazev, Y. V. Cheburkin, K. Sharma, Y. P. Knyazev, L. Orfi, I. Szabadkai, H. Daub, G. Keri, and A. Ullrich. 2008. AXL is a potential target for therapeutic intervention in breast cancer progression. *Cancer Res* 68: 1905-1915.
194. Bosurgi, L., J. H. Bernink, V. Delgado Cuevas, N. Gagliani, L. Joannas, E. T. Schmid, C. J. Booth, S. Ghosh, and C. V. Rothlin. 2013. Paradoxical role of the proto-oncogene Axl and Mer receptor tyrosine kinases in colon cancer. *Proc Natl Acad Sci U S A* 110: 13091-13096.
195. Dunne, P. D., D. G. McArt, J. K. Blayney, M. Kalimutho, S. Greer, T. Wang, S. Srivastava, C. W. Ong, K. Arthur, M. Loughrey, K. Redmond, D. B. Longley, M. Salto-Tellez, P. G. Johnston, and S. Van Schaeybroeck. 2014. AXL is a key regulator of inherent and chemotherapy-induced invasion and predicts a poor clinical outcome in early-stage colon cancer. *Clin Cancer Res* 20: 164-175.
196. Shieh, Y. S., C. Y. Lai, Y. R. Kao, S. G. Shiah, Y. W. Chu, H. S. Lee, and C. W. Wu. 2005. Expression of axl in lung adenocarcinoma and correlation with tumor progression. *Neoplasia* 7: 1058-1064.
197. Zhang, Z., J. C. Lee, L. Lin, V. Olivas, V. Au, T. LaFramboise, M. Abdel-Rahman, X. Wang, A. D. Levine, J. K. Rho, Y. J. Choi, C. M. Choi, S. W. Kim, S. J. Jang, Y. S. Park, W. S. Kim, D. H. Lee, J. S. Lee, V. A. Miller, M. Arcila, M. Ladanyi, P. Moonsamy, C. Sawyers, T. J. Boggon, P. C. Ma, C. Costa, M. Taron, R. Rosell, B. Halmos, and T. G. Bivona. 2012. Activation of the AXL kinase causes resistance to EGFR-targeted therapy in lung cancer. *Nat Genet* 44: 852-860.
198. Tsou, A. P., K. M. Wu, T. Y. Tsen, C. W. Chi, J. H. Chiu, W. Y. Lui, C. P. Hu, C. Chang, C. K. Chou, and S. F. Tsai. 1998. Parallel hybridization analysis of multiple protein kinase genes: identification of gene expression patterns characteristic of human hepatocellular carcinoma. *Genomics* 50: 331-340.
199. Tworkoski, K. A., J. T. Platt, A. Bacchiocchi, M. Bosenberg, T. J. Boggon, and D. F. Stern. 2013. MERTK controls melanoma cell migration and survival and differentially regulates cell behavior relative to AXL. *Pigment Cell Melanoma Res* 26: 527-541.
200. Koorstra, J. B., C. A. Karikari, G. Feldmann, S. Bisht, P. L. Rojas, G. J. Offerhaus, H. Alvarez, and A. Maitra. 2009. The Axl receptor tyrosine kinase confers an adverse prognostic influence in pancreatic cancer and represents a new therapeutic target. *Cancer Biol Ther* 8: 618-626.
201. Song, X., H. Wang, C. D. Logsdon, A. Rashid, J. B. Fleming, J. L. Abbruzzese, H. F. Gomez, D. B. Evans, and H. Wang. 2011. Overexpression of receptor tyrosine kinase Axl promotes tumor cell invasion and survival in pancreatic ductal adenocarcinoma. *Cancer* 117: 734-743.
202. Rankin, E. B., K. C. Fuh, T. E. Taylor, A. J. Krieg, M. Musser, J. Yuan, K. Wei, C. J. Kuo, T. A. Longacre, and A. J. Giaccia. 2010. AXL is an essential

factor and therapeutic target for metastatic ovarian cancer. *Cancer Res* 70: 7570-7579.
203. van Ginkel, P. R., R. L. Gee, R. L. Shearer, L. Subramanian, T. M. Walker, D. M. Albert, L. F. Meisner, B. C. Varnum, and A. S. Polans. 2004. Expression of the receptor tyrosine kinase Axl promotes ocular melanoma cell survival. *Cancer Res* 64: 128-134.
204. Ling, L., and H. J. Kung. 1995. Mitogenic signals and transforming potential of Nyk, a newly identified neural cell adhesion molecule-related receptor tyrosine kinase. *Mol Cell Biol* 15: 6582-6592.
205. Guttridge, K. L., J. C. Luft, T. L. Dawson, E. Kozlowska, N. P. Mahajan, B. Varnum, and H. S. Earp. 2002. Mer receptor tyrosine kinase signaling: prevention of apoptosis and alteration of cytoskeletal architecture without stimulation or proliferation. *J Biol Chem* 277: 24057-24066.
206. Wu, Y. M., D. R. Robinson, and H. J. Kung. 2004. Signal pathways in up-regulation of chemokines by tyrosine kinase MER/NYK in prostate cancer cells. *Cancer Res* 64: 7311-7320.
207. Goruppi, S., E. Ruaro, B. Varnum, and C. Schneider. 1999. Gas6-mediated survival in NIH3T3 cells activates stress signalling cascade and is independent of Ras. *Oncogene* 18: 4224-4236.
208. Fridell, Y. W., Y. Jin, L. A. Quilliam, A. Burchert, P. McCloskey, G. Spizz, B. Varnum, C. Der, and E. T. Liu. 1996. Differential activation of the Ras/extracellular-signal-regulated protein kinase pathway is responsible for the biological consequences induced by the Axl receptor tyrosine kinase. *Mol Cell Biol* 16: 135-145.
209. Sen, P., M. A. Wallet, Z. Yi, Y. Huang, M. Henderson, C. E. Mathews, H. S. Earp, G. Matsushima, A. S. J. Baldwin, and R. M. Tisch. 2007. Apoptotic cells induce Mer tyrosine kinase-dependent blockade of NF-kappaB activation in dendritic cells. *Blood* 109: 653-660.
210. Demarchi, F., R. Verardo, B. Varnum, C. Brancolini, and C. Schneider. 2001. Gas6 anti-apoptotic signaling requires NF-kappa B activation. *J Biol Chem* 276: 31738-31744.
211. Samatar, A. A., and P. I. Poulikakos. 2014. Targeting RAS-ERK signalling in cancer: promises and challenges. *Nat Rev Drug Discov* 13: 928-942.
212. Sawabu, T., H. Seno, T. Kawashima, A. Fukuda, Y. Uenoyama, M. Kawada, N. Kanda, A. Sekikawa, H. Fukui, M. Yanagita, H. Yoshibayashi, S. Satoh, Y. Sakai, T. Nakano, and T. Chiba. 2007. Growth arrest-specific gene 6 and Axl signaling enhances gastric cancer cell survival via Akt pathway. *Mol Carcinog* 46: 155-164.
213. Gustafsson, A., D. Martuszewska, M. Johansson, C. Ekman, S. Hafizi, B. Ljungberg, and B. Dahlback. 2009. Differential expression of Axl and Gas6 in renal cell carcinoma reflecting tumor advancement and survival. *Clin Cancer Res* 15: 4742-4749.
214. Zitzmann, K., J. Ruden, S. Brand, B. Goke, J. Lichtl, G. Spottl, and C. J. Auernhammer. 2010. Compensatory activation of Akt in response to mTOR and Raf inhibitors - a rationale for dual-targeted therapy approaches in neuroendocrine tumor disease. *Cancer Lett* 295: 100-109.

215. Gioeli, D., W. Wunderlich, J. Sebolt-Leopold, S. Bekiranov, J. D. Wulfkuhle, E. F. Petricoin, M. Conaway, and M. J. Weber. 2011. Compensatory pathways induced by MEK inhibition are effective drug targets for combination therapy against castration-resistant prostate cancer. *Mol Cancer Ther* 10: 1581-1590.
216. Christoph, S., D. Deryckere, J. Schlegel, J. K. Frazer, L. A. Batchelor, A. Y. Trakhimets, S. Sather, D. M. Hunter, C. T. Cummings, J. Liu, C. Yang, D. Kireev, C. Simpson, J. Norris-Drouin, E. A. Hull-Ryde, W. P. Janzen, G. L. Johnson, X. Wang, S. V. Frye, H. S. Earp, and D. K. Graham. 2013. UNC569, a novel small-molecule mer inhibitor with efficacy against acute lymphoblastic leukemia in vitro and in vivo. *Mol Cancer Ther* 12: 2367-2377.
217. Chen, J., K. Carey, and P. J. Godowski. 1997. Identification of Gas6 as a ligand for Mer, a neural cell adhesion molecule related receptor tyrosine kinase implicated in cellular transformation. *Oncogene* 14: 2033-2039.
218. Caberoy, N. B., G. Alvarado, J. L. Bigcas, and W. Li. 2012. Galectin-3 is a new MerTK-specific eat-me signal. *J Cell Physiol* 227: 401-407.
219. Caberoy, N. B., Y. Zhou, and W. Li. 2010. Tubby and tubby-like protein 1 are new MerTK ligands for phagocytosis. *EMBO J* 29: 3898-3910.
220. Bellosta, P., M. Costa, D. A. Lin, and C. Basilico. 1995. The receptor tyrosine kinase ARK mediates cell aggregation by homophilic binding. *Mol Cell Biol* 15: 614-625.
221. Tsou, W.-I., K. Q. Nguyen, R. Birge, and S. Kotenko. 2013. Apoptotic cell recognition receptors, Tyro3, Axl and Mer, demonstrate distinct patterns of ligand-inducible and ligand-independent receptor activation (P2016). *The Journal of Immunology* 190: 214.9.
222. Tauseef, M., S. Vogel, A. Dietrich, A. Malik, L. Birnbaumer, and D. Mehta. 2011. Tyrosine phosphorylation of STIM1 induced by TRPC6-Pyk2 cascade regulates store-operated calcium entry and endothelial permeability. *The FASEB Journal* 25: 1082.4.
223. Muz, B., M. Buggio, F. Azab, A. F. Trombino, M. Padval, and A. K. Azab. 2014. PYK2 Inhibitors Sensitize Hypoxia-Induced Drug Resistant Multiple Myeloma Cell. *Blood* 124: 4704-4704.
224. Lev, S., H. Moreno, R. Martinez, P. Canoll, E. Peles, J. M. Musacchio, G. D. Plowman, B. Rudy, and J. Schlessinger. 1995. Protein tyrosine kinase PYK2 involved in Ca(2+)-induced regulation of ion channel and MAP kinase functions. *Nature* 376: 737-745.
225. Xiong, W., and J. T. Parsons. 1997. Induction of apoptosis after expression of PYK2, a tyrosine kinase structurally related to focal adhesion kinase. *J Cell Biol* 139: 529-539.
226. Parsons, J. T., and S. J. Parsons. 1997. Src family protein tyrosine kinases: cooperating with growth factor and adhesion signaling pathways. *Curr Opin Cell Biol* 9: 187-192.
227. Tokiwa, G., I. Dikic, S. Lev, and J. Schlessinger. 1996. Activation of Pyk2 by stress signals and coupling with JNK signaling pathway. *Science* 273: 792-794.

228. Goldman, R. D., D. L. Spector, and A. C. Swedlund. 2005. *Live cell imaging: a laboratory manual*. Cold Spring Harbor Laboratory Press Cold Spring Harbor, NY:
229. Guma, M., J. Kashiwakura, B. Crain, Y. Kawakami, B. Beutler, G. S. Firestein, T. Kawakami, M. Karin, and M. Corr. 2010. JNK1 controls mast cell degranulation and IL-1{beta} production in inflammatory arthritis. *Proc Natl Acad Sci U S A* 107: 22122-22127.
230. Weston, C. R., and R. J. Davis. 2007. The JNK signal transduction pathway. *Curr Opin Cell Biol* 19: 142-149.
231. Karin, M. 1998. Mitogen-activated protein kinase cascades as regulators of stress responses. *Ann N Y Acad Sci* 851: 139-146.
232. Barr, R. K., and M. A. Bogoyevitch. 2001. The c-Jun N-terminal protein kinase family of mitogen-activated protein kinases (JNK MAPKs). *Int J Biochem Cell Biol* 33: 1047-1063.
233. Gupta, S., T. Barrett, A. J. Whitmarsh, J. Cavanagh, H. K. Sluss, B. Derijard, and R. J. Davis. 1996. Selective interaction of JNK protein kinase isoforms with transcription factors. *EMBO J* 15: 2760-2770.
234. Bogoyevitch, M. A., and B. Kobe. 2006. Uses for JNK: the many and varied substrates of the c-Jun N-terminal kinases. *Microbiol Mol Biol Rev* 70: 1061-1095.
235. Liu, J., and A. Lin. 2005. Role of JNK activation in apoptosis: a double-edged sword. *Cell Res* 15: 36-42.
236. Fey, D., D. R. Croucher, W. Kolch, and B. N. Kholodenko. 2012. Crosstalk and signaling switches in mitogen-activated protein kinase cascades. *Front Physiol* 3: 355.
237. Lopez-Bergami, P., C. Huang, J. S. Goydos, D. Yip, M. Bar-Eli, M. Herlyn, K. S. Smalley, A. Mahale, A. Eroshkin, S. Aaronson, and Z. Ronai. 2007. Rewired ERK-JNK signaling pathways in melanoma. *Cancer Cell* 11: 447-460.
238. Bennett, B. L., D. T. Sasaki, B. W. Murray, E. C. O'Leary, S. T. Sakata, W. Xu, J. C. Leisten, A. Motiwala, S. Pierce, Y. Satoh, S. S. Bhagwat, A. M. Manning, and D. W. Anderson. 2001. SP600125, an anthrapyrazolone inhibitor of Jun N-terminal kinase. *Proc Natl Acad Sci U S A* 98: 13681-13686.
239. Vultur, A., J. Villanueva, C. Krepler, G. Rajan, Q. Chen, M. Xiao, L. Li, P. A. Gimotty, M. Wilson, J. Hayden, F. Keeney, K. L. Nathanson, and M. Herlyn. 2014. MEK inhibition affects STAT3 signaling and invasion in human melanoma cell lines. *Oncogene* 33: 1850-1861.
240. Dai, B., J. Meng, M. Peyton, L. Girard, W. G. Bornmann, L. Ji, J. D. Minna, B. Fang, and J. A. Roth. 2011. STAT3 mediates resistance to MEK inhibitor through microRNA miR-17. *Cancer Res* 71: 3658-3668.
241. Yoon, Y. K., H. P. Kim, S. W. Han, Y. Oh do, S. A. Im, Y. J. Bang, and T. Y. Kim. 2010. KRAS mutant lung cancer cells are differentially responsive to MEK inhibitor due to AKT or STAT3 activation: implication for combinatorial approach. *Mol Carcinog* 49: 353-362.

242. Forbes, S. A., D. Beare, P. Gunasekaran, K. Leung, N. Bindal, H. Boutselakis, M. Ding, S. Bamford, C. Cole, and S. Ward. 2015. COSMIC: exploring the world's knowledge of somatic mutations in human cancer. *Nucleic acids research* 43: D805-D811.
243. Colombo, R., M. Caldarelli, M. Mennecozzi, M. L. Giorgini, F. Sola, P. Cappella, C. Perrera, S. R. Depaolini, L. Rusconi, U. Cucchi, N. Avanzi, J. A. Bertrand, R. T. Bossi, E. Pesenti, A. Galvani, A. Isacchi, F. Colotta, D. Donati, and J. Moll. 2010. Targeting the mitotic checkpoint for cancer therapy with NMS-P715, an inhibitor of MPS1 kinase. *Cancer Res* 70: 10255-10264.
244. Ferrandi, C., R. Ballerio, P. Gaillard, C. Giachetti, S. Carboni, P. A. Vitte, J. P. Gotteland, and R. Cirillo. 2004. Inhibition of c-Jun N-terminal kinase decreases cardiomyocyte apoptosis and infarct size after myocardial ischemia and reperfusion in anaesthetized rats. *Br J Pharmacol* 142: 953-960.
245. Zhang, T., F. Inesta-Vaquera, M. Niepel, J. Zhang, S. B. Ficarro, T. Machleidt, T. Xie, J. A. Marto, N. Kim, T. Sim, J. D. Laughlin, H. Park, P. V. LoGrasso, M. Patricelli, T. K. Nomanbhoy, P. K. Sorger, D. R. Alessi, and N. S. Gray. 2012. Discovery of potent and selective covalent inhibitors of JNK. *Chem Biol* 19: 140-154.
246. Beech, J., L. Saleh, J. Frentzel, H. Figler, I. R. J. Correa, B. Baker, C. Ramspacher, M. Marshall, S. Dasa, J. Linden, C. J. Noren, and K. A. Kelly. 2015. Multivalent Site-Specific Phage Modification Enhances the Binding Affinity of Receptor Ligands. *Bioconjug Chem*
247. Dente, L., C. Vetriani, A. Zucconi, G. Pelicci, L. Lanfrancone, P. G. Pelicci, and G. Cesareni. 1997. Modified phage peptide libraries as a tool to study specificity of phosphorylation and recognition of tyrosine containing peptides. *J Mol Biol* 269: 694-703.
248. Tian, F., M. L. Tsao, and P. G. Schultz. 2004. A phage display system with unnatural amino acids. *J Am Chem Soc* 126: 15962-15963.
249. Somers, K., P. Stinissen, and V. Somers. 2011. Citrulline-modified phage display: a novel high-throughput discovery approach for the identification of citrulline-containing ligands. *Proteomics* 11: 2550-2554.
250. Saleh, L., and C. J. Noren. 2011. Site-directed chemical modification of phage particles. *Phage Nanobiotechnology* 202-219.
251. Barrett, R. W., S. E. Cwirla, W. J. Dower, M. Gallop, and T. F. Woiwode. 2007. Compounds displayed on icosahedral phage and methods of using same.
252. Sandman, K. E., and C. J. Noren. 2000. The efficiency of Escherichia coli selenocysteine insertion is influenced by the immediate downstream nucleotide. *Nucleic Acids Res* 28: 755-761.
253. Sandman, K. E., J. S. Benner, and C. J. Noren. 2000. Phage display of selenopeptides. *J. Am. Chem. Soc*
254. Gorlatov, S. N., and T. C. Stadtman. 1998. Human thioredoxin reductase from HeLa cells: selective alkylation of selenocysteine in the protein inhibits

enzyme activity and reduction with NADPH influences affinity to heparin. *Proc Natl Acad Sci U S A* 95: 8520-8525.
255. Sandman, K. E., D. F. Tardiff, L. A. Neely, and C. J. Noren. 2003. Revised Escherichia coli selenocysteine insertion requirements determined by in vivo screening of combinatorial libraries of SECIS variants. *Nucleic Acids Res* 31: 2234-2241.
256. Fredholm, B. B., A. P. IJzerman, K. A. Jacobson, J. Linden, and C. E. Muller. 2011. International Union of Basic and Clinical Pharmacology. LXXXI. Nomenclature and classification of adenosine receptors--an update. *Pharmacol Rev* 63: 1-34.
257. Chen, J.-F., H. K. Eltzschig, and B. B. Fredholm. 2013. Adenosine receptors as drug targets—what are the challenges? *Nature Reviews Drug Discovery* 12: 265-286.
258. Cheng, Y., Y. M. Tao, J. F. Sun, Y. H. Wang, X. J. Xu, J. Chen, Z. Q. Chi, and J. G. Liu. 2010. Adenosine A(1) receptor agonist N(6)-cyclohexyl-adenosine induced phosphorylation of delta opioid receptor and desensitization of its signaling. *Acta Pharmacol Sin* 31: 784-790.
259. Olson, E. R., J. E. Naugle, X. Zhang, J. A. Bomser, and J. G. Meszaros. 2005. Inhibition of cardiac fibroblast proliferation and myofibroblast differentiation by resveratrol. *Am J Physiol Heart Circ Physiol* 288: H1131-H1138.
260. Huskens, J. 2006. Multivalent interactions at interfaces. *Curr Opin Chem Biol* 10: 537-543.
261. Robeva, A. S., R. Woodard, D. R. Luthin, H. E. Taylor, and J. Linden. 1996. Double tagging recombinant A1- and A2A-adenosine receptors with hexahistidine and the FLAG epitope. Development of an efficient generic protein purification procedure. *Biochem Pharmacol* 51: 545-555.
262. Brose, M. S., P. Volpe, M. Feldman, M. Kumar, I. Rishi, R. Gerrero, E. Einhorn, M. Herlyn, J. Minna, A. Nicholson, J. A. Roth, S. M. Albelda, H. Davies, C. Cox, G. Brignell, P. Stephens, P. A. Futreal, R. Wooster, M. R. Stratton, and B. L. Weber. 2002. BRAF and RAS mutations in human lung cancer and melanoma. *Cancer Res* 62: 6997-7000.
263. Meng, J., B. Dai, B. Fang, B. N. Bekele, W. G. Bornmann, D. Sun, Z. Peng, R. S. Herbst, V. Papadimitrakopoulou, J. D. Minna, M. Peyton, and J. A. Roth. 2010. Combination treatment with MEK and AKT inhibitors is more effective than each drug alone in human non-small cell lung cancer in vitro and in vivo. *PLoS One* 5: e14124.
264. Davies, B. R., A. Logie, J. S. McKay, P. Martin, S. Steele, R. Jenkins, M. Cockerill, S. Cartlidge, and P. D. Smith. 2007. AZD6244 (ARRY-142886), a potent inhibitor of mitogen-activated protein kinase/extracellular signal-regulated kinase kinase 1/2 kinases: mechanism of action in vivo, pharmacokinetic/pharmacodynamic relationship, and potential for combination in preclinical models. *Mol Cancer Ther* 6: 2209-2219.
265. Banerji, U., D. R. Camidge, H. M. Verheul, R. Agarwal, D. Sarker, S. B. Kaye, I. M. Desar, J. N. Timmer-Bonte, S. G. Eckhardt, K. D. Lewis, K. H. Brown, M. V. Cantarini, C. Morris, S. M. George, P. D. Smith, and C. M. van

Herpen. 2010. The first-in-human study of the hydrogen sulfate (Hyd-sulfate) capsule of the MEK1/2 inhibitor AZD6244 (ARRY-142886): a phase I open-label multicenter trial in patients with advanced cancer. *Clin Cancer Res* 16: 1613-1623.
266. Adjei, A. A., R. B. Cohen, W. Franklin, C. Morris, D. Wilson, J. R. Molina, L. J. Hanson, L. Gore, L. Chow, S. Leong, L. Maloney, G. Gordon, H. Simmons, A. Marlow, K. Litwiler, S. Brown, G. Poch, K. Kane, J. Haney, and S. G. Eckhardt. 2008. Phase I pharmacokinetic and pharmacodynamic study of the oral, small-molecule mitogen-activated protein kinase kinase 1/2 inhibitor AZD6244 (ARRY-142886) in patients with advanced cancers. *J Clin Oncol* 26: 2139-2146.
267. Infante, J. R., K. P. Papadopoulos, J. C. Bendell, A. Patnaik, H. A. Burris, D. Rasco, S. F. Jones, L. Smith, D. S. Cox, M. Durante, K. M. Bellew, J. J. Park, N. T. Le, and A. W. Tolcher. 2013. A phase 1b study of trametinib, an oral Mitogen-activated protein kinase kinase (MEK) inhibitor, in combination with gemcitabine in advanced solid tumours. *Eur J Cancer* 49: 2077-2085.
268. Eferl, R., R. Ricci, L. Kenner, R. Zenz, J. P. David, M. Rath, and E. F. Wagner. 2003. Liver tumor development. c-Jun antagonizes the proapoptotic activity of p53. *Cell* 112: 181-192.
269. Vleugel, M. M., A. E. Greijer, R. Bos, E. van der Wall, and P. J. van Diest. 2006. c-Jun activation is associated with proliferation and angiogenesis in invasive breast cancer. *Hum Pathol* 37: 668-674.
270. Maeda, S., and M. Karin. 2003. Oncogene at last--c-Jun promotes liver cancer in mice. *Cancer Cell* 3: 102-104.
271. Eferl, R., and E. F. Wagner. 2003. AP-1: a double-edged sword in tumorigenesis. *Nat Rev Cancer* 3: 859-868.
272. Jiao, X., S. Katiyar, N. E. Willmarth, M. Liu, X. Ma, N. Flomenberg, M. P. Lisanti, and R. G. Pestell. 2010. c-Jun induces mammary epithelial cellular invasion and breast cancer stem cell expansion. *J Biol Chem* 285: 8218-8226.
273. Patterson, K. I., T. Brummer, P. M. O'Brien, and R. J. Daly. 2009. Dual-specificity phosphatases: critical regulators with diverse cellular targets. *Biochem J* 418: 475-489.
274. Camps, M., A. Nichols, and S. Arkinstall. 2000. Dual specificity phosphatases: a gene family for control of MAP kinase function. *FASEB J* 14: 6-16.
275. Misra-Press, A., C. S. Rim, H. Yao, M. S. Roberson, and P. J. Stork. 1995. A novel mitogen-activated protein kinase phosphatase. Structure, expression, and regulation. *J Biol Chem* 270: 14587-14596.
276. Koivunen, E., W. Arap, H. Valtanen, A. Rainisalo, O. P. Medina, P. Heikkila, C. Kantor, C. G. Gahmberg, T. Salo, Y. T. Konttinen, T. Sorsa, E. Ruoslahti, and R. Pasqualini. 1999. Tumor targeting with a selective gelatinase inhibitor. *Nat Biotechnol* 17: 768-774.
277. Tveita, A., O. P. Rekvig, and S. N. Zykova. 2008. Glomerular matrix metalloproteinases and their regulators in the pathogenesis of lupus nephritis. *Arthritis Res Ther* 10: 229.

278. Hesek, D., M. Toth, S. O. Meroueh, S. Brown, H. Zhao, W. Sakr, R. Fridman, and S. Mobashery. 2006. Design and characterization of a metalloproteinase inhibitor-tethered resin for the detection of active MMPs in biological samples. *Chem Biol* 13: 379-386.
279. Wistuba, I. I., J. G. Gelovani, J. J. Jacoby, S. E. Davis, and R. S. Herbst. 2011. Methodological and practical challenges for personalized cancer therapies. *Nat Rev Clin Oncol* 8: 135-141.
280. Zimmer, L., F. Barlesi, M. Martinez-Garcia, V. Dieras, J. H. Schellens, J. P. Spano, M. R. Middleton, E. Calvo, L. Paz-Ares, J. Larkin, S. Pacey, M. Venturi, F. Kraeber-Bodere, J. J. Tessier, W. E. Eberhardt, M. Paques, E. Guarin, V. Meresse, and J. C. Soria. 2014. Phase I expansion and pharmacodynamic study of the oral MEK inhibitor RO4987655 (CH4987655) in selected patients with advanced cancer with RAS-RAF mutations. *Clin Cancer Res* 20: 4251-4261.
281. Bubici, C., and S. Papa. 2014. JNK signalling in cancer: in need of new, smarter therapeutic targets. *Br J Pharmacol* 171: 24-37.
282. Deutscher, S. L. 2010. Phage display in molecular imaging and diagnosis of cancer. *Chem Rev* 110: 3196-3211.